PREPARED FOR THE U.S. DEPARTMENT OF ENERGY,
UNDER CONTRACT DE-AC02-76-CHO-3073

RECEIVED
OCT 2 7 1997
OSTI

PPPL-3255
UC-427

PPPL-3255

Kinetic Description of Intense Nonneutral Beam Propagation Through a Periodic Solenoidal Focusing Field Based on the Nonlinear Vlasov-Maxwell Equations

by
Ronald C. Davidson and Chiping Chen

August 1997

DISTRIBUTION OF THIS DOCUMENT IS UNLIMITED
MASTER
DISTRIBUTION OF THIS DOCUMENT IS UNLIMITED

PPPL PRINCETON PLASMA PHYSICS LABORATORY

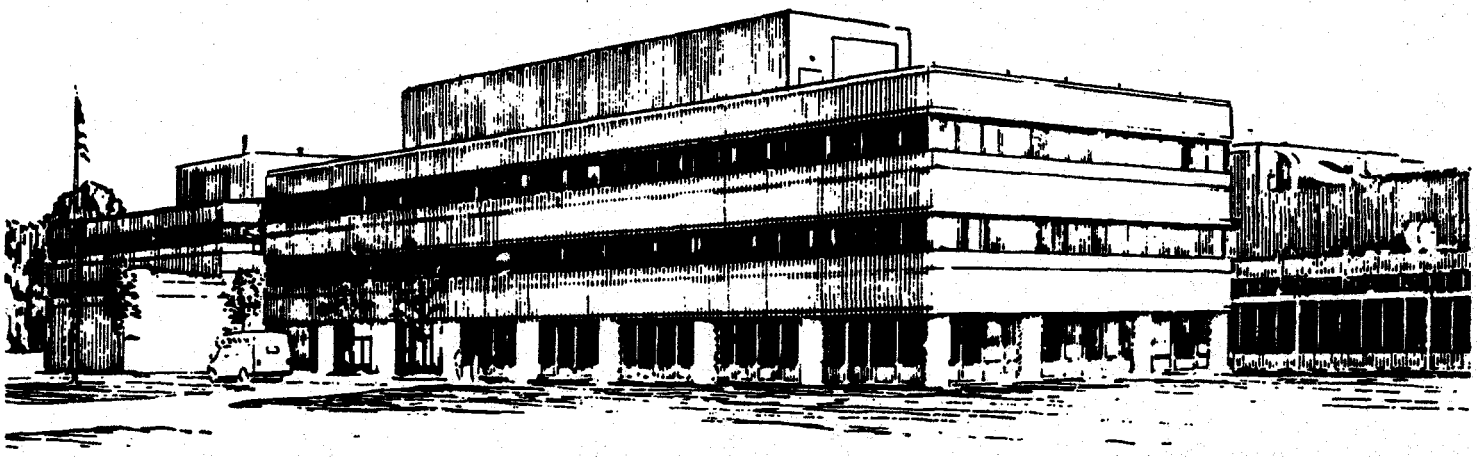

PRINCETON UNIVERSITY, PRINCETON, NEW JERSEY

PPPL Reports Disclaimer

This report was prepared as an account of work sponsored by an agency of the United States Government. Neither the United States Government nor any agency thereof, nor any of their employees, makes any warranty, express or implied, or assumes any legal liability of responsibility for the accuracy, completeness, or usefulness of any information, apparatus, product, or process disclosed, or represents that its use would not infringe privately owned rights. Reference herein to any specific commercial produce, process, or service by trade name, trademark, manufacturer, or otherwise, does not necessarily constitute or imply its endorsement, recommendation, or favoring by the United States Government or any agency thereof. The views and opinions of authors expressed herein do not necessarily state or reflect those of the United States Government or any agency thereof.

Notice

This report has been reproduced from the best available copy.
Available in paper copy and microfiche.

Number of pages in this report: 82

U.S. Department of Energy and Department of Energy Contractors can obtain copies of this report from:

Office of Scientific and Technical Information
P.O. Box 62
Oak Ridge, TN 37831
(615) 576-8401

This report is publicly available from the:

National Technical Information Service
Department of Commerce
5285 Port Royal Road
Springfield, VA 22161
(703) 487-4650

DISCLAIMER

Portions of this document may be illegible in electronic image products. Images are produced from the best available original document.

KINETIC DESCRIPTION OF INTENSE NONNEUTRAL BEAM PROPAGATION THROUGH A PERIODIC SOLENOIDAL FOCUSING FIELD BASED ON THE NONLINEAR VLASOV-MAXWELL EQUATIONS

Ronald C. Davidson
Plasma Physics Laboratory
Princeton University
Princeton, New Jersey 08543

Chiping Chen
Plasma Science and Fusion Center
Massachusetts Institute of Technology
Cambridge, Massachusetts 02139

ABSTRACT

A kinetic description of intense nonneutral beam propagation through a *periodic solenoidal focusing field* $B^{sol}(\vec{x}) = B_z(z)\vec{e}_z - (1/2)B_z'(z)(x\vec{e}_x + y\vec{e}_y)$ is developed, where $B_z(z+S) = B_z(z)$, and $S =$ const. is the axial periodicity length. The analysis is carried out for a *thin beam* with characteristic beam radius $r_b \ll S$, and directed axial momentum $\gamma_b m\beta_b c$ (in the z-direction) large compared with the transverse momentum and axial momentum spread of the beam particles. Making use of the nonlinear Vlasov-Maxwell equations for general distribution function $f_b(\vec{x},\vec{p},t)$ and self-consistent electrostatic field $\vec{E}^s(\vec{x},t) = -\nabla\phi^s(\vec{x},t)$ consistent with the thin-beam approximation, the kinetic model is used to investigate detailed beam equilibrium properties for a variety of distributions functions. Examples are presented both for the case of a uniform solenoidal focusing field $B_z(z) = B_0 =$ const. and for the case of a periodic solenoidal focusing field $B_z(z+S) = B_z(z)$. The nonlinear Vlasov-Maxwell equations are simplified in the thin-beam approximation, and an alternative Hamiltonian formulation is developed that is particularly well-suited to intense beam propagation in periodic focusing systems. For the case of a uniform focusing field, the nonlinear Vlasov-Maxwell equations are used to investigate a wide variety of azimuthally symmetric ($\partial/\partial\theta = 0$) intense beam equilibria characterized by $\partial/\partial t = 0 = \partial/\partial z$, ranging from distributions that are *isotropic* in momentum dependence in the frame of the beam, to *anisotropic*

distributions in which the momentum spreads are different in the axial and transverse directions. As a general remark, for a uniform focusing field, it is found that there is enormous latitude in the choice of equilibrium distribution function f_b^0, and the corresponding properties of the beam equilibrium. Introducing the axial coordinate $s = z$, use is made of the nonlinear Vlasov-Maxwell equations to investigate intense beam propagation in a *periodic* solenoidal field $B_z(s + S) = B_z(s)$, in which case the properties of the beam are *modulated as a function of* s by the focusing field. The nonlinear Vlasov equation is transformed to a frame of reference rotating at the Larmor frequency $\Omega_L(s) = -Z_i e B_z(s)/2\gamma_b mc$, and the description is further simplified by assuming azimuthal symmetry, in which case the canonical angular momentum is an exact single-particle constant of the motion. As an application of this general formalism, the specific example is considered of a periodically focused, rigid-rotor Vlasov equilibrium with step-function radial density profile and average azimuthal motion of the beam corresponding to a rigid rotation (in the Larmor frame) about the axis of symmetry. A wide range of beam properties are calculated, such as the average flow velocity, transverse temperature profile, and transverse thermal emittance. This example represents an important generalization of the familiar Kapchinskij-Vladimirskij beam distribution to allow for average beam rotation in the Larmor frame. Based on the present analysis, the Vlasov-Maxwell description of intense nonneutral beam propagation through a periodic solenoidal focusing field $\vec{B}^{sol}(\vec{x})$ is found to be remarkably tractable and rich in physics content. The Vlasov-Maxwell formalism developed here can be extended in a straightforward manner to investigate detailed stability behavior for perturbations about specific choices of beam equilibria.

TABLE OF CONTENTS

I. INTRODUCTION

Periodic focusing accelerators [1-4] have a wide range of applications ranging from basic scientific research, to applications [5-7] such as heavy ion fusion, tritium production and nuclear waste treatment. Of particular importance, at the high beam currents and charge density of practical interest, are the effects of the intense self fields produced by the beam space charge and current on detailed equilibrium, stability and transport properties. One of the challenges of intense beam propagation is to understand and avoid the effects of collective instabilities [8-17] and nonlinear mechanisms for halo formation [18-21], which become particularly virulent when space-charge forces are comparable to the external focusing force. Over the years, considerable theoretical progress has been made [8-24], both analytical and in numerical studies, in describing collective processes and the nonlinear beam dynamics for an intense beam propagating through a periodic focusing field. The equilibrium and stability properties of one particular distribution function, the Kapchinskij-Vladimirskij (KV) beam equilibrium [24], which has an inverted population in phase space, has received considerable attention. While providing useful insights, analyses restricted to the KV beam distribution tend to be limited in scope, since it is well known in plasma physics that the detailed nonlinear dynamics and equilibrium and stability properties can exhibit a sensitive dependence on the form of the distribution function $f_b(\vec{x},\vec{p},t)$.

It is the purpose of this article to develop and apply a *kinetic* description of intense nonneutral beam propagation through a peroidic solenoidal field $\vec{B}^{sol}(\vec{x})$ based on the nonlinear Vlasov-Maxwell equations for general distribution function $f_b(\vec{x},\vec{p},t)$. The present article uses the Vlasov-Maxwell formalism to investigate detailed beam equilibrium properties for a variety of distribution functions, both for the case of a uniform solenoidal focusing field $B_0\vec{e}_z$, where B_0 = const., and for a periodic solenoidal focusing field [25] $\vec{B}^{sol}(\vec{x}) = B_z(z)\vec{e}_z - (1/2)B_z'(z)(x\vec{e}_x + y\vec{e}_y)$, where $B_z(z+S) = B_z(z)$ and S is the axial periodicity length. The intense nonneutral beam propagates axially (the z-direction) through the applied field $\vec{B}^{sol}(\vec{x})$, and the beam is assumed to be *thin* with characteristic beam radius

r_b small in comparison with the axial periodicity length S of the focusing field. In addition, the average directed axial momentum $\gamma_b m\beta_b c$ of the beam particles is assumed to be large in comparison with the transverse particle momentum and the axial momentum spread. The self-field intensity, which is proportional to the beam current and density, is allowed to be arbitrarily large, subject only to the condition required for radial confinement of the beam particles by the applied field, and the requirement that Budker's parameter ν satisfy $\nu = N_b Z_i^2 e^2/mc^2 \ll \gamma_b$. Here, $N_b = \int dxdyn_b$ is the number of beam particles per unit axial length, $Z_i e$ is the charge, and $\gamma_b mc^2$ is the characteristic energy.

The organization of this paper is the following. The theoretical model and assumptions are presented in Sec. II. In Sec. III, the nonlinear Vlasov-Maxwell equations and the single-particle equations of motion are simplified in the context of these assumptions (Sec. III.A), and an alternative Hamiltonian formulation is developed that is particularly well-suited to describing intense beam propagation in periodic focusing systems (Sec. III.B). For the case of a uniform focusing field $B_0\vec{e}_z$ [26], in Sec. IV the kinetic formalism based on the nonlinear Vlasov-Maxwell equations is used to investigate a wide variety of azimuthally symmetric ($\partial/\partial\theta = 0$) intense beam equilibria characterized by $\partial/\partial t = 0 = \partial/\partial z$, ranging from distributions that are *isotropic* in momentum dependence in the frame of the beam (Sec. IV.A), to *anisotropic* distributions in which the momentum spreads are different in the axial and transverse directions (Sec. IV.B). A density inversion theorem is demonstrated (Sec. IV.C) for the class of anistropic distributions considered in Sec. IV.B, and a general radial force constraint condition is derived (Sec. IV.D) that relates the mean-square radius $\langle r^2 \rangle$ of the beam to the strength of the focusing field, the transverse thermal emittance ϵ_{th}, and other system parameters. As a general remark, for a uniform focusing field, it is found that there is enormous latitude in the choice of equilibrium distribution function. In Sec. V, introducing the axial coordinate $s = z$, we make use of the kinetic formalism based on the nonlinear Vlasov-Maxwell equations to investigate intense beam propagation in a periodic solenoidal field $B_z(s + S) = B_z(s)$, in which case the properties of the beam

are modulated as a function of s by the periodic focusing field. Following a transformation of the nonlinear Vlasov equation to a frame of reference rotating at the Larmor frequency $\Omega_L(s) = -Z_i e B_z(s)/2\gamma_b mc$ (Sec. V.A), the description is further simplified (Sec. V.B) by assuming azimuthal symmetry ($\partial/\partial\tilde{\theta} = 0$), in which case the canonical angular momentum $\tilde{P}_\theta$ is an exact single-particle constant of the motion. As an application of the general formalism developed in Sec. V.B, we consider the specific example (Sec. V.C) of a periodically focused rigid-rotor Vlasov equilibrium with step-function radial density profile and average azimuthal motion of the beam corresponding to a rigid rotation (in the Larmor frame) about the axis of symmetry. A wide range of beam properties are calculated, such as the average flow velocity, transverse temperature profile, and transverse thermal emittance. Finally, the method of characteristics is summarized (Sec. V.D) as an approach for solving the nonlinear Vlasov equation for intense beam systems with periodic focusing.

As a general remark, based on the analysis in Secs. II-V, a Vlasov-Mawell description of intense nonneutral beam propagation through a periodic solenoidal focusing field $\vec{B}^{sol}(\vec{x})$ is remarkably tractable and rich in physics content.

II. THEORETICAL MODEL AND ASSUMPTIONS

In the present analysis, we consider an intense nonneutral ion beam propagating in the z-direction with characteristic axial velocity $\beta_b c$ and kinematic energy $\gamma_b mc^2$ through a periodic focusing solenoidal magnetic field $\vec{B}^{sol}(\vec{x})$. In the electrostatic approximation, the distribution function $f_b(\vec{x},\vec{p},t)$ of the beam ions in the six-dimensional phase space $(\vec{x},\vec{p})$ evolves according to the nonlinear Vlasov equation [1,26]

$$\frac{\partial f_b}{\partial t} + \vec{v}\cdot\frac{\partial f_b}{\partial \vec{x}} + Z_i e\left[-\nabla\phi^s + \frac{1}{c}\vec{v}\times(\vec{B}^{sol}+\vec{B}^s)\right]\cdot\frac{\partial f_b}{\partial \vec{p}} = 0. \tag{1}$$

Here $\vec{E}^s(\vec{x},t) = -\nabla\phi^s(\vec{x},t)$ is the self-electric field due to the beam space charge, and $\vec{B}^s(x,t) = \nabla\times\vec{A}^s(\vec{x},t)$ is the self-magnetic field due to the current carried by the beam ions. Note in Eq. (1) that the inductive electric field, $-c^{-1}\partial\vec{A}^s/\partial t$, has been assumed to be negligibly small in comparison with $-\nabla\phi^s$. In Eq. (1), $+Z_i e$ is the ion charge, c is the speed of light in *vacuo*, and the mechanical momentum $\vec{p}$ and kinematic energy γmc^2 are related by

$$\begin{aligned} \vec{p} &= \gamma m\vec{v}, \\ \gamma mc^2 &= c(m^2c^2+\vec{p}^2)^{1/2}, \end{aligned} \tag{2}$$

where γ is the relativistic mass factor, and m is the ion rest mass. Of course the self-field potentials, $\phi^s(\vec{x},t)$ and $\vec{A}^s(\vec{x},t)$, occurring in Eq. (1) are determined self-consistently in terms of the beam charge density and axial current density from the Maxwell equations

$$\begin{aligned} \nabla^2\phi^s(\vec{x},t) &= -4\pi Z_i e n_b(\vec{x},t) \\ &= -4\pi Z_i e\int d^3\vec{p} f_b(\vec{x},\vec{p},t), \end{aligned} \tag{3}$$

and

$$\begin{aligned} \nabla^2\vec{A}^s(\vec{x},t) &= -4\pi Z_i e n_b(\vec{x},t)\vec{V}_b(\vec{x},t) \\ &= -4\pi Z_i e\int d^3\vec{p}\vec{v} f_b(\vec{x},\vec{p},t), \end{aligned} \tag{4}$$

where $n_b(\vec{x},t)$ is the density of beam ions and $\vec{V}_b(\vec{x},t)$ is the flow velocity. In the regime of practical interest, it is assumed that the characteristic beam radius r_b is small in comparison

with the axial periodicity length S of the focusing field, i.e.,

$$r_b^2 \ll S^2. \tag{5}$$

In this case, the applied solenoidal magnetic field can be expressed to good approximation in the beam interior as $\vec{B}^{sol}(\vec{x}) = \nabla \times \vec{A}_\perp^{sol}(\vec{x})$, where [25]

$$\vec{A}_\perp^{sol}(\vec{x}) = \frac{1}{2} B_z(z)(-y\vec{e}_x + x\vec{e}_y), \tag{6}$$

and

$$\vec{B}^{sol}(\vec{x}) = B_z(z)\vec{e}_z - \frac{1}{2} B_z'(z)(x\vec{e}_x + y\vec{e}_y). \tag{7}$$

Here, $\vec{e}_x$ and $\vec{e}_y$ are unit Cartesian vectors perpendicular to the beam propagation direction ($\vec{e}_z$), $x\vec{e}_x + y\vec{e}_y$ is the transverse displacement from the beam axis at $(x, y) = (0, 0)$, the superscript 'prime' denotes d/dz with $B_z'(z) = dB_z(z)/dz$, and the axial component of magnetic field satisfies

$$B_z(z + S) = B_z(z), \tag{8}$$

where S is the axial period of the focusing field.

Consistent with the *thin-beam approximation* in Eq. (5), the distribution of the beam ions described by $f_b(\vec{x}, \vec{p}, t)$ is assumed to have large momentum directed predominantly in the axial direction and centered about $p_z = \gamma_b m \beta_b c$, with a narrow spread in momentum satisfying

$$p_x^2,\ p_y^2,\ (p_z - \gamma_b m\beta_b c)^2,\ (p_z - \gamma_b m\beta_b c)\gamma_b m\beta_b c \ll \gamma_b^2 m^2 c^2. \tag{9}$$

Here, $\gamma_b = (1-\beta_b^2)^{-1/2}$ is the relativistic mass factor, and $\gamma_b mc^2$ is the characteristic kinematic energy associated with the axial motion. Also consistent with Eq. (9) and the thin beam approximation in Eq. (5), we neglect the self-magnetic field produced by transverse beam currents in Eq. (4) and approximate $\vec{A}^s(\vec{x}, t) = A_z^s(\vec{x}, t)\vec{e}_z$. Treating the axial variation of beam properties as a function of z as weak in comparison with transverse spatial variations, Eqs. (3) and (4) can then be approximated by [see also Eq. (5)]

$$\nabla_\perp^2 \phi^s = -4\pi Z_i e \int d^3\vec{p} f_b(\vec{x},\vec{p},t), \tag{10}$$

and

$$\nabla_\perp^2 A_z^s = -4\pi Z_i e \int d^3\vec{p} v_z f_b(\vec{x},\vec{p},t), \tag{11}$$

where $\nabla_\perp^2 = \partial^2/\partial x^2 + \partial^2/\partial y^2$. Finally, the present analysis also assumes that

$$\frac{\nu}{\gamma_b} \equiv N_b Z_i^2 e^2/\gamma_b m c^2 \ll 1, \tag{12}$$

where ν is Budker's parameter and $N_b = \int dxdy n_b = \int dxdy \int d^3\vec{p} f_b$ is the number of ions per unit axial length of the beam. Equation (12) is equivalent to the condition that $2c/\omega_{pb} \gg r_b$, where c/ω_{pb} is the collisionless skin depth, and $\omega_{pb} = (4\pi Z_i^2 e^2 n_b/\gamma_b m)^{1/2}$ is the characteristic ion plasma frequency. Equation (12) assures that the self-field intensity is sufficiently weak that

$$\left|\frac{Z_i e\phi^s}{\gamma_b m c^2}\right| \ll 1, \quad \left|\frac{Z_i e A_z^s}{\gamma_b m c^2}\right| \ll \beta_b. \tag{13}$$

However, the analysis does permit the self-field potential energy $Z_i e\phi^s$ to be comparable in magnitude with the transverse kinetic energy $(p_x^2 + p_y^2)/2\gamma_b m$ of a beam ion.

To summarize, the subsequent analysis is based on the nonlinear Vlasov-Maxwell equations (1), (10) and (11), supplemented by the definitions of $\vec{B}^{sol}$ and $\vec{A}_\perp^{sol}$ in Eqs. (6) and (7), and the thin-beam approximation as described by the inequalities in Eqs. (5), (9) and (12).

III. NONLINEAR VLASOV EQUATION AND SINGLE-PARTILCE EQUATIONS OF MOTION

We now simplify the single-particle equations of motion (Sec. III.A) and the nonlinear Vlasov-Maxwell equations (Sec. III.B) for beam propagation through a periodic focusing solenoidal field in the context of the theoretical model and assumptions summarized in Sec. II. Particular emphasis will be placed on the case where the beam distribution function and field configuration are azimuthally symmetric ($\partial/\partial\theta = 0$).

A. Single-Particle Equations of Motion

The Hamiltonian for particle motion in the field configuration described in Sec. II can be expressed as

$$\begin{aligned} H &= \gamma mc^2 + Z_i e\phi^s \\ &= c(m^2c^2 + \vec{p}^{\,2})^{1/2} + Z_i e\phi^s. \end{aligned} \tag{14}$$

Here, the mechanical momentum $\vec{p}$ is related to the generalized canonical momentum $\vec{P}$ by $\vec{p} = \vec{P} - (Z_i e/c)\vec{A}$, where $\vec{A} = \vec{A}_\perp^{sol} + A_z^s \vec{e}_z$ is the vector potential defined in Eqs. (6) and (11). Substituting in Eq. (14) then gives

$$H = c\left[m^2c^2 + \left(P_z - \frac{Z_i e}{c}A_z^s\right)^2 + \left(P_x - \frac{Z_i e}{c}A_x^{sol}\right)^2 + \left(P_y - \frac{Z_i e}{c}A_y^{sol}\right)^2\right]^{1/2} + Z_i e\phi^s. \tag{15}$$

The single-particle equations of motion are given by

$$\frac{d\vec{x}}{dt} = \frac{\partial H}{\partial \vec{P}}, \tag{16}$$

$$\frac{d\vec{P}}{dt} = -\frac{\partial H}{\partial \vec{x}}. \tag{17}$$

Substituting Eq. (15) into Eqs. (16) and (17), we obtain the expected result

$$\frac{d\vec{x}}{dt} = \frac{\vec{p}}{\gamma m}, \tag{18}$$

$$\frac{d\vec{p}}{dt} = Z_i e\left[-\nabla\phi^s + \frac{\vec{v}}{c} \times \nabla \times (\vec{A}_\perp^{sol} + A_z^s \vec{e}_z)\right]. \tag{19}$$

In obtaining Eqs. (18) and (19), use has been made of $d\vec{P}/dt = d\vec{p}/dt + (Z_i e/c)d\vec{A}/dt$, where $d\vec{A}/dt = \partial\vec{A}/\partial t + (\vec{v}\cdot\nabla)\vec{A}$. Furthermore, consistent with the electrostatic approximation made in Sec. II, we have neglected $c^{-1}\partial\vec{A}^s/\partial t$ in comparison with $\nabla\phi^s$ in Eqs. (18) and (19).

Comparing Eq. (1) with Eqs. (18) and (19), it is important to note that the orbit equations (18) and (19) are the characteristics of the nonlinear Vlasov equation (1). That is, Eq. (1) can be expressed in the equivalent form

$$\frac{df_b}{dt} = 0, \tag{20}$$

where d/dt denotes the total time derivative following the particle motion in Eqs. (18) and (19). From Eq. (14) we also find

$$\frac{dH}{dt} = \frac{\vec{p}}{\gamma m}\cdot\frac{d\vec{p}}{dt} + Z_i e\left(\vec{v}\cdot\nabla\phi^s + \frac{\partial\phi^s}{\partial t}\right) = Z_i e\frac{\partial\phi^s}{\partial t}, \tag{21}$$

where use has been made of Eqs. (18) and (19). That is, whenever $\phi^s(x,y,z,t)$ is time-stationary ($\partial/\partial t = 0$), the Hamiltonian H is an exact single-particle constant of the motion ($dH/dt = 0$). The canonical angular momentum P_θ defined by

$$P_\theta = xP_y - yP_x = x\left(p_y + \frac{Z_i e}{c}A_y^{sol}\right) - y\left(p_x + \frac{Z_i e}{c}A_x^{sol}\right) = xp_y - yp_x + \frac{Z_i e}{2c}(x^2+y^2)B_z(z) \tag{22}$$

is also a quantity of considerable physical importance. Here, $A_y^{sol} = (x/2)B_z(z)$ and $A_x^{sol} = -(y/2)B_z(z)$ follow from Eq. (6). From Eqs. (18), (19) and (22) it is readily shown that

$$\frac{dP_\theta}{dt} = -Z_i e\left(x\frac{\partial}{\partial y} - y\frac{\partial}{\partial x}\right)\phi^s. \tag{23}$$

Therefore, in circumstances where the beam distribution function and field profiles are azimuthally symmetric about the beam axis ($\partial\phi/\partial\theta = 0$), it follows from Eq. (23) that the canonical angular momentum P_θ is an exact single-particle constant of the motion ($dP_\theta/dt = 0$). If the electrostatic potential is independent of time *and* azimuthally symmetric, i.e., $\partial\phi^s/\partial t = 0$ and $\partial\phi^s/\partial\theta = 0$, then $\phi^s = \phi^s(r,z)$, and both H and P_θ are exact single-particle constants of the motion. In this case the *equilibrium* beam distribution function ($\partial f_b^0/\partial t = 0$) can be constructed from the single-particle consistants of the motion H

and P_θ with $f_b^0 = f_b^0(H, P_\theta)$. This follows because

$$\frac{d}{dt} f_b^0(H, P_\theta) = \frac{dH}{dt} \cdot \frac{\partial f_b^0}{\partial H} + \frac{dP_\theta}{dt} \cdot \frac{\partial f_b^0}{\partial P_\theta} = 0 \tag{24}$$

whenever $dH/dt = 0 = dP_\theta/dt$.

A further important quantity characterizing the single-particle motion is the axial canonical momentum $P_z = p_z + (Z_i e/c)A_z^s$. Neglecting $\partial A_z^s/\partial t$ consistent with the electrostatic approximation in Sec. II, some straightforward algebra that makes use of Eqs. (18) and (19) gives

$$\frac{dP_z}{dt} = \frac{d}{dt}\left(p_z + \frac{Z_i e}{c} A_z^s\right) = Z_i e \frac{\partial}{\partial z}\left[-\phi^s + \frac{1}{c} v_z A_z^s + \frac{1}{2c} B_z(z)(x v_y - y v_x)\right], \tag{25}$$

where use has been made of Eqs. (6) and (7), and $dA_z^s/dt = (\vec{v}_\perp \cdot \partial/\partial \vec{x}_\perp) A_z^s + v_z \partial A_z^s/\partial z$ with $B_y^s = -\partial A_z^s/\partial x$ and $B_x^s = \partial A_z^s/\partial y$. In circumstances where the beam properties are axially uniform with $\partial \phi^s/\partial z = 0 = \partial A_z^s/\partial z$, and the solenoidal field is uniform with $B_z(z) = B_0 =$ const. (independent of z), then $\partial/\partial z = 0$ on the right-hand side of Eq. (25) and it follows trivially that the axial canonical momentum P_z is an exact single-particle constant of the motion ($dP_z/dt = 0$). Note that this does *not* imply that the axial mechanical momentum is conserved, because $dp_z/dt = (Z_i e/c)(\vec{v} \times \vec{B}^s)_z \neq 0$ generally follows from Eq. (25) even when $\partial/\partial z = 0$.

To summarize, if field quantities are time independent ($\partial/\partial t = 0$), azimuthally symmetric ($\partial/\partial \theta = 0$), *and* independent of z ($\partial/\partial z = 0$), then H, P_θ, and P_z are all single-particle constants of the motion, and the *equilibrium* beam distribution function (with $\partial f_b^0/\partial t = 0$) can be constructed from H, P_θ, and P_z with $f_b^0 = f_b^0(H, P_\theta, P_z)$. This follows because

$$\frac{d}{dt} f_b^0(H, P_\theta, P_z) = \frac{dH}{dt} \cdot \frac{\partial f_b^0}{\partial H} + \frac{dP_\theta}{dt} \cdot \frac{\partial f_b^0}{\partial P_\theta} + \frac{dP_z}{dt} \cdot \frac{\partial f_b^0}{\partial P_z} = 0 \tag{26}$$

whenever $dH/dt = dP_\theta/dt = dP_z/dt = 0$.

A further point is evident from Eq. (25). In circumstances where the periodic focusing field $B_z(z)$ produces a *slow* axial modulation of ϕ^s and A_z^s, then the z-variation on the right-hand side of Eq. (25) is *weak* in comparison with spatial variations perpendicular to

the beam propagation direction. That is, $|\partial/\partial z| \ll |\partial/\partial x|$, $|\partial/\partial y|$, consistent with the thin-beam approximation in Sec. II. It then follows from Eq. (25) and the perpendicular components of Eqs. (18) and (19) that the change in p_z (or P_z) is small in comparison with changes in the transverse momenta p_x and p_y. Specifically, a simple estimate shows that the variation in axial momentum Δp_z over one lattice period S is smaller than Δp_x or Δp_y by a factor of order of $r_b/S \ll 1$. Although the axial canonical momentum P_z is not an exact constant of the motion when there is a slow variation in the focusing field $B_z(z)$, it is clear from Eq. (25) that the changes in P_z are small.

The dynamical equations are further simplified in Sec. III.B in the context of the thin-beam approximation and the assumption of narrow spread in axial momentum summarized in Sec. II. For future reference, throughout the remainder of this article we make use of a simple relation between the self-field vector potential A_z^s and the electrostatic potential ϕ^s calculated from Eqs. (10) and (11). Because the distribution of beam particles is assumed to have axial momentum strongly peaked around $p_z = \gamma_b m \beta_b c$, an important consequence of Eqs. (9), (11) and (13) is that the axial current density $Z_i e \int d^3\vec{p} v_z f_b$ occurring in Eq. (11) is given to good approximation by

$$J_z = Z_i e \int d^3\vec{p} v_z f_b \cong Z_i e \beta_b c \int d^3\vec{p} f_b, \tag{27}$$

where $n_b = \int d^3\vec{p} f_b$ is the ion density. Comparing Eqs. (10) and (11), and making use of Eq. (27) we conclude that A_z^s can be approximated by

$$A_z^s = \beta_b \phi^s \tag{28}$$

in the present analysis.

B. Alternative Hamiltonian Formulation and Nonlinear Vlasov Equation

The discussion in Sec. III.A has been a fairly general treatment of the particle motion based on the relativistic Hamiltonian in Eqs. (14) and (15). We now examine the particle dynamics making explicit use of the thin-beam approximations in Eqs. (5) and (13), and

the assumption of narrow momentum spread about $p_z = \gamma_b m \beta_b c$ in Eq. (9). This can be done by making direct use of the form of the Hamiltonian H in Eqs. (14) and (15), and the equations of motion in Eqs. (16) and (17) (see Appendix A). Alternatively, we adopt here the approach often used in accelerator physics [2] and transform from the canonical conjugate variables (x, P_x), (y, P_y) and (z, P_z) to new canonical conjugate variables (x, P_x), (y, P_y) and $(t, -H)$. This is done by making use of Eq. (15) to eliminate the canonical momentum P_z in the axial direction, which is the principle direction of beam propagation, in favor of the Hamiltonian H defined in Eq. (15). Furthermore, as is customary in accelerator physics, we denote by s the configuration space coordinate measured along the principle direction of beam propagation, i.e.,

$$s = z. \tag{29}$$

We assume that all particles are moving in the forward direction with $p_z = P_z - (Z_i e/c)A_z^s > 0$, and make use Eq. (15) to introduce a new Hamiltonian $\mathcal{H}(x, P_x; y, P_y; t, -H; s)$ defined by

$$\mathcal{H}(x, P_x; y, P_y; t, -H; s) = -P_z(x, P_x; y, P_y; t, -H; s). \tag{30}$$

Solving Eq. (15) for $(P_z - Z_i e A_z^s/c)^2$ and taking the positive square root readily gives

$$\mathcal{H} = -\left[\left(\frac{H}{c} - \frac{Z_i e}{c}\phi^s\right)^2 - m^2c^2 - \left(P_x - \frac{Z_i e}{c}A_x^{sol}\right)^2 - \left(P_y - \frac{Z_i e}{c}A_y^{sol}\right)^2\right]^{1/2} - \frac{Z_i e}{c}A_z^s, \tag{31}$$

where $A_z^s = \beta_b \phi^s$, and A_x^{sol} and A_y^{sol} are defined in Eq. (6). In terms of the new Hamiltonian $\mathcal{H}$, it is readily shown that the equations of motion are given by

$$\begin{aligned}
\frac{dx}{ds} &= \frac{\partial \mathcal{H}}{\partial P_x}, \quad \frac{dP_x}{ds} = -\frac{\partial \mathcal{H}}{\partial x}, \\
\frac{dy}{ds} &= \frac{\partial \mathcal{H}}{\partial P_y}, \quad \frac{dP_y}{ds} = -\frac{\partial \mathcal{H}}{\partial y}, \\
\frac{dt}{ds} &= \frac{\partial \mathcal{H}}{\partial(-H)}, \quad \frac{d(-H)}{ds} = -\frac{\partial \mathcal{H}}{\partial t}.
\end{aligned} \tag{32}$$

The quantity $dt/ds = dt/dz$ in Eq. (32) will be recognized as v_z^{-1}, where v_z is the axial velocity. It will become apparent in the subsequent analysis that several simplications occur

when the Hamiltonian representation in Eq. (31) is used, particularly when system properties are time-stationary ($\partial/\partial t = 0$).

Treating s as the dynamical variable following the particle motion, the nonlinear Vlasov equation for the distribution function $f_b(x, P_x; y, P_y; t, -H; s)$ in the new variables can be expressed as $df_b/ds = 0$, or equivalently,

$$\frac{\partial f_b}{\partial s} + t'\frac{\partial f_b}{\partial t} + x'\frac{\partial f_b}{\partial x} + y'\frac{\partial f_b}{\partial y} + P_x'\frac{\partial f_b}{\partial P_x} + P_y'\frac{\partial f_b}{\partial P_y} + (-H')\frac{\partial f_b}{\partial(-H)} = 0. \tag{33}$$

Here, a superscript 'prime' denotes d/ds, e.g., $t' = dt/ds$, $x' = dx/ds$, etc. The nonlinear Vlasov equation (33) is *fully equivalent* to Eq. (1) and the analysis based on the dynamical variables used in Sec. III.A. What is apparent from Eqs. (32) and (33), however, are the simplifications that occur naturally when *equilibrium* beam properties are considered, corresponding to $\partial/\partial t = 0$. Treating $\phi^s(x, y, s, t)$ as time-independent ($\partial\phi^s/\partial t = 0$) in the subsequent analysis, it follows from Eqs. (28) and (31) that $\mathcal{H}$ does not depend explicitly on t. Therefore $\partial\mathcal{H}/\partial t = 0$, and

$$\frac{d}{ds}(-H) = 0 \tag{34}$$

follows from Eq. (32). Furthermore, the corresponding time-independent equilibrium distribution function $f_b = f_b^0(x, P_x; y, P_y; -H, s)$ necessarily satisfies $\partial f_b/\partial t = 0$ in Eq. (33). Setting $-H' = -dH/ds = 0$ and $\partial f_b/\partial t = 0$ in Eq. (33) then gives

$$\frac{\partial f_b^0}{\partial s} + x'\frac{\partial f_b^0}{\partial x} + y'\frac{\partial f_b^0}{\partial y} + P_x'\frac{\partial f_b^0}{\partial P_x} + P_y'\frac{\partial f_b^0}{\partial P_y} = 0 \tag{35}$$

for the evolution of $f_b^0(x, P_x; y, P_y; -H, s)$. Here, ϕ^s and $A_z^s = \beta_b\phi^s$ are determined self-consistently in terms of f_b^0 from Poisson's equation (10). Moreover, the characteristics x', y', P_x' and P_y' of the nonlinear Vlasov equation (35) are determined from Eq. (32). Note also in Eq. (35) that the energy constant of the motion, $-H$, occurs parametrically as a variable in the argument of the distribution function f_b^0.

We now simplify Eqs. (31) and (32) and the characteristics of the Vlasov equation (35) by making use of the thin-beam approximation in Eqs. (5) and (13), and the assumption

of narrow momentum spread about $p_z = \gamma_b m \beta_b c$ in Eq. (9). In this regard, we define the effective kinematic momentum of a beam particle by

$$p_b = (H^2/c^2 - m^2c^2)^{1/2} \tag{36}$$

and denote $p_b = \gamma_b m \beta_b c$, where $\gamma_b mc^2 = H$ and $\gamma_b = (1 - \beta_b^2)^{-1/2}$. While Eq. (36) implies that p_b, γ_b and β_b are (known) functions of H, keep in mind that the distribution of beam particles has a very narrow spread in momentum and energy. Making use of Eqs. (9) and (13), and assuming p_x^2, $p_y^2 \ll p_b^2$, we Taylor expand Eq. (31) to quadratic order in the transverse canonical momenta, and retain terms linear in the electrostatic potential ϕ^s. Equation (31) can then be approximated by

$$\mathcal{H} = -p_b + \frac{1}{2p_b}\left[\left(P_x - \frac{Z_i e}{c}A_x^{sol}\right)^2 + \left(P_y - \frac{Z_i e}{c}A_y^{sol}\right)^2\right] + \frac{HZ_i e}{p_b c^2}\phi^s - \frac{Z_i e}{c}A_z^s, \tag{37}$$

where $p_b(H) = \gamma_b m \beta_b c$ is defined in Eq. (36) and $H = \gamma_b mc^2$. Making use of $A_z^s = \beta_b \phi^s$ from Eq. (28), the expression for $\mathcal{H}$ in Eq. (37) becomes

$$\mathcal{H} = -\gamma_b m \beta_b c + \frac{1}{2\gamma_b m \beta_b c}\left[\left(P_x - \frac{Z_i e}{c}A_x^{sol}\right)^2 + \left(P_y - \frac{Z_i e}{c}A_y^{sol}\right)^2\right] + \frac{Z_i e}{\gamma_b^2 \beta_b c}\phi^s, \tag{38}$$

where use has been made of $(1-\beta_b^2)\phi^s = \phi^s/\gamma_b^2$, and $\phi^s(x,y,s)$ is determined self-consistently in terms of f_b^0 from Poisson's equation (10).

Solution to the nonlinear Vlasov equation (35) requires determination of the transverse orbits $x(s)$ and $y(s)$ from Eq. (32). To the level of accuracy of the expression for $\mathcal{H}$ in Eq. (38), we readily find from $dx/ds = \partial\mathcal{H}/\partial P_x$ and $dP_x/ds = -\partial\mathcal{H}/\partial x$ that

$$\frac{dx}{ds} = \frac{1}{\gamma_b m \beta_b c}\left(P_x - \frac{Z_i e}{c}A_x^{sol}\right) \equiv \frac{p_x}{\gamma_b m \beta_b c}, \tag{39}$$

$$\frac{dP_x}{ds} \equiv \frac{d}{ds}\left(p_x + \frac{Z_i e}{c}A_x^{sol}\right) = -\frac{Z_i e}{\gamma_b^2 \beta_b c}\frac{\partial \phi^s}{\partial x} + \frac{Z_i e B_z(s)}{2\gamma_b m \beta_b c^2}\left(P_y - \frac{Z_i e}{c}A_y^{sol}\right), \tag{40}$$

where $A_x^{sol}(x,y,s) = -yB_z(s)/2$ and $A_y^{sol}(x,y,s) = xB_z(s)/2$, and use has been made of $\partial B_y^{sol}/\partial x = B_z(s)/2$. Similarly, from Eqs. (32) and (38), the y-motion is determined from

$$\frac{dy}{ds} = \frac{1}{\gamma_b m \beta_b c}\left(P_y - \frac{Z_i e}{c}A_y^{sol}\right) \equiv \frac{p_y}{\gamma_b m \beta_b c}, \tag{41}$$

$$\frac{dP_y}{ds} \equiv \frac{d}{ds}\left(p_y + \frac{Z_i e}{c} A_y^{sol}\right) = -\frac{Z_i e}{\gamma_b^2 \beta_b c}\frac{\partial \phi^s}{\partial y} - \frac{Z_i e B_z(s)}{2\gamma_b m \beta_b c^2}\left(P_x - \frac{Z_i e}{c} A_x^{sol}\right). \tag{42}$$

We introduce the normalized Larmor frequency $\sqrt{\kappa_z(s)}$ and normalized electrostatic potential $\psi(x,y,s)$ defined by

$$\sqrt{\kappa_z(s)} = \frac{Z_i e B_z(s)}{2\gamma_b m \beta_b c^2}, \tag{43}$$

$$\psi(x,y,s) = \frac{Z_i e}{\gamma_b^3 m \beta_b^2 c^2}\phi^s(x,y,s). \tag{44}$$

Substituting $p_x = \gamma_b m \beta_b c dx/ds$ into Eq. (40) and $p_y = \gamma_b m \beta_b c dy/ds$ into Eq. (42) then gives the orbit equations for $x(s)$ and $y(s)$,

$$\frac{d^2x}{ds^2} - 2\sqrt{\kappa_z(s)}\frac{dy}{ds} - y\frac{d}{ds}\sqrt{\kappa_z(s)} = -\frac{\partial \psi}{\partial x}, \tag{45}$$

$$\frac{d^2y}{ds^2} + 2\sqrt{\kappa_z(s)}\frac{dx}{ds} + x\frac{d}{ds}\sqrt{\kappa_z(s)} = -\frac{\partial \psi}{\partial y}, \tag{46}$$

In Eqs. (45) and (46), $\psi(x,y,s)$ is determined in terms of the density of particles $n_b(x,y,s) = \int d^3\vec{p} f_b^0$ from Poisson's equation (10), which can be expressed as

$$\left(\frac{\partial^2}{\partial x^2} + \frac{\partial^2}{\partial y^2}\right)\psi = -\frac{4\pi Z_i^2 e^2}{\gamma_b^3 m \beta_b^2 c^2}\int d^3\vec{p} f_b^0. \tag{47}$$

As a further point, in circumstances where f_b^0 and ψ are azimuthally symmetric about the beam axis and depend on x and y only through the radial coordinate $r = (x^2+y^2)^{1/2}$, it follows that $\partial f_b^0/\partial\theta = 0 = \partial\psi/\partial\theta$, where $\partial/\partial\theta = x\partial/\partial y - y\partial/\partial x$. Equations (45) and (46) then give

$$\frac{dP_\theta}{ds} = \frac{d}{ds}(xP_y - yP_x) = 0, \tag{48}$$

corresponding to conservation of canonical angular momentum P_θ. Here, P_θ can be expressed as

$$(\gamma_b m \beta_b c)^{-1} P_\theta = x\frac{dy}{ds} - y\frac{dx}{ds} + \sqrt{\kappa_z(s)}(x^2+y^2), \tag{49}$$

which should be compared with Eq. (22). Therefore, as expected, whenever $\partial/\partial\theta = 0$ the canonical angular momentum is an exact single-particle constant of the motion ($dP_\theta/ds = 0$). We conclude that if field quantities are both time independent ($\partial/\partial t = 0$) and azimuthally

symmetric ($\partial/\partial\theta = 0$), then H and P_θ are single-particle constants of the motion. In this case, the equilibrium distribution function ($\partial f_b^0/\partial s = 0$) can be constructed from $-H$ and P_θ with $f_b^0 = f_b^0(-H, P_\theta)$. This follows because

$$\frac{d}{ds} f_b^0(-H, P_\theta) = \frac{d(-H)}{ds}\frac{\partial f_b^0}{\partial(-H)} + \frac{dP_\theta}{ds}\frac{\partial f_b^0}{\partial P_\theta} = 0 \tag{50}$$

whenever $d(-H)/ds = 0 = dP_\theta/ds$. Of course, if other single-particle constants of the motion C_j with $dC_j/ds = 0$ follow from Eqs. (45) and (46), then $f_b^0 = f_b^0(-H, P_\theta, C_j)$ necessarily solves the nonlinear Vlasov equation (35) with $(d/ds)f_b^0(-H, P_\theta, C_j) = 0$, where d/ds denotes the total derivative with respect to s in Eq. (35) (see Sec. V).

In Sec. V, we will make use of Eqs. (35) and (45)-(47) to investigate periodically focused beam equilibria for a solenoidal focusing field described by Eq. (7) with $B_z(s+S) = B_z(s)$. For future reference, it is convenent to transform the transverse dynamical equations (45) and (46) to a frame of reference rotating about the beam axis at the local Larmor frequency defined in normalized units by $\Omega_L(s) = -\sqrt{\kappa_z(s)} = -Z_i e B_z(s)/2\gamma_b m\beta_b c^2$. We introduce the accumulated phase of rotation from s_0 to s defined by $\theta_L(s) = -\int_{s_0}^{s} ds\sqrt{\kappa_z(s)}$, where $d\theta_L/ds = \Omega_L$. Then the transverse orbits, $\tilde{x}(s)$ and $\tilde{y}(s)$, in the rotating frame, are related to $x(s)$ and $y(s)$ in the laboratory frame by

$$\begin{aligned} x(s) &= \tilde{x}(s)\cos\theta_L(s) - \tilde{y}(s)\sin\theta_L(s), \\ y(s) &= \tilde{x}(s)\sin\theta_L(s) + \tilde{y}(s)\cos\theta_L(s). \end{aligned} \tag{51}$$

We further assume that the beam equilibrium properties are azimuthally symmetric ($\partial/\partial\theta = 0$), so that $\psi(x, y, s) = \psi(r, s)$ in Eqs. (45) and (46), where $r = (x^2 + y^2)^{1/2} = (\tilde{x}^2 + \tilde{y}^2)^{1/2}$. In this case,

$$\frac{\partial\psi}{\partial x} = \frac{x}{r}\frac{\partial\psi}{\partial r}, \quad \frac{\partial\psi}{\partial y} = \frac{y}{r}\frac{\partial\psi}{\partial r}, \tag{52}$$

where $\psi(r, s)$ is determined in terms of $n_b^0(r, s) = \int d^3\vec{p} f_b^0$ from Poisson's equation (47), which can be expressed as

$$\frac{1}{r}\frac{\partial}{\partial r} r \frac{\partial}{\partial r}\psi = -\frac{4\pi Z_i^2 e^2}{\gamma_b^3 m\beta_b^2 c^2}\int d^3\vec{p} f_b^0. \tag{53}$$

Substituting Eq. (52) into Eqs. (45) and (46), and making use of Eq. (51), it is readily shown that the transverse orbits $\tilde{x}(s)$ and $\tilde{y}(s)$ in the Larmor frame solve the dynamical equations

$$\frac{d^2\tilde{x}}{ds^2} + \left[\kappa_z(s) + \frac{1}{r}\frac{\partial\psi}{\partial r}\right]\tilde{x} = 0, \tag{54}$$

$$\frac{d^2\tilde{y}}{ds^2} + \left[\kappa_z(s) + \frac{1}{r}\frac{\partial\psi}{\partial r}\right]\tilde{y} = 0, \tag{55}$$

where $\kappa_z(s) = [Z_i e B_z(s)/2\gamma_b m\beta_b c^2]^2$, and $\psi(r,s)$ satisfies Poisson's equation (53) with $r = (\tilde{x}^2+\tilde{y}^2)^{1/2}$. Note from Eqs. (54) and (55) that the dynamical equations for $\tilde{x}(s)$ and $\tilde{y}(s)$ are identical in structure. In the laboratory frame, the x- and y-motions are naturally coupled by the magnetic force contributions in Eqs. (45) and (46). On the other hand, in the Larmor frame, it is evident from Eqs. (54) and (55) that the magnetic forces in the $\tilde{x}$- and $\tilde{y}$-directions are *decoupled* and *restoring* (because $\kappa_z > 0$), with $F_{\tilde{x}}^{magn} = -\kappa_z\tilde{x}$ and $F_{\tilde{y}}^{magn} = -\kappa_z\tilde{y}$. The $\tilde{x}$- and $\tilde{y}$-motions determined from Eqs. (54) and (55) are generally coupled through the electric field contribution proportional to $r^{-1}\partial\psi/\partial r$, where $r = (\tilde{x}^2 + \tilde{y}^2)^{1/2}$. This is true except for the special case where the beam density is uniform in the beam interior, in which case ψ is proportional to r^2, e.g., when f_b^0 corresponds to the Kapchinskij-Vladimirskij distribution function [24]. Conservation of canonical angular momentum also takes on a particularly simple form in the Larmor frame. For $\partial/\partial\theta = 0$, we note that

$$\frac{d}{ds}\left(\tilde{x}\frac{d\tilde{y}}{ds} - \tilde{y}\frac{d\tilde{x}}{ds}\right) = 0 \tag{56}$$

follows trivially from Eqs. (54) and (55). From (56), conservation of canonical angular momentum in the Larmor frame then becomes $dP_\Theta/ds = 0$, where

$$(\gamma_b m\beta_b c)^{-1} P_\Theta = \tilde{x}\frac{d\tilde{y}}{ds} - \tilde{y}\frac{d\tilde{x}}{ds}. \tag{57}$$

Some of the simplifications evident in Eqs. (54) and (55) from transforming to the Larmor frame will be utilized, as appropriate, in Sec. V.

IV. INTENSE BEAM EQUILIBRIA IN A UNIFORM SOLENOIDAL FOCUSING FIELD

In this section we consider intense ion beam equilibria ($\partial/\partial t = 0$) in the special circumstances where the applied solenoidal field $\vec{B}^{sol}(\vec{x})$ is a uniform focusing field with

$$B_z(s) = B_0 = \text{ const.} \tag{58}$$

It is further assumed that all equilibrium properties are azimuthally symmetric ($\partial/\partial\theta = 0$) about the beam axis and independent of axial coordinate ($\partial/\partial z = 0$). While limited in scope because $\partial/\partial\theta = \partial/\partial z = 0$ is assumed, we will find that the analysis in this section permits a broad range of beam equilibria f_b^0 to be considered [26], with correpondingly different equilibrium profiles for the beam density, pressure, etc., as well as different stability properties depending on the choice of f_b^0. In this regard, the analysis in this section is best viewed as a *smooth-beam approximation* to a periodic solenoidal focusing system, which provides valuable insights into the properties of intense nonneutral ion beams and can be used to benchmark numerical simulation codes and understand laboratory experiments.

Using the notation and formalism developed in Sec. III.A, for $\partial/\partial\theta = 0$ and $\partial/\partial z = 0$, it follows from Eqs. (23) and (25) that the canonical angular momentum P_θ and axial canonical momentum P_z are exact single-particle constants of the motion ($dP_\theta/dt = 0 = dP_z/dt$), where

$$P_\theta = rp_\theta + \frac{Z_i e B_0}{2c} r^2, \tag{59}$$

and

$$P_z = p_z + \frac{Z_i e}{c} A_z^s(r). \tag{60}$$

Here, $A_z^s(r) = \beta_b \phi^s(r)$ follows from Eq. (28), and $\vec{p} = (p_r, p_\theta, p_z)$ is the mechanical momentum in cylindrical coordinates (r, θ, z). Similarly, for $\partial\phi^s/\partial t = 0$, the Hamiltonian H defined in Eq. (14) or Eq. (15) is a conserved quantity ($dH/dt = 0$). Consistent with the thin-beam approximation in Eqs. (5) and (13), and the assumption of narrow momentum spread in Eq. (9), we expand the expression for H in Eq. (14) about $p_z = \gamma_b m \beta_b c$, and retain terms to

quadratic order in $\delta p_z = p_z - \gamma_b m\beta_b c$, p_x and p_y. This readily gives the approximate form

$$H = \gamma_b mc^2 + \frac{1}{2\gamma_b m}[2\gamma_b m\beta_b c\delta p_z + (\delta p_z)^2 + p_x^2 + p_y^2] + Z_i e\phi^s. \tag{61}$$

In Eq. (61), $\gamma_b = (1-\beta_b^2)^{-1/2}$ is the relativistic mass factor, and $\phi^s = \phi^s(r)$ when $\partial/\partial z = 0$. Expressing $p_x = P_x - (Z_i e/c)A_x^{sol}$, $p_y = P_y - (Z_i e/c)A_y^{sol}$ and $p_z = P_z - (Z_i e/c)A_z^s$, where (P_x, P_y, P_z) is the canonical momentum, Eqs. (16), (17) and (61) can readily be used to determine the dynamical equations of motion consistent with the thin-beam approximation (see Appendix), although a detailed knowledge of the particle orbits is not required for the Vlasov equilibrium analysis in this section. For future reference, it is convenient in Eq. (61) to eliminate the linear term δp_z in favor of P_z, i.e., $\delta p_z = P_z - (Z_i e/c)A_z^s - \gamma_b m\beta_b c$. This readily gives

$$H = \frac{1}{\gamma_b}mc^2 + V_b P_z + \frac{1}{2\gamma_b m}[(\delta p_z)^2 + p_x^2 + p_y^2] + \frac{Z_i e}{\gamma_b^2}\phi^s, \tag{62}$$

where $V_b \equiv \beta_b c$, and use has been made of $\gamma_b mc^2 - \gamma_b m\beta_b^2 c^2 = mc^2/\gamma_b$ and $\phi^s - \beta_b A_z^s = \phi^s/\gamma_b^2$. Equation (62) provides a useful expression for the linear combination $H - V_b P_z$. Because H and P_z are individually conserved quantities, it follows that $H - V_b P_z$ is also a constant of the motion with $d(H - V_b P_z)/dt = 0$. It should also be pointed out that the expression $H - V_b P_z$ in Eq. (62) can be obtained by Lorentz transformation of the full relativistic expression for $H - V_b P_z$ to a frame of reference moving with axial velocity $V_b\vec{e}_z$ relative to the laboratory frame, and expanding the kinematic energy for small momentum in the beam frame.

To summarize, for $\partial/\partial\theta = \partial/\partial z = \partial/\partial t = 0$ and uniform focusing field $B_z(z) = B_0 =$ const., the canonical angular momentum P_θ, axial canonical momentum P_z, and energy H, defined in Eqs. (59), (60) and (62), respectively, are single-particle constants of the motion in the equilibrium field configuration [26]. Therefore, as discussed in Sec. III.A [see Eq. (26)], the equilibrium distribution function (with $\partial f_b^0/\partial t = 0$) can be constructed from H, P_θ and P_z, i.e.,

$$f_b^0 = f_b^0(H, P_\theta, P_z). \tag{63}$$

In general there is considerable latitude in specifying the functional form of f_b^0 in Eq. (63),

although the specific choice of distribution function should be guided by experiment, including the technique used for beam formation. Because the expressions for P_z and H in Eqs. (60) and (62) depend explicitly on $A_z^s = \beta_b \phi^s$ and ϕ^s, it is clear that any equilibrium analysis based on Eq. (63) must be supplemented by a self-consistent determination of the electrostatic potential $\phi^s(r)$ from Poisson's equation (10), i.e.,

$$\frac{1}{r}\frac{\partial}{\partial r} r \frac{\partial}{\partial r}\phi^s = -4\pi Z_i e \int d^3\vec{p} f_b^0(H, P_\theta, P_z), \tag{64}$$

where $n_b^0(r) = \int d^3\vec{p} f_b^0$ is the ion density.

In the remainder of Sec. IV, we present several examples of intense beam equilibria in a uniform focusing field $B_z(s) = B_0 = \text{const.}$ for two classes of distribution function f_b^0, corresponding to isotropic (Sec. IV.A) and anisotropic (Sec. IV.B) equilibria in the beam frame. Finally, a density inversion theorem is developed (Sec. IV.C), permitting a determination of the distribution function from the density profile $n_b^0(r)$, and a generalized force constraint is derived (Sec. IV.D) that relates the mean square beam radius $\langle r^2 \rangle$ to the transverse thermal emittance ϵ_{th} and other system parameters for general choice of distribution function f_b^0.

A. Isotropic Beam Distribution and Thermal Equilibrium

A very interesting class of *isotropic* beam equilibria occurs when $f_b^0(H, P_\theta, P_z)$ depends on the constants of the motion P_θ, P_z and H defined in Eqs. (59)-(61) exclusively through a linear combination. In this case, f_b^0 is of the form

$$f_b^0 = f_b^0(H + \Omega_b P_\theta - V_b P_z), \tag{65}$$

where Ω_b and V_b are constants related to the angular velocity of mean rotation and the average axial velocity of the beam particles (see below). No matter how complicated the functional form of the distribution function $f_b^0(H + \Omega_b P_\theta - V_b P_z)$, or the corresponding radial dependence of the self-consistent equilibrium profiles for beam density $n_b^0(r) = \int d^3\vec{p} f_b^0$, radial electric field $E_r = -\partial\phi^s/\partial r$, etc., a very important stability theorem pertaining to the entire class of nonneutral beam equilibria described by Eq. (65) has been developed by Davidson

[26]. Specifically, whenever the distribution function $f_b^0(H+\Omega_b P_\theta - V_b P_z)$ is a monotonically decreasing function of the argument $H+\Omega_b P_\theta - V_b P_z$, the beam equilibrium is stable to small-amplitude electrostatic and transverse electromagnetic perturbations. Indeed, this class of distribution functions can be shown to be *nonlinearly stable* to electromagnetic perturbations with arbitrary polarization. The reason can be summarized briefly as follows. In a frame of reference moving the the average velocity of the beam, the distribution function f_b^0 in Eq. (65) is *isotropic*. Therefore, for a one-component nonneutral beam, whenever $f_b^0(H+\Omega_b P_\theta - V_b P_z)$ is a monotonically decreasing function, no free energy is available to drive instability.

Returning to Eq. (65), the combination $H - V_b P_z$ is determined in terms of $(\delta p_z)^2$, $p_x^2 + p_y^2 = p_r^2 + p_\theta^2$, and ϕ^s from Eq. (62). Making use of Eqs. (59) and (62), and expressing $p_\theta^2 + 2\gamma_b m\Omega_b r p_\theta = (p_\theta + \gamma_b m\Omega_b r)^2 - \gamma_b^2 m^2 \Omega_b^2 r^2$, it is readily shown that

$$H + \Omega_b P_\theta - V_b P_z = \frac{1}{\gamma_b} mc^2 + \frac{1}{2\gamma_b m}[p_r^2 + (p_\theta + \gamma_b m\Omega_b r)^2 + (p_z - \gamma_b m\beta_b c)^2] + V(r). \quad (66)$$

Here, $\delta p_z = p_z - \gamma_b m\beta_b c$, $V_b = \beta_b c$, and $V(r)$ is the effective potential defined by

$$V(r) = \frac{1}{2}\gamma_b m\left[\left(\frac{\Omega_{cb}}{2}\right)^2 - \left(\Omega_b - \frac{\Omega_{cb}}{2}\right)^2\right] r^2 + \frac{Z_i e}{\gamma_b^2}\phi^s(r), \quad (67)$$

where $r = (x^2+y^2)^{1/2}$ is the radial distance from the beam axis, and $\Omega_{cb} = Z_i eB_0/\gamma_b mc$ is the relativistic cyclotron frequency in the focusing magnetic field B_0. Whatever the functional form chosen for $f_b^0(H + \Omega_b P_\theta - V_b P_z)$, it is clear from Eqs. (66) and (67) that certain simple properties of the beam equilibria follow for the general class of distribution functions in Eq. (65). For example, the average macroscopic velocity $\vec{V}_b(\vec{x})$ is readily shown to be

$$\vec{V}_b = \frac{\int d^3\vec{p}(\vec{p}/\gamma_b m) f_b^0}{\int d^3\vec{p} f_b^0} = \beta_b c\vec{e}_z - \Omega_b r\vec{e}_\theta, \quad (68)$$

where use has been made of Eqs. (65) and (66). Evidently, from Eq. (68), the average beam motion corresponds to a constant axial velocity $\beta_b c$ plus a rigid rotation about the beam axis at constant angular velocity $-\Omega_b$. The coefficient of r^2 in the definition of the effective potential $V(r)$ in Eq. (67) is proportional to $(\Omega_{cb}/2)^2 - (\Omega_b - \Omega_{cb}/2)^2 = \Omega_b\Omega_{cb} - \Omega_b^2$, which is required to be *positive* for the (focusing) magnetic force to exceed the (defocusing)

centrifugal force due to beam rotation. Note that this coefficient acquires its largest positive value, $(\Omega_{cb}/2)^2$, whenever the beam rotation frequency is equal to the Larmor frequency, i.e., $\Omega_b = \Omega_{cb}/2$. Note also that this coefficient is negative (defocusing) whenever $\Omega_b < 0$ or $\Omega_b > \Omega_{cb}$. In these ranges of Ω_b, the beam equilibrium is not radially confined. A further interesting general equilibrium property pertaining to the class of distribution functions described by Eq. (65) relates to the pressure tensor P_b defined in the usual manner as the average flux relative to the mean of momentum relative to the mean. From Eqs. (65) and (66), it is readily shown that

$$\mathsf{P}_b(\vec{x}) = (\gamma_b m)^{-1} \int d^3\vec{p}(\vec{p} - \gamma_b m\vec{V}_b)(\vec{p} - \gamma_b m\vec{V}_b) f_b^0 = P_b(r)\mathsf{I}. \tag{69}$$

Here, $\mathsf{I} = \vec{e}_r\vec{e}_r + \vec{e}_\theta\vec{e}_\theta + \vec{e}_z\vec{e}_z$ is the unit dyadic, and $P_b(r)$ is the scalar pressure defined in terms of the average kinetic energy of random motion (relative to the mean) by

$$P_b(r) = n_b^0(r)T_b(r) = \frac{1}{3\gamma_b m}\int d^3\vec{p}\,[p_r^2 + (p_\theta + \gamma_b m\Omega_b r)^2 + (p_z - \gamma_b m\beta_b c)^2] f_b^0. \tag{70}$$

Therefore, for the class of Vlasov equilibria described by Eq. (66), the beam pressure is *isotropic*. Moreover, once the radial dependence of the scalar pressure $P_b(r)$ and density $n_b^0(r) = \int d^3\vec{p} f_b^0$ are calculated for specific choice of f_b^0, Eq. (70) can be used to determine the effective temperature profile $T_b(r) = P_b(r)/n_b^0(r)$.

Thermal Equilibrium Distribution

We now consider the specific choice of distribution function f_b^0 corresponding to thermal equilibrium [26], i.e.,

$$f_b^0 = \frac{\hat{n}_b \exp(mc^2/\gamma_b k_B T)}{(2\pi\gamma_b m k_B T)^{3/2}} \exp\left(-\frac{H + \Omega_b P_\theta - V_b P_z}{k_B T}\right). \tag{71}$$

Here, k_B is Boltzmann's constant, and Ω_b, $V_b = \beta_b c$, $\hat{n}_b$ and T are constant parameters. We substitute Eq. (66) into Eq. (71) and evaluate the density profile $n_b^0(r) = \int d^3\vec{p} f_b^0$. Because the momentum dependence of f_b^0 has the form of a shifted Maxwellian, this readily gives

$$n_b^0(r) = \hat{n}_b \exp\left\{-\frac{\gamma_b m}{2k_B T}\left[(\Omega_b\Omega_{cb} - \Omega_b^2)r^2 + \frac{2Z_i e}{\gamma_b^3 m}\phi^s\right]\right\}. \tag{72}$$

Without loss of generality we take $\phi^s(r=0)=0$ so that $\hat{n}_b = n_b^0(r=0)$ can be identified with the density on-axis. Substituting Eq. (72) into Poisson's equation (64) gives a nonlinear differential equation for the electrostatic potential $\phi^s(r)$, which can generally be solved numerically. Once the functional form of $\phi^s(r)$ is determined self-consistently, the radial dependence of the density profile $n_b^0(r)$ can be obtained from Eq. (72). As a general remark, provided that the defocusing effects of beam rotation and space charge do not exceed the focusing effect of the applied solenoidal field, the density profile calculated from Eqs. (64) and (72) is bell-shaped, assuming a maximum value of $\hat{n}_b$ at $r=0$, and decreasing monotonically as r increases. The important control parameter that defines the condition for radially confined beam equilibria can be determined by examining Eqs. (64) and (72) near the beam axis (small values of r), where $n_b^0(r) \cong \hat{n}_b$ and $\phi^s(r) \cong -\pi Z_i e \hat{n}_b r^2$. The condition for $n_b^0(r)$ to decrease as r increases from $r=0$, which is also the condition that $(d^2V/dr^2)_{r=0} > 0$, where $V(r)$ is the effective potential defined in Eq. (67), can be expressed as

$$\hat{\omega}_\beta^2 \equiv (\Omega_{cb}/2)^2 - \hat{\omega}_{pb}^2/2\gamma_b^2 > (\Omega_b - \Omega_{cb}/2)^2. \tag{73}$$

Here, $\hat{\omega}_{pb}^2 = 4\pi Z_i^2 e^2 \hat{n}_b/\gamma_b m$ is the on-axis plasma frequency-squared, use has been made of $\Omega_b\Omega_{cb} - \Omega_b^2 = (\Omega_{cb}/2)^2 - (\Omega_b - \Omega_{cb}/2)^2$, and $\hat{\omega}_\beta$ is the betatron frequency for small-amplitude oscillations in the transverse orbit (in the rotating frame) near the beam axis. Whenever $\hat{\omega}_\beta^2$ is 'closely tuned' to $(\Omega_b - \Omega_{cb}/2)^2$, the density profile calculated from Eqs. (64) and (72) tends to be radially broad in units of the Debye length $\lambda_D = (\gamma_b^2 k_B T/4\pi\hat{n}_b Z_i^2 e^2)^{1/2}$, with $n_b^0(r) \cong \hat{n}_b = \text{const.}$ in the beam interior ($0 \le r < r_b$), and decreases abruptly to expoentially small values of over a narrow sheath region about a Debye length in thickness [26]. Typical numerical results obtained from Eqs. (64) and (72) are presented in Fig. 1, where $n_b^0(r)/\hat{n}_b$ is plotted versus r/λ_D.

A further interesting equilibrium property is the scalar pressure $P_b(r)$ defined in Eq. (70). Substituting Eqs. (66) and (71) into Eq. (70) readily gives the pressure profile

$$P_b(r) = n_b^0(r) k_B T, \tag{74}$$

where T = const. is the thermal equilibrium temperature. As expected from Eqs. (65) and (71), the temperature is isotropic ($T_\perp = T_\parallel = T$) in thermal equilibrium, and independent of radius r. It should also be pointed out that radial force balance on a beam fluid element is readily derived by taking the r-derivative of Eq. (72). This gives

$$k_B T \frac{\partial n_b^0}{\partial r} = -\gamma_b m n_b^0 (\Omega_b \Omega_{cb} - \Omega_b^2) r + \frac{Z_i e}{\gamma_b^2} n_b^0 E_r, \tag{75}$$

where $E_r = -\partial \phi^s / \partial r$ is the equilibrium radial electric field determined from Poisson's equation (64). Equation (75) is simply a statement of radial force balance between the (outward) pressure gradient, centrifugal and electric forces and the (inward) $V_{\theta b} \vec{e}_\theta \times B_0 \vec{e}_z$ magnetic force on a fluid element. It should be emphasized that for the general class of isotropic beam equilibria described by Eq. (65), a force balance equation identical in form to Eq. (75) can be derived with $k_B T \partial n_b^0 / \partial r$ replaced by $\partial P_b / \partial r$, where $P_b(r)$ is the scalar pressure defined in terms of f_b^0 by Eq. (70).

It is customary in accelerator physics to define the statistical average $\langle \psi \rangle$ of a function ψ defined on the phase space (x, y, p_x, p_y, p_z) by

$$\langle \psi \rangle = N_b^{-1} \int dx dy dp_x dp_y dp_z \psi f_b^0. \tag{76}$$

Here, $\int dx dy \cdots = 2\pi \int_0^\infty dr r \cdots$ for azimuthally symmetric f_b^0 and ψ with $\partial / \partial \theta = 0$, and $N_b = \int dx dy dp_x dp_y dp_z f_b^0 = 2\pi \int_0^\infty dr r n_b^0(r)$ is the number of beam ions per unit axial length. For example, making use of the definition of canonical angular momentum P_θ in Eq. (59), it follows from Eqs. (66) and (76) that

$$\langle P_\theta \rangle = \gamma_b m (\Omega_{cb}/2 - \Omega_b) \langle r^2 \rangle \tag{77}$$

for the choice of thermal equilibrium distribution f_b^0 in Eq. (71), and indeed for the entire class of isotropic rigid-rotor Vlasov equilibria $f_b^0(H + \Omega_b P_\theta - V_b P_z)$ described by Eq. (65). Equation (77) is a powerful constraint condition that relates the average $\langle P_\theta \rangle$ directly to the angular rotation velocity Ω_b and the mean-square radius $\langle r^2 \rangle$ of the beam, no matter how complex the functional form of the density profile $n_b^0(r)$. A second constraint condition can

be obtained directly from the radial force balance equation (75). We make use of Poisson's equation (64) to express $E_r = \partial\phi^s/\partial r = (4\pi Z_i e/r)\int_0^r dr r n_b^0(r)$, and operate on Eq. (75) with $2\pi\int_0^\infty dr r^2 \cdots$. Some straightforward integration by parts and rearrangement of terms gives

$$[(\Omega_{cb}/2)^2 - (\Omega_b - \Omega_{cb}/2)^2]\langle r^2\rangle = \frac{2k_B T}{\gamma_b m} + \frac{Z_i^2 e^2 N_b}{\gamma_b^3 m}, \tag{78}$$

which relates the mean-square beam radius $\langle r^2\rangle$ to the temperature T and the number of particles per unit axial length N_b. Equation (77) can be used (for example) to eliminate $(\Omega_b - \Omega_{cb}/2)^2$ in favor of $\langle P_\theta\rangle^2$ in Eq. (78). Equation (78) can then be expressed as

$$(\Omega_{cb}/2)^2\langle r^2\rangle \; - \; \frac{Z_i^2 e^2 N_b}{\gamma_b^3 m} = \frac{1}{\langle r^2\rangle}\left[\frac{\langle P_\theta\rangle^2}{\gamma_b^2 m^2} + \frac{2k_B T}{\gamma_b m}\langle r^2\rangle\right]. \tag{79}$$

It is convenient to introduce the self-field perveance K, solenoidal field focusing coefficient κ_{z0}, root-mean-square *transverse thermal emittance* ϵ_{th} (emittance relative to the average rotational motion in the laboratory frame), and effective beam radius r_b, defined by [1,25]

$$K = \frac{2Z_i^2 e^2 N_b}{\gamma_b^3 m\beta_b^2 c^2},$$

$$\kappa_{z0} = \left(\frac{Z_i e B_0}{2\gamma_b m\beta_b c^2}\right)^2 = \left(\frac{\Omega_{cb}}{2\beta_b c}\right)^2, \tag{80}$$

$$\epsilon_{th}^2 = \frac{4}{\gamma_b^2 m^2\beta_b^2 c^2}\langle r^2\rangle\langle p_r^2 + (p_\theta + \gamma_b m\Omega_b r)^2\rangle,$$

$$r_b^2 = 2\langle r^2\rangle.$$

Making use of Eqs. (70),(74) and (80), the condition in Eq. (79) can be expressed as

$$\left(\kappa_{z0} - \frac{K}{r_b^2}\right) r_b = \frac{1}{r_b^3}\left(\epsilon_{th}^2 + \frac{4\langle P_\theta\rangle^2}{\gamma_b^2 m^2\beta_b^2 c^2}\right). \tag{81}$$

Equation (81) is identical in form to the familiar envelope equation [25] in the smooth-beam approximation ($d^2 r_b/ds^2 = 0$), allowing for average beam rotation relative to the Larmor frame, i.e., $\langle P_\theta\rangle \neq 0$ whenever $\Omega_b \neq \Omega_{cb}/2$ [see Eq. (77)].

Monoenergetic Beam Distribution

As a second example of an isotropic beam equilibrium $f_b^0(H+\Omega_b P_\theta - V_b P_z)$, we consider the case where the distribution function of beam ions is monoenergetic in the moving frame, i.e.,

$$f_b^0 = \frac{\hat{n}_b}{4\pi\gamma_b m(3\gamma_b m\hat{T}_b)^{1/2}}\delta\left(H+\Omega_b P_\theta - V_b P_z - \frac{3}{2}\hat{T}_b - \frac{mc^2}{\gamma_b}\right). \tag{82}$$

Here, $H+\Omega_b P_\theta - V_b P_z$ is defined in terms of r and the mechanical momentum variables (p_r, p_θ, p_z) in Eq. (66), and $\hat{n}_b$ and $\hat{T}_b$ are positive constants which will be identified below with the on-axis ($r=0$) values of beam density and temperature, respectively. It is convenient to introduce the shifted momentum variables $(\tilde{p}_r, \tilde{p}_\theta, \tilde{p}_z)$ and normalized potential $\psi_b(r)$ defined by

$$\tilde{p}_r = p_r, \quad \tilde{p}_\theta = p_\theta + \gamma_b m\Omega_b r, \quad \tilde{p}_z = p_z - \gamma_b m\beta_b c, \quad \psi_b(r) = 1 - \frac{2V(r)}{3\hat{T}_b}. \tag{83}$$

Making use of Eqs. (66) and (83), the distribution fucntion in Eq. (82) can then be expressed as

$$f_b^0 = \frac{\hat{n}_b}{2\pi(3\gamma_b m\hat{T}_b)^{1/2}}\delta[\,\tilde{p}^2 - 3\gamma_b m\hat{T}_b\psi_b(r)], \tag{84}$$

where $\psi_b(r)$ and $V(r)$ are defined in Eqs. (83) and (67), respectively. The density profile $n_b^0(r) = \int d^3\vec{p} f_b^0$ calculated from Eq. (84) is non-zero only for $\psi_b(r) \geq 0$ and zero whenever $\psi_b(r) < 0$. Therefore, the outer beam radius r_b is calculated self-consistently from $\psi_b(r_b) = 0$, or equivalently, $V(r_b) = 3\hat{T}_b/2$.

Expressing $\int d^3\tilde{\vec{p}}\cdots = 4\pi\int_0^\infty d\tilde{p}\tilde{p}^2\cdots$, where $\tilde{p}^2 = \tilde{p}_r^2 + \tilde{p}_\theta^2 + \tilde{p}_z^2$, it is readily shown that the density profile $n_b^0(r) = \int d^3\tilde{\vec{p}} f_b^0$ calculated from Eq. (84) is given by

$$n_b^0(r) = \begin{cases} \hat{n}_b[\psi_b(r)]^{1/2}, & 0 \leq r < r_b, \\ 0, & r > r_b, \end{cases} \tag{85}$$

where $\psi_b(r) = 1 - 2V(r)/3\hat{T}_b$ and $V(r_b) = 3\hat{T}_b/2$. Similarly, substituting Eq. (84) into Eq. (70), the temperature profile $T_b(r)$ for the choice of monoenergetic beam distribution in Eq. (82) is readily shown to be

$$T_b(r) = \hat{T}_b\psi_b(r) \tag{86}$$

over the radial extent of the beam ($0 \leq r < r_b$).

Note from Eqs. (85) and (86) that the pressure profile $P_b(r) = n_b^0(r)T_b(r)$ $= (\hat{T}_b/\hat{n}_b^2)[n_b^0(r)]^3$ scales as the cube of the local density $n_b^0(r)$. Also, $\psi_b(r) = 1 - 2V(r)/3\hat{T}_b$ decreases monotonically from $\psi_b(r = 0) = 1$ on the beam axis to $\psi_b(r = r_b) = 0$ at the outer beam radius r_b where $V(r_b) = 3\hat{T}_b/2$. Correspondingly, the density profile $n_b^0(r)$ and temperature profile $T_b(r)$ defined in Eqs. (85) and (86) decrease monotonically from maximum values of $\hat{n}_b$ and $\hat{T}_b$, respectively, at $r = 0$, to zero at the beam edge $r = r_b$. To determine the radial dependence of $n_b^0(r)$ self-consistently, it is necessary to substitute Eq. (85) into Poisson's equation (64). Making use of $\psi_b(r) = 1 - 2V(r)/3\hat{T}_b$, where $V(r)$ is defined in Eq. (67), some straightforward algebra gives the nonlinear differential equation for $\psi_b(r)$,

$$\frac{1}{r}\frac{\partial}{\partial r}r\frac{\partial}{\partial r}\psi_b(r) = -\frac{1}{\lambda_D^2}\left\{\frac{2\gamma_b^2}{\hat{\omega}_{pb}^2}\left[\left(\frac{\Omega_{cb}}{2}\right)^2 - \left(\Omega_b - \frac{\Omega_{cb}}{2}\right)^2\right] - [\psi_b(r)]^{1/2}\right\}. \tag{87}$$

Here, an effective Debye length defined by $\lambda_D = (3\gamma_b^2\hat{T}_b/8\pi Z_i^2 e^2 \hat{n}_b)^{1/2}$ has been introduced as a radial scale length, and $\hat{\omega}_{pb}^2 = 4\pi Z_i^2 e^2/\gamma_b m$ is the on-axis value of plasma frequency-squared. In Eq. (87), $\psi_b(0) = 1$, and for physically allowed solutions $\psi_b(r)$ must decrease as r increases from $r = 0$. This readily gives the condition

$$\frac{2\gamma_b^2}{\hat{\omega}_{pb}^2}\left[\left(\frac{\Omega_{cb}}{2}\right)^2 - \left(\Omega_b - \frac{\Omega_{cb}}{2}\right)^2\right] \equiv 1 + \epsilon > 1, \tag{88}$$

which is required for existence of radially confined equilibrium solutions. Note that Eq. (88) is identical to the inequality in Eq. (73). Furthermore, whenever $0 < \epsilon \ll 1$ is satisfied, it is found from Eq. (87) that radial profile is very broad in units of the Debye length λ_D. That is, $\psi_b(r)$ decreases monotonically to zero at $\psi_b(r = r_b) = 0$, where $r_b \gg \lambda_D$. Although an analytical solution for $\psi_b(r)$ does not appear to be accessible from Eq. (87), numerical solutions are readily obtained for $\psi_b(r)$ versus r/r_b and different values of the dimensionless parameter ϵ defined in Eq. (88). Typical numerical results are shown in Fig. 2, where $n_b^0(r)/\hat{n}_b = [\psi_b(r)]^{1/2}$ and $T_b(r)/\hat{T}_b = \psi_b(r)$ are plotted versus r/r_b for several values of ϵ. As expected, the beam radius satisfies $r_b \gg \lambda_D$ whenever ϵ is sufficiently small. Other

equilibrium properties can also be calculated for the choice of monoenergetic distribution function in Eqs. (82) and (84). For example, as in Eq. (77), it is readily shown that the average canonical angular momentum $\langle P_\theta \rangle$ is related to the mean-square radius by $\langle P_\theta \rangle = \gamma_b m(\Omega_{cb}/2 - \Omega_b)\langle r^2 \rangle$.

General Isotropic Beam Distribution

Equilibrium properties can also be calculated for other choices of isotropic distrubution function $f_b^0(H + \Omega_b P_\theta - V_b P_z)$. For completeness, we establish here useful expressions for the density and pressure profiles as well as the nonlinear Poisson equation for general choice of f_b^0. It is convenient to introduce $\tilde{p}^2 = p_r^2 + (p_\theta + \gamma_b m \Omega_b r)^2 + (p_z - \gamma_b m \beta_b c)^2$, and make use of Eq. (66) to express $H + \Omega_b P_\theta - V_b P_z = (2\gamma_b m)^{-1}\tilde{p}^2 + V_0(r)$, where $V_0(r) = V(r) + mc^2/\gamma_b$, and $V(r)$ is the effective potential defined in terms of $\phi^s(r)$ and other equilibrium parameters in Eq. (67). Some straightforward algebra then shows that the density profile $n_b^0(r) = \int d^3\vec{p} f_b^0$ and pressure profile $P_b(r) = (2/3)\int d^3\vec{p}(\tilde{p}^2/2\gamma_b m) f_b^0$ can be expressed as

$$n_b^0(r) = 2\pi(2\gamma_b m)^{3/2} \int_{V_0(r)}^{\infty} dU [U - V_0(r)]^{1/2} f_b^0(U), \tag{89}$$

and

$$P_b(r) = \frac{4\pi}{3}(2\gamma_b m)^{3/2} \int_{V_0(r)}^{\infty} dU [U - V_0(r)]^{3/2} f_b^0(U). \tag{90}$$

Here, we have introduced the integration variable $U = \tilde{p}^2/2\gamma_b m + V_0(r)$. Comparison of Eqs. (89) and (90) shows that $\partial P_b/\partial V_0 = -n_b^0(r)$, or equivalently, $\partial P_b/\partial r = -n_b^0(r)\partial V_0/\partial r$. Making use of Eq. (67) to evaluate $\partial V_0/\partial r = \partial V/\partial r$ then gives

$$\frac{\partial P_b}{\partial r} = -\gamma_b m n_b^0(\Omega_b \Omega_{cb} - \Omega_b^2) r + \frac{Z_i e}{\gamma_b^2} n_b^0 E_r, \tag{91}$$

where $E_r = -\partial\phi^s/\partial r$ is the radial electric field. Equation (91) will be recognized as the condition for radial force balance on a fluid element for general choice of equilibrium distribution function f_b^0 [compare with Eq. (75)].

The effective potential $V_0(r)$ occurring in Eqs. (89) and (90) must of course be determined self-consistently from Poisson's equation (64). Making use of the definition of $V(r) = V_0(r) -$

mc^2/γ_b in Eq. (67), and the expression for $n_b^0(r)$ in Eq. (89), Poisson's equation (64) can be expressed in the equivalent form

$$\frac{1}{r}\frac{\partial}{\partial r}r\frac{\partial}{\partial r}V_0(r) = 2\gamma_b m\left[\left(\frac{\Omega_{cb}}{2}\right)^2 - \left(\Omega_b - \frac{\Omega_{cb}}{2}\right)^2 - \frac{\hat{\omega}_{pb}^2}{2\gamma_b^2}F(V_0)\right]. \tag{92}$$

In Eq. (92), $\hat{\omega}_{pb}^2 = 4\pi\hat{n}_b Z_i^2 e^2/\gamma_b m$, where $\hat{n}_b = 2\pi(2\gamma_b m)^{3/2}\int_{mc^2/\gamma_b}^{\infty} dU[U - mc^2/\gamma_b]^{1/2} f_b^0(U)$ is the on-axis ($r = 0$) beam density, and $F(V_0)$ is defined by

$$F(V_0) = \frac{\int_{V_0(r)}^{\infty} dU[U - V_0(r)]^{1/2} f_b^0(U)}{\int_{mc^2/\gamma_b}^{\infty} dU[U - mc^2/\gamma_b]^{1/2} f_b^0(U)}. \tag{93}$$

For the special case of the monoenergetic distribution in Eq. (82), we make the identification $V_0(r) = mc^2/\gamma_b + (3\hat{T}_b/2)[1 - \psi_b(r)]$, and Eq. (92) reduces exactly to Eq. (87) for $\psi_b(r)$, as expected.

For the general choice of distribution function $f_b^0(U)$, the solution for $V_0(r)$ is required to increase monotonically from its on-axis value $V_0(r = 0) = mc^2/\gamma_b$ as r is increased. This assures radial confinement of the beam equilibrium and that the density profile $n_b^0(r)$ defined in Eq. (89) decreases as a function of increasing r. From Eq. (93), $F(V_0) = 1$ at $r = 0$ where $V_0(r = 0) = mc^2/\gamma_b$. Examination of Eqs. (92) and (93) then shows that the condition for $V_0(r)$ to increase monotonically as r is increased is identical to the inequality in Eq. (88). While further examples of isotropic beam equilibria $f_b^0(H + \Omega_b P_\theta - V_b P_z)$ will not be considered here, it is clear that Eqs. (89)-(93) can be used to investigate equilibrium properties for a variety of choices of f_b^0.

B. Anisotropic Beam Distributions

In this section, for a uniform solenoidal focusing field with $B_z(s) = B_0 = \text{const.}$, we consider *anisotropic* beam equilibria $f_b^0(H, P_\theta, P_z)$ in which the average kinetic energy spread (relative to the mean) in the transverse (r, θ) plane differs from that in the axial direction. Such anisotropics are well known in plasma physics to provide the free energy to drive various collective modes and instabilities [26]. Examining the δp_z contributions to the expanded Hamiltonian H in Eq. (61), and expressing $\delta p_z \equiv p_z - \gamma_b m\beta_b c = \delta P_z - (Z_i e/c)A_z^s$, it is

readily shown that

$$\frac{1}{2\gamma_b m}[2\gamma_b m\beta_b c(\delta p_z)+(\delta p_z)^2]=\beta_b c\delta P_z-Z_i e\beta_b A_z^s+\frac{(\delta P_z)^2}{2\gamma_b m}-\frac{Z_i eA_z^s}{\gamma_b mc}\delta P_z+\frac{(Z_i eA_z^s)^2}{2\gamma_b mc^2}, \quad (94)$$

where $A_z^s(r)=\beta_b\phi^s(r)$ follows from Eq. (28). Comparing the size of the terms on the right-hand side of Eq. (94), we conclude that the fourth term is negligibly small in comparison with the first, and the fifth term is negligibly small in comparison with the second, by virtue of the assumption $|Z_i eA_z^s/\gamma_b mc^2|\ll\beta_b$ in Eq. (13). Therefore, in the remainder of Sec. IV, we approximate

$$\frac{1}{2\gamma_b m}[2\gamma_b mc(\delta p_z)+(\delta p_z)^2]=\beta_b c\delta P_z-Z_i e\beta_b A_z^s+\frac{(\delta P_z)^2}{2\gamma_b m} \quad (95)$$

in application of the Hamiltonian H in Eq. (61). Making use of Eqs. (61) and (95), a Hamiltonian $H_\perp$ for the *perpendicular* motion is introduced, where $H_\perp$ is defined by

$$H_\perp\equiv H-\gamma_b mc^2-\beta_b c\delta P_z-\frac{(\delta P_z)^2}{2\gamma_b m}=\frac{1}{2\gamma_b m}(p_r^2+p_\theta^2)+\frac{Z_i e}{\gamma_b^2}\phi^s. \quad (96)$$

In Eq. (96), $p_r^2+p_\theta^2=p_x^2+p_y^2$, and use has been made of $\phi^s-\beta_b A_z^s=\phi^s/\gamma_b^2$. Because $H_\perp$ is constructed from the constants of the motion H and P_z, the perpendicular Hamiltonian $H_\perp$ is also a constant of the motion to the level of accuracy of Eq. (95).

In the remainder of this section, we consider anisotropic beam equilibria $f_b^0(H,P_\theta,P_z)$ of the form

$$f_b^0=F_b(H_\perp+\Omega_b P_\theta)G(P_z), \quad (97)$$

where P_θ, P_z, and $H_\perp$ are defined in Eqs. (59), (60) and (96), respectively, and equilibrium properties are assumed to be azimuthally symmetric ($\partial/\partial\theta=0$) and independent of axial coordinate ($\partial/\partial z=0$). Making use of Eqs. (59) and (96), the argument $H_\perp+\Omega_b P_\theta$ occurring in Eq. (97) can be expressed as

$$H_\perp+\Omega_b P_\theta=\frac{1}{2\gamma_b m}[p_r^2+(p_\theta+\gamma_b m\Omega_b r)^2]+V(r), \quad (98)$$

where $V(r)$ is the effective potenital defined in terms of r and the electrostatic potential $\phi^s(r)$ in Eq. (67). As in Sec. IV.A, $\Omega_b=$ const. corresponds to the angular velocity of mean

rotation of the beam, i.e., $V_{\theta b}(r) = (\gamma_b m)^{-1}(\int d^3\vec{p}p_\theta f_b^0)/(\int d^3\vec{p}f_b^0) = -\Omega_b r$ for general choice of $F_b(H_\perp + \Omega_b P_\theta)$ and $G(P_z)$. In addition, the distribution in axial canonical momentum $G(P_z)$ is assumed to be strongly peaked about $P_z \equiv p_z + (Z_i e/c)A_z^s(r) = \gamma_b m\beta_b c = \text{const.}$, where $A_z^s = \beta_b \phi^s$. Of course many choices are possible for the functional form of $G(P_z)$, such as a symmetric step-function centered at $P_z = \gamma_b m\beta_b c$, or a resonance distribution, or a Gaussian distribution, to mention a few examples. For the case of a Gaussian distribution, we express

$$G(P_z) = \frac{1}{(2\pi\gamma_b m T_{\|b})^{1/2}} \exp\left[-\frac{(P_z - \gamma_b m\beta_b c)^2}{2\gamma_b m T_{\|b}}\right], \tag{99}$$

where $T_{\|b} = \text{const.}$ is an effective *temperature* associated with the axial motion, and $G(P_z)$ has been normalized according to $\int_{-\infty}^{\infty} dp_z G(P_z) = 1$. For general perpendicular distribution function $F_b(H_\perp + \Omega_b P_\theta)$, and $G(P_z)$ specified by Eq. (99), it is readily shown that the average axial flow velocity is $V_{zb} = (\gamma_b m)^{-1}(\int d^3\vec{p}p_z f_b^0)/(\int d^3\vec{p}f_b^0) = \beta_b c(1 + Z_i e A_z^s/\gamma_b m\beta_b c^2)$. Because $|Z_i e A_z^s/\gamma_b m c^2| \ll \beta_b$ is assumed in Eq. (13), it follows that the axial flow velocity is given to good approximation by $V_{zb} = \beta_b c = \text{const.}$ Similarly, the z-z component of the pressure tensor, which provides a measure of the axial velocity spread of the beam particles, is given by

$$P_{\|b}(r) \equiv \gamma_b m \int d^3\vec{p}(p_z/\gamma_b m - V_{zb})^2 f_b^0 = n_b^0(r) T_{\|b}. \tag{100}$$

Here, use has been made of Eqs. (97) and (99), and the density profile $n_b^0(r) = \int d^3\vec{p}f_b^0$ can be expressed as

$$n_b^0(r) = \int d^2\vec{p}F_b(H_\perp + \Omega_b P_\theta), \tag{101}$$

where $\int d^2\vec{p}\cdots = \int dp_r dp_\theta \cdots$. Note from (100) that the axial temperature is uniform and equal to $T_{\|b} = \text{const.}$ for the choice of $G(P_z)$ in Eq. (99). Of course, in the cold limit with $T_{\|b} \to 0$, Eq. (99) gives $G(P_z) \to \delta(P_z - \gamma_b m\beta_b c)$. Finally, making use of Eqs. (97) and (99), the pressure tensor defined as in Eq. (69) is found to be of the form $\mathsf{P}_b(\vec{x}) = P_{\perp b}(r)(\vec{e}_r\vec{e}_r + \vec{e}_\theta\vec{e}_\theta) + P_{\|b}(r)\vec{e}_z\vec{e}_z$, which is diagonal, but generally *anisotropic*. Here, $P_{\|b}(r)$

is the parallel pressure defined in Eq. (100), and the perpendicular pressure is defined by

$$P_{\perp b}(r) \equiv \frac{1}{2\gamma_b m}\int d^3\vec{p}\,[p_r^2 + (p_\theta + \gamma_b m\Omega_b r)^2]f_b^0$$

$$= \frac{1}{2\gamma_b m}\int d^2\vec{p}\,[p_r^2 + (p_\theta + \gamma_b m\Omega_b r)^2]F_b(H_\perp + \Omega_b P_\theta) \tag{102}$$

$$= n_b^0(r)T_{\perp b}(r).$$

Once the radial dependence of $P_{\perp b}(r)$ and $n_b^0(r)$ are calculated from Eqs. (101) and (102) for specific choice of $F_b(H_\perp + \Omega_b P_\theta)$, Eq. (102) can be used to determine the radial profile of the effective perpendicular temperature $T_{\perp b}(r) \equiv P_{\perp b}(r)/n_b^0(r)$.

The perpendicular and parallel distribution functions in Eq. (97) can be specified independently. In the remainder of Sec. IV.B, assuming the normalization $\int_{-\infty}^{\infty} dp_z G(P_z) = 1$, we make use of Eqs. (101) and (102) to determine the density and pressure profiles for various choices of $F_b(H_\perp + \Omega_b P_\theta)$, where $H_\perp + \Omega_b P_\theta$ is defined in Eq. (98). In this regard, it is convenient to express $\tilde{p}_\perp^2 = p_r^2 + (p_\theta + \gamma_b m\Omega_b r)^2$, and represent $\int d^2\vec{p}\cdots = \int_{-\infty}^{\infty} dp_r \int_{-\infty}^{\infty} dp_\theta \cdots = \pi\int_0^\infty d\tilde{p}_\perp^2 \cdots$ in Eqs. (101) and (102). This density and perpendicular pressure profiles can then be expressed as

$$n_b^0(r) = \pi\int_0^\infty d\tilde{p}_\perp^2 F_b\left[\frac{\tilde{p}_\perp^2}{2\gamma_b m} + V(r)\right], \tag{103}$$

$$n_b^0(r)T_{\perp b}(r) = \pi\int_0^\infty d\tilde{p}_\perp^2 \frac{\tilde{p}_\perp^2}{2\gamma_b m} F_b\left[\frac{\tilde{p}_\perp^2}{2\gamma_b m} + V(r)\right], \tag{104}$$

where $V(r) = (\gamma_b m/2)(\Omega_b\Omega_{cb} - \Omega_b^2)r^2 + (Z_i e/\gamma_b^2)\phi^s(r)$ is defined in Eq. (67). Of course, for specified $F_b(H_\perp + \Omega_b P_\theta)$, the electrostatic potential $\phi^s(r)$ must be determined self-consistently from Poisson's equation (64), which becomes

$$\frac{1}{r}\frac{\partial}{\partial r}r\frac{\partial}{\partial r}\phi^s = -4\pi^2 Z_i e\int_0^\infty d\tilde{p}_\perp^2 F_b\left[\frac{\tilde{p}_\perp^2}{2\gamma_b m} + V(r)\right]. \tag{105}$$

Depending on the choice of $F_b(H_\perp + \Omega_b P_\theta)$, Eq. (105) is generally a nonlinear differential equation for $\phi^s(r)$.

Thermal Equilibrium Transverse Distribution

As a first example, we consider the case where $F_b(H_\perp + \Omega_b P_\theta)$ is specified by

$$F_b = \frac{\hat{n}_b}{2\pi\gamma_b m T_{\perp b}} \exp\left(-\frac{H_\perp + \Omega_b P_\theta}{T_{\perp b}}\right), \tag{106}$$

where $\hat{n}_b$ and $T_{\perp b}$ are positive constants. Substituting Eq. (106) into Eqs. (103) and (104) readily gives

$$n_b^0(r) = \hat{n}_b \exp\left\{-\frac{\gamma_b m}{2T_{\perp b}}\left[(\Omega_b\Omega_{cb} - \Omega_b^2)r^2 + \frac{2Z_i e}{\gamma_b^3 m}\phi^s\right]\right\}, \tag{107}$$

and $P_{\perp b}(r) = n_b^0(r)T_{\perp b}$. As expected, the transverse temperature profile calculated from Eq. (106) is isothermal with $T_{\perp b}(r) = T_{\perp b} = \text{const}$. Furthermore, Eq. (107) is identical to the expression for $n_b^0(r)$ in Eq. (72) obtained for the isotropic thermal equilibrium distribution in Eq. (71), provided we make the replacement $k_B T \rightarrow T_{\perp b}$ in Eq. (72). The essential difference between Eq. (71) and Eq. (97), with $F_b(H_\perp + \Omega_b P_z)$ specified by Eq. (106), is that Eq. (97) allows for an energy anisotropy ($T_{\perp b} \neq T_{\parallel b}$) between the perpendicular and parallel directions, whereas Eq. (71) does not. Because of the similarity between Eqs. (72) and (107), virtually all of the analysis in Sec. IV.A pertaining to the choice of f_b^0 in Eq. (71) can be applied to Eq. (106), provided we make the replacements $k_B T \rightarrow T_{\perp b}$. This includes the condition for radially confined equilibria [Eq. (73)], self-consistent profiles for $n_b^0(r)$ (Fig. 1), and radial force balance equation [Eq. (75)], and constraint conditions on $\langle r^2 \rangle$ and $\langle P_\theta \rangle$ [Eqs. (77)-(79)].

Monoenergetic Transverse Distribution

As a second example, we consider the case where the transverse distribution function $F_b(H_\perp + \Omega_b P_\theta)$ is *monoenergetic* with [26]

$$F_b(H_\perp + \Omega_b P_\theta) = \frac{\hat{n}_b}{2\pi\gamma_b m}\delta(H_\perp + \Omega_b P_\theta - \hat{T}_{\perp b}), \tag{108}$$

where $\hat{n}_b$ and $\hat{T}_{\perp b}$ are positive constants. Substituting Eq. (108) into Eq. (103) gives the density profile

$$n_b^0(r) = \hat{n}_b \int_0^\infty d\left(\frac{\tilde{p}_\perp^2}{2\gamma_b m}\right)\delta\left[\frac{\tilde{p}_\perp^2}{2\gamma_b m} + V(r) - \hat{T}_{\perp b}\right], \tag{109}$$

where $V(r)$ is defined in Eq. (67). As in Sec. IV.A, we take $\phi^s(r=0)=0$, and therefore $V(r=0)=0$. It is clear from Eq. (109) that $n_b^0(r)=0$ whenever $V(r)>\hat{T}_{\perp b}$, and $n_b^0(r)=\hat{n}_b=$ const. whenever $0\le V(r)<\hat{T}_{\perp b}$. Therefore, as $V(r)$ increases (from zero) with increasing r, the outer beam radius r_b is determined from $V(r_b)=\hat{T}_{\perp b}$. Carrying out the integration over $\tilde{p}_\perp^2$ in Eq. (109) thus gives the rectangular density profile (Fig. 3)

$$n_b^0(r)=\begin{cases}\hat{n}_b=\text{const.}, & 0\le r<r_b,\\ 0, & r>r_b.\end{cases} \tag{110}$$

Substituting Eq. (110) into Poisson's equation (105), we obtain for the electrostatic potential

$$\phi^s(r)=\begin{cases}-Z_i e\pi\hat{n}_b r^2, & 0\le r<r_b,\\ -Z_i e\pi\hat{n}_b r_b^2[1+2\ln(r/r_b)], & r>r_b.\end{cases} \tag{111}$$

Making use of Eq. (67), the effective potential $V(r)$ in the beam interior ($0\le r<r_b$) can be expressed as

$$V(r)=\frac{1}{2}\gamma_b m\left[\left(\frac{\Omega_{cb}}{2}\right)^2-\left(\Omega_b-\frac{\Omega_{cb}}{2}\right)^2\right]r^2-\frac{Z_i^2e^2N_b}{\gamma_b^2}\frac{r^2}{r_b^2}, \tag{112}$$

where $N_b=2\pi\int_0^\infty dr r n_b^0(r)=\pi\hat{n}_b r_b^2$ is the number of particles per unit axial length. As noted earlier, the outer beam radius r_b is determined from $V(r_b)=\hat{T}_{\perp b}$, which can be expressed as

$$\left[\left(\frac{\Omega_{cb}}{2}\right)^2-\left(\Omega_b-\frac{\Omega_{cb}}{2}\right)^2\right]r_b^2=\frac{2\hat{T}_{\perp b}}{\gamma_b m}+\frac{2Z_i^2e^2N_b}{\gamma_b^3 m}. \tag{113}$$

Equation (113) can be used to determine the beam radius r_b in terms of Ω_b, $\hat{T}_{\perp b}$, N_b and other system parameters. Because $\langle r^2\rangle=r_b^2/2$ for the uniform density profile in Eq. (110), note that Eq. (113) is similar in form to the constraint conditon obtained in Eq. (78) for the thermal equilibrium distribution f_b^0 in Eq. (71). Furthermore, because $\langle P_\theta\rangle=\gamma_b m(\Omega_{cb}/2-\Omega_b)\langle r^2\rangle$ for the entire class of anisotropic rigid-rotor equilibria described by Eq. (97), the angular rotation term proportional to $(\Omega_b-\Omega_{cb}/2)^2$ in Eq. (113) can be eliminated in favor of $\langle P_\theta\rangle/\gamma_b m\langle r^2\rangle$.

Comparing Eqs. (112) and (113), it follows that $\hat{T}_{\perp b}-V(r)=\hat{T}_{\perp b}(1-r^2/r_b^2)$ in the beam interior ($0\le r<r_b$). Substituting Eq. (108) into Eq. (104) for the transverse pressure

profile, we obtain

$$n_b^0(r)T_{\perp b}(r) = \hat{n}_b \int_0^\infty d\left(\frac{\tilde{p}_\perp^2}{2\gamma_b m}\right) \frac{\tilde{p}_\perp^2}{2\gamma_b m} \delta\left[\frac{\tilde{p}_\perp^2}{2\gamma_b m} - \hat{T}_{\perp b}\left(1 - \frac{r^2}{r_b^2}\right)\right] \tag{114}$$

for $0 \le r < r_b$. Equation (114) readily gives the parabolic temperature profile (Fig. 3)

$$T_{\perp b}(r) = \hat{T}_{\perp b}\left(1 - \frac{r^2}{r_b^2}\right), \quad 0 \le r < r_b, \tag{115}$$

which decreases from a maximum value of $\hat{T}_{\perp b}$ at $r = 0$, to zero at the beam edge ($r = r_b$). Note that $T_{\perp b}(r = r_b) = 0$ is expected for the monoenergetic transverse distribution in Eq. (108) because $r = r_b$ represents the outer envelope of turning points in the transverse orbits.

Step-Function Transverse Distribution

As a third example, we consider the case where the transverse distribution function $F_b(H_\perp + \Omega_b P_\theta)$ is specified by the step-function distribution [17]

$$F_b = \frac{\hat{n}_b}{2\pi\gamma_b m \hat{T}_{\perp b}} U\left(\frac{H_\perp + \Omega_b P_\theta}{\hat{T}_{\perp b}}\right). \tag{116}$$

Here, $\hat{n}_b$ and $\hat{T}_{\perp b}$ are positive constants and $U(x)$ is the unit step-function defined by $U(x) = 1$ for $0 \le x < 1$, and $U(x) = 0$ for $x > 1$. Note that $\hat{T}_{\perp b} = \text{const.}$ is the maximum allowed value of $H_\perp + \Omega_b P_\theta$ in Eq. (116). Substituting Eq. (116) into the expressions for $n_b^0(r)$ and $n_b^0(r)T_{\perp b}(r)$ in Eqs. (103) and (104) readily gives

$$n_b^0(r) = \begin{cases} \hat{n}_b[1 - V(r)/\hat{T}_{\perp b}], & 0 \le r < r_b, \\ 0, & r > r_b, \end{cases} \tag{117}$$

and

$$n_b^0(r)T_{\perp b}(r) = \hat{n}_b \hat{T}_{\perp b}\left[1 - \frac{V(r)}{\hat{T}_{\perp b}}\right]^2 = \frac{\hat{T}_{\perp b}}{\hat{n}_b}[n_b^0(r)]^2 \tag{118}$$

for $0 \le r < r_b$. Here, the outer beam radius r_b is determined from $V(r_b) = \hat{T}_{\perp b}$. Note from Eq. (117), as $V(r)$ increases from zero at $r = 0$ to $V(r_b) = \hat{T}_{\perp b}$ at $r = r_b$, the density decreases from $n_b^0(r = 0) = \hat{n}_b$ to $n_b^0(r = r_b) = 0$. Furthermore, the perpendicular pressure in Eq. (118) scales *double adiabatically*, with $P_{\perp b}(r)$ proportional to $[n_b^0(r)]^2$.

To determine the effective potential $V(r) = (\gamma_b m/2)(\Omega_b\Omega_{cb} - \Omega_b^2)r^2 + (Z_i e/\gamma_b^2)\phi^s(r)$ self-consistently, we substitute Eqs. (116) and (117) into Poisson's equation (105). This readily yields the (linear) Bessel's equation for $V(r)$,

$$\frac{1}{r}\frac{\partial}{\partial r}r\frac{\partial}{\partial r}V = 2\gamma_b m\left[\Omega_b\Omega_{cb} - \Omega_b^2 - \frac{\hat{\omega}_{pb}^2}{2\gamma_b^2}\left(1 - \frac{V}{\hat{T}_{\perp b}}\right)\right] \tag{119}$$

in the beam interior ($0 \leq r < r_b$). Here, $\hat{\omega}_{pb}^2 = 4\pi\hat{n}_b Z_i^2 e^2/\gamma_b m$ is the on-axis plasma frequency-squared. Solving Eq. (119) for $V(r)$, and defining $\lambda_D^2 = \gamma_b^2\hat{T}_{\perp b}/4\pi\hat{n}_b Z_i^2 e^2$, we obtain

$$V(r) = 2\gamma_b m\lambda_D^2\left(\Omega_b\Omega_{cb} - \Omega_b^2 - \frac{\hat{\omega}_{pb}^2}{2\gamma_b^2}\right)\left[I_0\left(\frac{r}{\lambda_D}\right) - 1\right], \quad 0 \leq r < r_b, \tag{120}$$

where $I_0(x)$ is the modified Bessel function of the first kind of order zero. Setting $V(r = r_b) = \hat{T}_{\perp b}$ then gives

$$I_0\left(\frac{r_b}{\lambda_D}\right) = 1 + \frac{\omega_{pb}^2/2\gamma_b^2}{\Omega_b\Omega_{cb} - \Omega_b^2 - \hat{\omega}_{pb}^2/2\gamma_b^2}, \tag{121}$$

which is a nonlinear transcendental equation that determines the normalized beam radius r_b/λ_D self-consistently. Note from Eq. (121) that the beam radius r_b is large in comparison with the effective Debye length λ_D whenever $(\Omega_b\Omega_{cb} - \Omega_b^2)$ is 'closely tuned' to $\hat{\omega}_{pb}^2/2\gamma_b^2$.

Finally, substituting Eqs. (120) and (121) into Eq. (117) gives for the density profile (Fig. 4)

$$n_b^0(r) = \hat{n}_b\frac{I_0(r_b/\lambda_D) - I_0(r/\lambda_D)}{I_0(r_b/\lambda_D) - 1} \tag{122}$$

in the beam interior ($0 \leq r < r_b$), and $n_b^0(r) = 0$ for $r > r_b$. Note from Eq. (122) that $n_b^0(r = 0) = \hat{n}_b$ and $n_b^0(r = r_b) = 0$, as expected. Here, use is made of $I_0(0) = 1$.

As a fourth and final example for a uniform focusing field $B_z(z) = B_0 = \text{const.}$, following development of the density inversion theorem in Sec. IV.C, we will consider the case where the density profile has the *parabolic* form $n_b^0(r) = \hat{n}_b(1 - r^2/r_b^2)$ for $0 \leq r < r_b$.

C. Density Inversion Theorem

For the class of anisotropic beam distributions $f_b^0 = F_b(H_\perp + \Omega_b P_\theta)G(P_z)$ in Eq. (97), the configuration- and mometum-space dependences of f_b^0 are so interconnected [see Eq. (98)]

that a specification of the radial dependence of a macroscopic equilibrium profile, such as the density $n_b^0(r) = \int d^3\vec{p} f_b^0$, is sufficient information to reconstruct the detailed functional form [26] the transverse distribution function $F_b(H_\perp + \Omega_b P_\theta)$. To illustrate this point, we note from Eq. (103) that the density profile $n_b^0(r)$ depends on the radial coordinate r exclusively through the effective potential $V(r) = (\gamma_b m/2)(\Omega_b\Omega_{cb} - \Omega_b^2)r^2 + (Z_i e/\gamma_b^2)\phi^s(r)$ defined in Eq. (67). Taking the derivative of $n_b^0(V)$ with respect to V in Eq. (103) gives

$$\frac{\partial n_b^0}{\partial V} = (2\pi\gamma_b m)\int_0^\infty dU \frac{\partial}{\partial U} F_b[U + V(r)], \tag{123}$$

where the variable $U = \vec{p}_\perp^2/2\gamma_b m$ has been introduced in Eq. (123). Assuming that $F_b[U + V(r)]_{U\to\infty} = 0$, and integrating by parts on the right-hand side of Eq. (123) gives

$$F_b(H_\perp + \Omega_b P_\theta) = -\frac{1}{2\pi\gamma_b m}\left(\frac{\partial n_b^0}{\partial V}\right)_{V=H_\perp+\Omega_b P_\theta} \tag{124}$$

for the transverse distribution function $F_b(H_\perp + \Omega_b P_\theta)$.

The density inversion theorem can be summarized as follows. For specified $n_b^0(r)$ we calculate the electrostatic potential $\phi^s(r)$ from Poisson's equation $r^{-1}(\partial/\partial r)(r\partial\phi^s/\partial r) = -4\pi Z_i e n_b^0(r)$, and the effective potential $V(r)$ from the definition $V(r) = (\gamma_b m/2)(\Omega_b\Omega_{cb} - \Omega_b^2)r^2 + (Z_i e\gamma_b^2)\phi^s(r)$ in Eq. (67). Solving then for r(V), assumed to be monotonic, we evaluate $\partial n_b^0/\partial V = (\partial n_b^0/\partial r)(\partial r/\partial V)$ in Eq. (124), which determines the transverse distribution function $F_b(H_\perp + \Omega_b P_\theta)$.

By any measure, this *density inversion theorem* is a remarkable result, which can be used to determine the (assumed) distribution functions $F_b(H_\perp + \Omega_b P_\theta)$ in Eqs. (106), (108), and (116) from the (derived) density profiles in Eqs. (107), (110) and (122), respectively. To illustrate this point, we consider the *prescribed* parabolic density profile (Fig. 5)

$$n_b^0(r) = \begin{cases} \hat{n}_b(1 - r^2/r_b^2), & 0 \le r < r_b, \\ 0, & r > r_b. \end{cases} \tag{125}$$

Making use of Poisson's equation (105) and the definition of the effective potential $V(r)$ in Eq. (67) gives

$$V(r) = \frac{\gamma_b m}{2}\left[(\Omega_b\Omega_{cb} - \Omega_b^2)r^2 - \frac{\hat{\omega}_{pb}^2 r^2}{2\gamma_b^2}\left(1 - \frac{r^2}{4r_b^2}\right)\right] \tag{126}$$

for $0 \leq r < r_b$. Inverting Eq. (126) for $r^2(V)$ gives

$$\frac{r^2(V)}{r_b^2} = \left[\left(\frac{\Omega_b\Omega_{cb} - \Omega_b^2 - \hat{\omega}_{pb}^2/2\gamma_b^2}{\hat{\omega}_{pb}^2/4\gamma_b^2}\right)^2 + \frac{16V}{\gamma_b m r_b^2 \hat{\omega}_{pb}^2/\gamma_b^2}\right]^{1/2} - \frac{\Omega_b\Omega_{cb} - \Omega_b^2 - \hat{\omega}_{pb}^2/2\gamma_b^2}{\hat{\omega}_{pb}^2/4\gamma_b^2}, \quad (127)$$

where $\hat{\omega}_{pb}^2 = 4\pi\hat{n}_b Z_i^2 e^2/\gamma_b m$. Substituting Eq. (127) into Eq. (125) and evaluating $\partial n_b^0/\partial V$, it is readily shown from the density inversion theorem in Eq. (124) that the transverse distribution function $F_b(H_\perp + \Omega_b P_\theta)$ which is consistent with the parabolic density profile assumed in Eq. (125) is given by

$$F_b = \frac{\hat{n}_b}{2\pi\gamma_b m}\left(\frac{\gamma_b m r_b^2 \hat{\omega}_{pb}^2}{32\gamma_b^2}\right)$$

$$\times \left[\frac{\gamma_b m \hat{\omega}_{pb}^2 r_b^2}{16\gamma_b^2}\left(\frac{\Omega_b\Omega_{cb} - \Omega_b^2 - \hat{\omega}_{pb}^2/2\gamma_b^2}{\hat{\omega}_{pb}^2/4\gamma_b^2}\right)^2 + H_\perp + \Omega_b P_\theta\right]^{-1/2} U\left(\frac{H_\perp + \Omega_b P_\theta}{\hat{T}_{\perp b}}\right). \quad (128)$$

In Eq. (128), $U(x)$ is the unit step-function defined by $U(x) = 1$ for $0 \leq x < 1$, and $U(x) = 0$ for $x > 1$. Note from Eqs. (125)-(128) that the outer beam radius r_b is determined from $V(r_b) = \hat{T}_{\perp b} = \text{const.}$, which can be expressed as

$$\frac{2\hat{T}_{\perp b}}{\gamma_b m} = (\Omega_b\Omega_{cb} - \Omega_b^2)r_b^2 - \frac{3\hat{\omega}_{pb}^2}{8\gamma_b^2} r_b^2. \quad (129)$$

For the parabolic density profile in Eq. (125), the number of particles per unit length is $N_b = 2\pi \int_0^\infty dr r n_b^0(r) = \pi\hat{n}_b r_b^2/2$. Therefore, Eq. (129) can be expressed as

$$\left[\left(\frac{\Omega_{cb}}{2}\right)^2 - \left(\Omega_b - \frac{\Omega_{cb}}{2}\right)^2\right] r_b^2 = \frac{2\hat{T}_{\perp b}}{\gamma_b m} + \frac{3Z_i^2 e^2 N_b}{\gamma_b^3 m}. \quad (130)$$

Note that $\langle r^2 \rangle = r_b^2/3$ for the parabolic density profile in Eq. (125), and that Eq. (130) can be used to determine r_b^2 self-consistently in terms of Ω_b, $\hat{T}_{\perp b}$ and N_b for a broad range of system parameters. Not surprisingly, Eq. (130) is similar in form to Eq. (113) derived for a uniform density beam.

To summarize, the density inversion theorem in Eq. (124) applies to the entire class of anisotropic beam distributions f_b^0 in Eq. (97) and is clearly a very powerful result. For specified density profile $n_b^0(r)$, the corresponding expression for $V(r)$ is inverted to determine

$r(V)$. Equation (124) can then be used to determine directly the transverse distribution function $F_b(H_\perp + \Omega_b P_\theta)$ that self-consistently generates the assumed density profile $n_b^0(r)$.

D. Force Constraint Relating the Mean-Square Radius $\langle r^2 \rangle$ to the Transverse Thermal Emittance

The entire class of anisotropic beam distributions $f_b^0 = F_b(H_\perp + \Omega_b P_\theta)G(P_z)$ in Eq. (97) can be characterized by a universal force constraint condition that relates the mean-square radius $\langle r^2 \rangle$ to the transverse thermal emittance ϵ_{th}, number of beam particles per unit axial length N_b, and angular rotation velocity Ω_b. This constraint condition is analogous to Eqs. (113) and (130) extended to arbitrary choice of $F_b(H_\perp + \Omega_b P_\theta)$.

From Eq. (104) and some straightforward integration by parts, it is readily shown that $\partial P_{\perp b}/\partial r = -n_b^0(r)\partial V(r)/\partial r$, where $V(r)$ is the effective potential defined in Eq. (67), and $P_{\perp b} = n_b^0(r)T_{\perp b}(r)$ is the perpendicular pressure defined in Eq. (102). This gives the condition for local radial force balance, which can be expressed as

$$\frac{\partial P_{\perp b}}{\partial r} = -\gamma_b m n_b^0(\Omega_b \Omega_{cb} - \Omega_b^2)r + \frac{4\pi Z_i^2 e^2}{\gamma_b^2}\frac{n_b^0}{r}\int_0^r dr r n_b^0(r). \tag{131}$$

Here, Poisson's equation (105) has been integrated to give $\partial\phi^s/\partial r = -(4\pi Z_i e/r)\int_0^r dr r n_b^0(r)$, and Eq. (131) is valid for general choice of transverse distribution function $F_b(H_\perp + \Omega_b P_\theta)$. Comparing Eq. (76) and Eq. (102), it is clear that the spatial average of $P_{\perp b}(r)$ and the statistical average $\langle p_r^2 + (p_\theta + \gamma_b m \Omega_b r)^2 \rangle$ are related by

$$2\pi \int_0^\infty dr r P_{\perp b} = \frac{N_b}{2\gamma_b m}\langle p_r^2 + (p_\theta + \gamma_b m \Omega_b r)^2 \rangle = \frac{N_b}{8}\frac{\gamma_b m \beta_b^2 c^2 \epsilon_{th}^2}{\langle r^2 \rangle}, \tag{132}$$

where $\epsilon_{th}^2 = (4/\gamma_b^2 m^2 \beta_b^2 c^2)\langle r^2 \rangle \langle p_r^2 + (p_\theta + \gamma_b m \Omega_b r)^2 \rangle$ is the unnormalized transverse thermal emittance defined in Eq. (80). Returning to Eq. (131), we operate with $2\pi \int_0^\infty dr r^2 \cdots$ and carry out some straightforward integration by parts that assumes $P_{\perp b}(r \to \infty) = 0$. This gives

$$\frac{4\pi}{\gamma_b m N_b}\int_0^\infty dr r P_{\perp b} = (\Omega_b \Omega_{cb} - \Omega_b^2)\langle r^2 \rangle - \frac{Z_i^2 e^2 N_b}{\gamma_b^3 m}, \tag{133}$$

where $\langle r^2 \rangle = (2\pi/N_b)\int_0^\infty dr r^3 n_b^0(r)$ and $N_b = 2\pi\int_0^\infty dr r n_b^0(r)$. Expressing $\Omega_b\Omega_{cb} - \Omega_b^2 = (\Omega_{cb}/2)^2 - (\Omega_b - \Omega_{cb}/2)^2$, and making use of $\langle P_\theta \rangle = \gamma_b m(\Omega_{cb}/2 - \Omega_b)\langle r^2 \rangle$ to eliminate $(\Omega_b - \Omega_{cb}/2)^2$, the constraint condition in Eq. (133) can be expressed in the equivalent form

$$(\Omega_{cb}/2)^2\langle r^2 \rangle - \frac{Z_i^2 e^2 N_b}{\gamma_b^3 m} = \frac{1}{\langle r^2 \rangle}\left[\frac{\langle P_\theta \rangle^2}{\gamma_b^2 m^2} + \frac{1}{4}\beta_b^2 c^2 \epsilon_{th}^2\right], \tag{134}$$

where use has been made of Eq. (132) to express $2\pi\int_0^\infty dr r P_{\perp b}$ in terms of the thermal emittance.

Equation (134) is a powerful constraint condition that relates the mean-square radius $\langle r^2 \rangle$ to N_b, $\langle P_\theta \rangle$ and ϵ_{th} for the entire class of *anistropic* beam equilibria $f_b^0 = F_b(H_\perp + \Omega_b P_\theta)G(P_z)$ in Eq. (97), no matter how complicated the corresponding self-consistent profiles for the density $n_b^0(r)$ and perpendicular pressure $P_{\perp b}(r)$. Indeed, because the local radial force balance equations (91) and (131) are identical in form, the constraint condition in Eq. (134) also applies to the entire class of isotropic beam equilibria $f_b^0 = f_b^0(H - V_b P_z + \Omega_b P_\theta)$ in Eq. (65). Finally, only in the special case where $\langle P_\theta \rangle = 0$ and $\Omega_b = \Omega_{cb}/2$ is the term proportional to $\langle P_\theta \rangle^2$ absent in Eq. (134).

V. INTENSE BEAM EQUILIBRIA IN A PERIODIC FOCUSING SOLENOIDAL FIELD

A. Theoretical Model and Basic Equations

We now consider the case of a periodic focusing solenoidal field $B_z(s+S) = B_z(s)$ described by Eq. (7), and employ the formalism developed in Sec. III.B that utilizes the nonlinear Vlasov-Poisson equations (35) and (47) to advance the distribution function $f_b^0(x, P_x; y, P_y; -H, s)$ and the normalized effective potential $\psi(x, y, s) = (Z_i e/\gamma_b^3 m\beta_b^2 c^2)$ $\times \phi^s(x, y, s)$. Here, the characteristics of the nonlinear Vlasov equation (35) are given in Eqs. (39)-(42), and the transverse particle orbits $x(s)$ and $y(s)$ satisfy Eqs. (45) and (46). As discussed in Sec. III.B, the advantage of transforming to the new canonical variables $(x, P_x; y, P_y; t, -H; s)$ is that for time-stationary equilibria with $\partial\phi^s/\partial t = 0$ and $\partial f_b/\partial t = 0$, it necessarily follows that $d(-H)/ds = 0$. The formalism developed in Sec. III.B, while consistent with the thin-beam approximation in Sec. II, is otherwise quite general and can incorporate a (small) spread in axial momentum p_z or total energy H of the beam particles. [See discussion following Eqs. (36) and (37) where $p_b(H) = \gamma_b m\beta_b c$ depends on H.] For our purposes here, however, we specialize to the case where the spread in H is negligibly small and express

$$f_b^0(x, P_x; y, P_y; -H, s) = \beta_b(H)\delta(H - \hat{\gamma}_b mc^2)\tilde{F}_b(x, P_x; y, P_y; s), \tag{135}$$

where $\hat{\gamma}_b = \text{const.}$, and $H = \gamma_b(H)mc^2 = [m^2c^4 + c^2p_b^2(H)]^{1/2}$ and $\beta_b(H) = [1 - \gamma_b^{-2}(H)]^{1/2}$. From Eq. (31) or Eq. (38), for a thin beam with small transverse momentum consistent with Eqs. (9) and (13), it follows from Eq. (135) that

$$\int dp_z f_b^0 = \int dH \frac{\partial p_z}{\partial H} f_b^0 = \tilde{F}_b(x, P_x; y, P_y; s), \tag{136}$$

where use has been made of Eq. (31) and

$$\frac{\partial p_z}{\partial H} \cong \frac{H/c}{(H^2/c^2 - m^2c^2)^{1/2}} = \frac{1}{\beta_b(H)}. \tag{137}$$

Substituting Eq. (135) into Eq. (35) and operating with $\int dp_z \cdots = \int dH(\partial p_z/\partial H)\cdots$ then gives for the evolution of the reduced distribution function $\tilde{F}_b(x, P_x; y, P_y; s)$

$$\frac{\partial \tilde{F}_b}{\partial s} + x' \frac{\partial \tilde{F}_b}{\partial x} + y' \frac{\partial \tilde{F}_b}{\partial y} + P_x' \frac{\partial \tilde{F}_b}{\partial P_x} + P_y' \frac{\partial \tilde{F}_b}{\partial P_y} = 0. \tag{138}$$

Here, the characteristics x', y', P_x' and P_y' of Eq. (138) are defined by Eqs. (39)-(42) (for simplicity of notation, we drop the 'hat' on $\hat{\gamma}_b$ and $\hat{\beta}_b$), and $\psi(x, y, s) = (Z_i e/\gamma_b^3 m\beta_b^2 c^2)\phi^s(x, y, s)$ solves Eq. (47), where the beam density $n_b(x, y, s) = \int d^3\vec{p} f_b^0$ is expressed in terms of $\tilde{F}_b$ as

$$n_b(x, y, s) = \int dP_x dP_y \tilde{F}_b. \tag{139}$$

For notational simplicity in the analysis of Eq. (138), it is convenient to introduce the normalized transverse canonical momenta defined by $\hat{P}_x \equiv P_x/\gamma_b m\beta_b c$ and $\hat{P}_y \equiv P_y/\gamma_b m\beta_b c$, and the normalized transverse Hamiltonian $\hat{H}_\perp = H_\perp/\gamma_b mc$ defined by [see Eq. (38)]

$$\hat{H}_\perp = \frac{1}{2}[\hat{P}_x + y\sqrt{\kappa_z(s)}]^2 + \frac{1}{2}[\hat{P}_y - x\sqrt{\kappa_z(s)}]^2 + \psi(x, y, s). \tag{140}$$

In Eq. (140), $\sqrt{\kappa_z(s)} = Z_i e B_z(s)/2\gamma_b m\beta_b c^2$ is the solenoidal coupling coefficient defined in Eq. (43), and $\psi(x, y, s) = (Z_i e/\gamma_b^3 m\beta_b^2 c^2)\phi^s(x, y, s)$ is the normalized potential defined in Eq. (44). We readily find from $dx/ds = \partial\hat{H}_\perp/\partial\hat{P}_x$ and $d\hat{P}_x/ds = -\partial\hat{H}_\perp/\partial x$,

$$\frac{dx}{ds} = \hat{P}_x + y\sqrt{\kappa_z(s)}, \tag{141}$$

$$\frac{d\hat{P}_x}{ds} = -\frac{\partial\psi}{\partial x} + \sqrt{\kappa_z(s)}[\hat{P}_y - x\sqrt{\kappa_z(s)}], \tag{142}$$

and from $dy/ds = \partial\hat{H}_\perp/\partial\hat{P}_y$ and $d\hat{P}_y/ds = -\partial\hat{H}_\perp/\partial y$,

$$\frac{dy}{ds} = \hat{P}_y - x\sqrt{\kappa_z(s)}, \tag{143}$$

$$\frac{d\hat{P}_y}{ds} = -\frac{\partial\psi}{\partial y} - \sqrt{\kappa_z(s)}[\hat{P}_x + y\sqrt{\kappa_z(s)}]. \tag{144}$$

Equations (141)-(144), derived from the transverse Hamiltonian in Eq. (140), are equivalent to the dynamical equations (39)-(42) obtained in Sec. III.B, but are now expressed in terms

of the convenient quantities $\hat{P}_x$ and $\hat{P}_y$, $\kappa_z(s)$, and ψ. We further express Eq. (138) in terms of the variables $(x, \hat{P}_x; y, \hat{P}_y; s)$ and introduce the distribution function F_b defined by

$$F_b(x, \hat{P}_x; y, \hat{P}_y; s) = (\gamma_b m \beta_b c)^2 \tilde{F}_b, \tag{145}$$

which is scaled by the constant factor $(\gamma_b m \beta_b c)^2$ relative to $\tilde{F}_b$. Making use of Eqs. (139) and (145) to express $n_b = \int dP_x dP_y \tilde{F}_b = \int d\hat{P}_x d\hat{P}_y F_b$, the nonlinear Vlasov-Poisson equations (47) and (138) become

$$\frac{\partial F_b}{\partial s} + x' \frac{\partial F_b}{\partial x} + y' \frac{\partial F_b}{\partial y} + \hat{P}'_x \frac{\partial F_b}{\partial \hat{P}_x} + \hat{P}'_y \frac{\partial F_b}{\partial \hat{P}_y} = 0, \tag{146}$$

and

$$\left(\frac{\partial^2}{\partial x^2} + \frac{\partial^2}{\partial y^2} \right) \psi = - \frac{4\pi Z_i^2 e^2}{\gamma_b^3 m \beta_b^2 c^2} \int d\hat{P}_x d\hat{P}_y F_b. \tag{147}$$

Equation (146) describes the nonlinear evolution of the distribution function $F_b(x, \hat{P}_x; y, \hat{P}_y; s)$ determined self-consistently in terms of $\psi(x, y, s)$ from Poisson's equation (147). Moreover, the characteristics x', $\hat{P}'_x$, y' and $\hat{P}'_y$ of the nonlinear Vlasov equation (146) are given directly in terms of $(x, \hat{P}_x; y, \hat{P}_y; s)$ by Eqs. (141)-(144). Equations (146) and (147) have a wide range of applicability consistent with the thin-beam approximation and the (albert restrictive) assumption of negligibly small spread in total energy H and axial momentum spread made in Eqs. (135)-(137). No assumption of azimuthal symmetry $(\partial/\partial\theta = 0)$ has yet been made in Eqs. (146) and (147).

It was noted briefly in Sec. III.B that simplifications occur in the transverse orbit equations by transforming to the Larmor frame of reference rotating with normalized angular velocity $\Omega_L(s) = d\theta_L/ds \equiv -\sqrt{\kappa_z(s)}$ relative to the laboratory frame. We now perform a canonical transformation from laboratory-frame variables $(x, \hat{P}_x; y, \hat{P}_y)$ to Larmor-frame variables $(\tilde{x}, \tilde{P}_x; \tilde{y}, \tilde{P}_y)$ by introducing the generating function

$$F_2(\tilde{x}, \tilde{P}_x; \tilde{y}, \tilde{P}_y; s) = [x \cos\theta_L(s) + y \sin\theta_L(s)]\tilde{P}_x + [-x \sin\theta_L(s) + y \cos\theta_L(s)]\tilde{P}_y, \tag{148}$$

where $\theta_L(s) = -\int_{s_0}^{s} ds \sqrt{\kappa_z(s)}$. The generating function in Eq. (148) defines the transforma-

tion

$$\begin{aligned} \tilde{x} &= \partial F_2/\partial \tilde{P}_x = x\cos\theta_L + y\sin\theta_L, \\ \tilde{y} &= \partial F_2/\partial \tilde{P}_y = -x\sin\theta_L + y\cos\theta_L, \end{aligned} \tag{149}$$

and

$$\begin{aligned} \hat{P}_x &= \partial F_2/\partial x = \tilde{P}_x\cos\theta_L - \tilde{P}_y\sin\theta_L, \\ \hat{P}_y &= \partial F_2/\partial y = \tilde{P}_x\sin\theta_L + \tilde{P}_y\cos\theta_L, \end{aligned} \tag{150}$$

or equivalently,

$$\begin{aligned} \tilde{P}_x &= \hat{P}_x\cos\theta_L + \hat{P}_y\sin\theta_L, \\ \tilde{P}_y &= -\hat{P}_x\sin\theta_L + \hat{P}_y\cos\theta_L. \end{aligned} \tag{151}$$

The new perpendicular Hamiltonian in the Larmor frame is $\tilde{H}_\perp = \hat{H}_\perp + \partial F_2/\partial s$ expressed in Larmor-frame variables $(\tilde{x}, \tilde{P}_x; \tilde{y}, \tilde{P}_y)$. From Eq. (148) and $d\theta_L/ds = -\sqrt{\kappa_z(s)}$, we obtain

$$\frac{\partial F_2}{\partial s} = -\sqrt{\kappa_z}(-x\sin\theta_L + y\cos\theta_L)\tilde{P}_x + \sqrt{\kappa_z}(x\cos\theta_L + y\sin\theta_L)\tilde{P}_y = \sqrt{\kappa_z}(x\hat{P}_y - y\hat{P}_x), \tag{152}$$

where use is made of Eq. (150). From Eqs. (140) and (152), it follows that

$$\tilde{H}_\perp = \hat{H}_\perp + \frac{\partial F_2}{\partial s} = \frac{1}{2}(\hat{P}_x^2 + \hat{P}_y^2) + \frac{1}{2}\kappa_z(x^2 + y^2) + \psi. \tag{153}$$

Making use of Eqs. (149) and (151) to express $\hat{P}_x^2 + \hat{P}_y^2 = \tilde{P}_x^2 + \tilde{P}_y^2$ and $x^2 + y^2 = \tilde{x}^2 + \tilde{y}^2$, the new transverse Hamiltonian $\tilde{H}_\perp$ expressed in Larmor-frame variables is given by

$$\tilde{H}_\perp(\tilde{x}, \tilde{P}_x; \tilde{y}, \tilde{P}_y; s) = \frac{1}{2}(\tilde{P}_x^2 + \tilde{P}_y^2) + \frac{1}{2}\kappa_z(s)(\tilde{x}^2 + \tilde{y}^2) + \psi(\tilde{x}, \tilde{y}, s). \tag{154}$$

The equations of motion in the Larmor frame are given by $d\tilde{x}/ds = \partial\tilde{H}_\perp/\partial\tilde{P}_x$, $d\tilde{P}_x/ds = -\partial\tilde{H}_\perp/\partial\tilde{x}$, $d\tilde{y}/ds = \partial\tilde{H}_\perp/\partial\tilde{P}_y$ and $d\tilde{P}_y/ds = -\partial\tilde{H}_\perp/\partial\tilde{y}$. From Eq. (154) we readily obtain

$$\frac{d\tilde{x}}{ds} = \tilde{P}_x, \quad \frac{d\tilde{P}_x}{ds} = -\kappa_z\tilde{x} - \frac{\partial\psi}{\partial\tilde{x}}, \tag{155}$$

$$\frac{d\tilde{y}}{ds} = \tilde{P}_y, \quad \frac{d\tilde{P}_y}{ds} = -\kappa_z\tilde{y} - \frac{\partial\psi}{\partial\tilde{y}}. \tag{156}$$

The nonlinear Vlasov-Poisson equations (146) and (147) for $F_b(\tilde{x}, \tilde{P}_x; \tilde{y}, \tilde{P}_y; s)$ and $\psi(\tilde{x}, \tilde{y}, s)$ in Larmor-frame variables become

$$\frac{\partial F_b}{\partial s} + \tilde{x}'\frac{\partial F_b}{\partial\tilde{x}} + \tilde{y}'\frac{\partial F_b}{\partial\tilde{y}} + \tilde{P}_x'\frac{\partial F_b}{\partial\tilde{P}_x} + \tilde{P}_y'\frac{\partial F_b}{\partial\tilde{P}_y} = 0, \tag{157}$$

$$\left(\frac{\partial^2}{\partial\tilde{x}^2}+\frac{\partial^2}{\partial\tilde{y}^2}\right)\psi = -\frac{4\pi Z_b^2 e^2}{\gamma_b^3 m\beta_b^2 c^2}\int d\tilde{P}_x d\tilde{P}_y F_b. \tag{158}$$

The characteristics $\tilde{x}'$, $\tilde{y}'$, $\tilde{P}_x'$ and $\tilde{P}_y'$ of the nonlinear Vlasov equation (157) are defined in terms of $(\tilde{x}, \tilde{P}_x; \tilde{y}, \tilde{P}_y; s)$ by Eqs. (155) and (156). Therefore, Eq. (157) can be expressed in the equivalent form

$$\frac{\partial F_b}{\partial s}+\tilde{P}_x\frac{\partial F_b}{\partial\tilde{x}}+\tilde{P}_y\frac{\partial F_b}{\partial\tilde{y}}-\left(\kappa_x\tilde{x}+\frac{\partial\psi}{\partial\tilde{x}}\right)\frac{\partial F_b}{\partial\tilde{P}_x}-\left(\kappa_y\tilde{y}+\frac{\partial\psi}{\partial\tilde{y}}\right)\frac{\partial F_b}{\partial\tilde{P}_y}=0, \tag{159}$$

where $\psi(\tilde{x}, \tilde{y}, s)$ is determined in terms of $F_b(\tilde{x}, \tilde{P}_x; \tilde{y}, \tilde{P}_y; s)$ by means of Poisson's equation (158).

The Vlasov-Poisson equations (158) and (159) can be used to investigate the nonlinear evolution of the distribution function F_b in the four-dimensional phase space $(\tilde{x}, \tilde{P}_x; \tilde{y}, \tilde{P}_y)$ for a wide range of system parameters and 'initial' conditions (at $s = s_0$, say). Indeed, Eqs. (158) and (159) generally allow for both radial ($\partial/\partial\tilde{r} \neq 0$) and azimuthal ($\partial/\partial\tilde{\theta} \neq 0$) variations in the effective potential ψ and distribution function F_b.

B. Vlasov-Poisson Description for Azimuthally Symmetric Beam Propagation ($\partial/\partial\tilde{\theta} \equiv 0$)

In the remainder of Sec. V, we specialize to the case where the distribution function F_b and effective potencial ψ are azimuthally symmetric ($\partial/\partial\tilde{\theta} \equiv 0$), i.e., depend on $\tilde{x}$ and $\tilde{y}$ exclusively through the radial coordinate $\tilde{r} \equiv (\tilde{x}^2+\tilde{y}^2)^{1/2}$. As noted in Sec. III.B, this leads to several simplifications in the transverse particle dynamics [see Eqs. (52)-(56)], and therefore in the nonlinear Vlasov-Poisson equations (158) and (159). For $\partial/\partial\tilde{\theta} \equiv 0$, it follows that $\psi = \psi(\tilde{r}, s)$, and $\partial\psi/\partial\tilde{x} \equiv (\tilde{x}/\tilde{r})\partial\psi/\partial\tilde{r}$ and $\partial\psi/\partial\tilde{y} \equiv (\tilde{y}/\tilde{r})\partial\psi/\partial\tilde{r}$. Therefore, from the orbit equations (155) and (156) it is readily shown that

$$\frac{d}{ds}\tilde{P}_\theta = \frac{d}{ds}(\tilde{x}\tilde{P}_y - \tilde{y}\tilde{P}_x) = 0, \tag{160}$$

corresponding to conservation of canonical angular momentum $\tilde{P}_\theta$ (in the Larmor frame). Two options are available for analyzing Eqs. (158) and (159) when $\partial/\partial\tilde{\theta} = 0$. One approach

is to transform directly to the variables $(\tilde{r}, \tilde{P}_r; \tilde{\theta}, \tilde{P}_\theta; s)$ in cylindrical coordinates, imposing $\partial\psi/\partial\tilde{\theta} = 0 = \partial F_b/\partial\tilde{\theta}$ *ab initio*. The other is to continue the analysis of Eq. (159) in a Cartesian representation, imposing the condition that $\psi = \psi(\tilde{r}, s)$. We discuss these two approaches separately.

First, transforming directly to a cylindrical representation, we express $\tilde{P}_x^2 + \tilde{P}_y^2 = \tilde{P}_r^2 + \tilde{P}_\theta^2/\tilde{r}^2$ and $\tilde{r}^2 = \tilde{x}^2 + \tilde{y}^2$ in the expression for the perpendicular Hamiltonian $\tilde{H}_\perp$ in Eq. (154). This gives

$$\tilde{H}_\perp(\tilde{r}, \tilde{P}_r; \tilde{\theta}, \tilde{P}_\theta; s) = \frac{1}{2}\left(\tilde{P}_r^2 + \frac{\tilde{P}_\theta^2}{\tilde{r}^2}\right) + \frac{1}{2}\kappa_z(s)\tilde{r}^2 + \psi(\tilde{r}, s). \tag{161}$$

The equations of motion are $d\tilde{r}/ds = \partial\tilde{H}_\perp/\partial\tilde{P}_r$, $d\tilde{P}_r/ds = -\partial\tilde{H}_\perp/\partial\tilde{r}$, $d\tilde{\theta}/ds = \partial\tilde{H}_\perp/\partial\tilde{P}_\theta$ and $d\tilde{P}_\theta/ds = -\partial\tilde{H}_\perp/\partial\tilde{\theta}$. Because $\partial\tilde{H}_\perp/\partial\tilde{\theta} = 0$, this readily gives

$$\frac{d\tilde{r}}{ds} = \tilde{P}_r, \quad \frac{d\tilde{P}_r}{ds} = -\kappa_z\tilde{r} + \frac{\tilde{P}_\theta^2}{\tilde{r}^3} - \frac{\partial\psi}{\partial\tilde{r}} \tag{162}$$

$$\frac{d\tilde{\theta}}{ds} = \frac{\tilde{P}_\theta}{\tilde{r}^2}, \quad \frac{d}{ds}\tilde{P}_\theta = 0. \tag{163}$$

Note from Eq. (163) that $d\tilde{P}_\theta/ds = 0$, as expected. For azimutally symmetric beam distributions with $\partial F_b/\partial\tilde{\theta} = 0$, it follows from Eqs. (159), (162) and (163) that the nonlinear Vlasov equation for $F_b(\tilde{r}, \tilde{P}_r; \tilde{P}_\theta; s)$ can be expressed as

$$\frac{\partial F_b}{\partial s} + \tilde{P}_r\frac{\partial F_b}{\partial\tilde{r}} - \left(\kappa_z\tilde{r} - \frac{\tilde{P}_\theta^2}{\tilde{r}^3} + \frac{\partial\psi}{\partial\tilde{r}}\right)\frac{\partial F_b}{\partial\tilde{P}_r} = 0, \tag{164}$$

where $\kappa_z(s + S) = \kappa_z(s)$ generally depends on s, and $\psi(\tilde{r}, s)$ is determined self-consistently from Poisson's equation

$$\frac{1}{\tilde{r}}\frac{\partial}{\partial\tilde{r}}\tilde{r}\frac{\partial\psi}{\partial\tilde{r}} = -\frac{4\pi Z_i^2 e^2}{\gamma_b^3 m\beta_b^2 c^2}\frac{1}{\tilde{r}}\int d\tilde{P}_r d\tilde{P}_\theta F_b. \tag{165}$$

Here, use has been made of $\int d\tilde{P}_x d\tilde{P}_y \cdots = \tilde{r}^{-1}\int d\tilde{P}_r d\tilde{P}_\theta \cdots$. There are some advantages to the cylindrical representation used in Eqs. (164) and (165). First, Eq. (164) takes explicit advantage, from the outset, of the fact that $\tilde{P}_\theta$ is a single-particle constant of the motion when $\partial/\partial\tilde{\theta} = 0$. Second, the characteristics of Eq. (164) involve calculation of the radial orbits in the *two-dimensional* phase space $(\tilde{r}, \tilde{P}_r)$. Indeed, Eq. (164) is particularly well suited to

integration using the method of characteristics (see Sec. V.D for a brief discussion). Finally, Eq. (164) can readly be used to describe equilibrium properties ($\partial/\partial s = 0$) for intense beam propagation parallel to a *uniform* focusing field with $\kappa_z(s) = \kappa_{z0} = \text{const.}$ (independent of s). For s-independent $\psi(\tilde{r})$, it follows from Eq. (161) that $\tilde{H}_\perp$ (as well as $\tilde{P}_\theta$) is an exact single-particle constant of the motion ($d\tilde{H}_\perp/ds = 0$). In this case the *equilibrium* beam distribution ($\partial F_b^0/\partial s = 0$) can be constructed from the single-particle constants of the motion $\tilde{H}_\perp$ and $\tilde{P}_\theta$ with $F_b^0 = F_b^0(\tilde{H}_\perp, \tilde{P}_\theta)$ (see also the discussion in Sec. III.A). That is, $F_b^0(\tilde{H}_\perp, \tilde{P}_\theta)$ solves the nonlinear Vlasov equation (164) exactly, because $(d/ds)F_b^0(\tilde{H}_\perp, \tilde{P}_\theta) = 0$ whenever $d\tilde{H}_\perp/ds = 0 = d\tilde{P}_\theta/ds$. In this regard, is should be noted that distributions of the form $F_b^0(\tilde{H}_\perp + \tilde{\Omega}_b\tilde{P}_\theta)$, where $\tilde{\Omega}_b = \text{const.}$, correspond exactly to the class of rigid-rotor Vlasov-equilibria considered in Sec. IV.B. Here, of course, $-\tilde{\Omega}_b = \text{const.}$ is the (appropriately normalized) angular rotation velocity *in the Larmor frame.*

We now return to the Cartesian representation of the nonlinear Vlasov equation in Eq. (159), allowing for axial variation of $\kappa_z(s + S) = \kappa(s)$, but assuming $\partial\psi/\partial\tilde{\theta} = 0$, i.e., $\psi = \psi(\tilde{r}, s)$. Making use of $\partial\psi/\partial\tilde{x} = (\tilde{x}/\tilde{r})\partial\psi/\partial\tilde{r}$ and $\partial\psi/\partial\tilde{y} = (\tilde{y}/\tilde{r})\partial\psi/\partial\tilde{r}$, the Vlasov equation (159) can be expressed as

$$\frac{\partial F_b}{\partial s} + \tilde{P}_x\frac{\partial F_b}{\partial \tilde{x}} + \tilde{P}_y\frac{\partial F_b}{\partial \tilde{y}} - \left(\kappa_z\tilde{x} + \frac{1}{\tilde{r}}\frac{\partial\psi}{\partial\tilde{r}}\tilde{x}\right)\frac{\partial F_b}{\partial \tilde{P}_x} - \left(\kappa_z\tilde{y} + \frac{1}{\tilde{r}}\frac{\partial\psi}{\partial\tilde{r}}\tilde{y}\right)\frac{\partial F_b}{\partial \tilde{P}_y} = 0. \tag{166}$$

The characteristics of Eq. (166) are identical to the orbit equations (54) and (55) for $\tilde{x}(s)$ and $\tilde{y}(s)$. Following Courant and Snyder [28], it is convenient when analyzing the particle motion to express the transverse orbits as

$$\tilde{x}(s) = Aw(s)\cos\left(\int_{s_0}^{s}\frac{ds}{w^2(s)} + \phi_0\right), \quad \tilde{y}(s) = Aw(s)\sin\left(\int_{s_0}^{s}\frac{ds}{w^2(s)} + \phi_0\right), \tag{167}$$

where A and ϕ_0 are constants (independent of s) and $w(s)$ is the so-called *envelope function.* Note from Eq. (167) that

$$\tilde{r}^2(s) = \tilde{x}^2(s) + \tilde{y}^2(s) = A^2w^2(s). \tag{168}$$

The equation advancing $w(s)$ is readily obtained by substituting the expression for $\tilde{x}(s)$ or $\tilde{y}(s)$ in Eq. (167) into Eq. (54) or Eq. (55). For example, it follows from Eq. (167) that the

$\tilde{x}$-motion satisties

$$\frac{d\tilde{x}}{ds} = A\frac{dw}{ds}\cos\left(\int_{s_0}^{s}\frac{ds}{w^2(s)} + \phi_0\right) - \frac{A}{w}\sin\left(\int_{s_0}^{s}\frac{ds}{w^2(s)} + \phi_0\right) = \frac{1}{w}\frac{dw}{ds}\tilde{x} - \frac{1}{w^2}\tilde{y}, \tag{169}$$

$$\frac{d^2\tilde{x}}{ds^2} = A\left(\frac{d^2w}{ds^2} - \frac{1}{w^3}\right)\cos\left(\int_{s_0}^{s}\frac{ds}{w^2(s)} + \phi_0\right) = \frac{1}{w}\left(\frac{d^2w}{ds^2} - \frac{1}{w^3}\right)\tilde{x}. \tag{170}$$

Analogous equations can be obtained for $d\tilde{y}/ds$ and $d^2\tilde{y}/ds^2$. Substituting Eq. (170) into Eq. (54), and defining the self-field coupling coefficient $\kappa_s(s)$ by

$$\kappa_s(s) = -\left[\frac{1}{\tilde{r}}\frac{\partial}{\partial\tilde{r}}\psi(\tilde{r},s)\right]_{\tilde{r}=Aw(s)}, \tag{171}$$

it follows directly that the envelope function $w(s+S) = w(s)$ solves

$$\frac{d^2}{ds^2}w(s) + [\kappa_z(s) - \kappa_s(s)]w(s) = \frac{1}{w^3(s)}. \tag{172}$$

Equation (172) can also be obtained in a similar manner by substituting the espression for $\tilde{y}(s)$ in Eq. (167) into Eq. (55). In the special case where the density profile is radially uniform with $n_b(\tilde{r},s) = \hat{n}_b(s) = N_b/\pi r_b^2(s)$ for $0 \le \tilde{r} < r_b(s)$, and $n_b(\tilde{r},s) = 0$ for $\tilde{r} > r_b(s)$, we note from Poisson's equation (158), when $\partial\psi/\partial\tilde{\theta} = 0$, that $\psi = -(1/2)(K/r_b^2)\tilde{r}^2$ in the beam interior ($0 \le \tilde{r} < r_b$). Here, $K = 2N_bZ_i^2e^2/\gamma_b^3m\beta_b^2c^2$ is the self-field perveance, and $N_b = 2\pi\int_0^\infty d\tilde{r}\,\tilde{r}\,n_b$ is the number of particles per unit axial length. In this case, the expression for $\kappa_s(s)$ in Eq. (171) reduces to the familiar result $\kappa_s(s) = K/r_b^2(s)$. In general, however, for *nonuniform* density profile $n_b(\tilde{r},s)$, the coefficient $\kappa_s(s)$ in Eq. (171) depends explicity on $Aw(s)$, thereby increasing the complexity and nonlinearity of Eq. (172) for the envelope function $w(s)$.

The azimuthal symmetry of $\psi(\tilde{r},s)$ places powerful constraints on the transverse orbits $\tilde{x}(s)$ and $\tilde{y}(s)$. Denoting $\tilde{x}' = d\tilde{x}/ds$, $\tilde{y}' = d\tilde{y}/ds$, and $w' = dw/ds$, it is readily shown from Eq. (167) that

$$\tilde{x}^2 + \tilde{y}^2 = w^2A^2,$$

$$\tilde{x}'^2 + \tilde{y}'^2 = \left(w'^2 + \frac{1}{w^2}\right)A^2,$$

$$\frac{\tilde{x}^2}{w^2} + w^2\left(\tilde{x}' - \frac{w'}{w}\tilde{x}\right)^2 = A^2, \tag{173}$$
$$\frac{\tilde{y}^2}{w^2} + w^2\left(\tilde{y}' - \frac{w'}{w}\tilde{y}\right)^2 = A^2,$$
$$x\tilde{y}' - y\tilde{x}' = A^2.$$

Here, $A =$ const., and $w(s+S) = w(s)$ solves the nonlinear envelope equation (172). Note that the constraint condition $x\tilde{y}' - y\tilde{x}' = A^2$ in Eq. (173) corresponds to conservation of canonical angular momentum. In addition, the third and fourth constraints conditions in Eq. (173) corresponds to conservation of the phase space area (equal to πA^2) in the phase spaces $(\tilde{x}, \tilde{x}')$ and $(\tilde{y}, \tilde{y}')$ for the $\tilde{x}$- and $\tilde{y}$-orbits. Here, for radially nonuniform density profile $n_b(\tilde{r}, s)$, we reiterate that the solution for $w(s)$ obtained from Eq. (172) generally depends on A, as evident from the expression for $\kappa_s(s)$ and Eq. (171).

We now perform a canonical transformation from Larmor-frame variables $(\tilde{x}, \tilde{P}_x; \tilde{y}, \tilde{P}_y)$ to new variables $(X, P_X; Y, P_Y)$ by introducing the generating function F_2 defined by

$$F_2(\tilde{x}, P_X; \tilde{y}, P_Y; s) = \frac{\tilde{x}}{w}\left(P_X + \frac{\tilde{x}}{2}\frac{dw}{ds}\right) + \frac{\tilde{y}}{w}\left(P_Y + \frac{\tilde{y}}{2}\frac{dw}{ds}\right), \tag{174}$$

where the envelope function $w(s)$ solves Eq. (172). The generating function in Eq. (174) defines the transformation

$$X = \frac{\partial F_2}{\partial P_X} = \frac{\tilde{x}}{w}, \quad Y = \frac{\partial F_2}{\partial P_Y} = \frac{\tilde{y}}{w}, \tag{175}$$

and

$$\tilde{P}_x = \frac{\partial F_2}{\partial \tilde{x}} = \frac{1}{w}\left(P_X + \tilde{x}\frac{dw}{ds}\right), \quad \tilde{P}_y = \frac{\partial F_2}{\partial \tilde{y}} = \frac{1}{w}\left(P_Y + \tilde{y}\frac{dw}{ds}\right). \tag{176}$$

The new Hamiltonian $H_\perp$ expressed in the variables $(X, P_X; Y, P_Y; s)$ is given by $H_\perp = \tilde{H}_\perp + \partial F_2/\partial s$, where $\tilde{H}_\perp$ and F_2 are defined in Eqs. (154) and (174), respectively. Evaluating $\partial F_2/\partial s$ from Eq. (174) and making use of the expression for $\tilde{H}_\perp$ in Eq. (154), we obtain for $H_\perp(X, P_X; Y, P_Y; s)$

$$H_\perp = \frac{1}{2w^2}(P_X^2 + P_Y^2) + \psi + \frac{1}{2}w^2(X^2 + Y^2)\left[\frac{1}{w}\frac{d^2w}{ds^2} + \kappa_z(s)\right]. \tag{177}$$

Here, use has been made of Eqs. (175) and (176) to eliminate $(\tilde{x}, \tilde{P}_x; \tilde{y}, \tilde{P}_y)$ in favor of $(X, P_X; Y, P_Y)$. Making use of Eq. (172) to express $w^{-1}\, d^2w/ds^2 + \kappa_x(s) = \kappa_s(s) + 1/w^4$, Eq. (177) becomes

$$H_\perp(X, P_X; Y, P_Y; s) = \frac{1}{2w^2(s)}(P_X^2 + P_Y^2 + X^2 + Y^2) + \delta\psi\Big(w(s)R, s\Big). \tag{178}$$

Here, from Eq. (171) and (177), the effective potential $\delta\psi$ occuring in Eq. (178) is defined by

$$\delta\psi(wR, s) \equiv \left[\psi(\tilde{r}, s) - \frac{1}{2}\tilde{r}\frac{\partial}{\partial\tilde{r}}\psi(\tilde{r}, s)\right]_{\tilde{r}=wR} = -\frac{1}{2}\left\{\tilde{r}^3\frac{\partial}{\partial\tilde{r}}\left[\frac{1}{\tilde{r}^2}\psi(\tilde{r}, s)\right]\right\}_{\tilde{r}=wR} \tag{179}$$

and $R^2 = (X^2 + Y^2) = (\tilde{x}^2 + \tilde{y}^2)/w^2(s) = \tilde{r}^2/w^2(s)$ follows from Eq. (175). It should be emphasized that $\delta\psi$ is directly related to the radial nonuniformity in the density profile $n_b(\tilde{r}, s)$. For example, if F_b corresponds to the Kapchinskij-Vladimirskij (KV) distribution [24], then the density profile is radially uniform with $n_b(\tilde{r}, s) = \hat{n}_b(s) = N_b/\pi r_b^2(s)$ for $0 \le \tilde{r} < r_b(s)$, and $n_b(\tilde{r}, s) = 0$ for $r > r_b(s)$. As noted in the discussion following Eq. (172), for this case $\psi(\tilde{r}, s) = -(1/2)(K/r_b^2)\tilde{r}^2$ in the beam interior ($0 \le \tilde{r} < r_b$), and therefore $\delta\psi = 0$ follows directly from Eq. (179). Consequently, the term proportional to $\delta\psi$ in Eq. (176) should be viewed as a measure of the departure of the system from a KV-like beam distribution with characteristic step-function density profile and parabolic potential ($\psi \propto \tilde{r}^2$) in the beam interior.

The equations of motion in terms of the new variables $(X, P_X; Y, P_Y)$ are given by $dX/ds = \partial H_\perp/\partial P_X$, $dP_X/ds = -\partial H_\perp/\partial X$, $dY/ds = \partial H_\perp/\partial P_Y$ and $dP_Y/ds = -\partial H_\perp/\partial Y$, where $H_\perp(X, P_X; Y, P_Y; s)$ is defined in Eq. (178). For azimuthally symmetric $\delta\psi(wR, s)$, if follows that $\partial\delta\psi/\partial X = (X/R)\partial\delta\psi/\partial R$ and $\partial\delta\psi/\partial Y = (Y/R)\partial\delta\psi/\partial R$. Therefore, the orbit equations become

$$\frac{dX}{ds} = \frac{P_X}{w^2(s)}, \quad \frac{dP_X}{ds} = -\frac{X}{w^2(s)} - \frac{X}{R}\frac{\partial\delta\psi}{\partial R}, \tag{180}$$

$$\frac{dY}{ds} = \frac{P_Y}{w^2(s)}, \quad \frac{dP_Y}{ds} = -\frac{Y}{w^2(s)} - \frac{Y}{R}\frac{\partial\delta\psi}{\partial R}, \tag{181}$$

where $R = (X^2 + Y^2)^{1/2}$, $\delta\psi\big(w(s)R, s\big)$ is defined in Eq. (179), and the envelope function $w(s+S) = w(s)$ solves Eq. (172). In terms of the new variables, the nonlinear Vlasov equation (166) gives for the evolution of $F_b(X, P_X; Y, P_Y; s)$

$$\frac{\partial F_b}{\partial s} + \frac{P_X}{w^2}\frac{\partial F_b}{\partial X} + \frac{P_Y}{w^2}\frac{\partial F_b}{\partial Y} - \left(\frac{X}{w^2} + \frac{X}{R}\frac{\partial \delta\psi}{\partial R}\right)\frac{\partial F_b}{\partial P_X} - \left(\frac{Y}{w^2} + \frac{Y}{R}\frac{\partial \delta\psi}{\partial R}\right)\frac{\partial F_b}{\partial P_Y} = 0. \qquad (182)$$

The effective potential $\delta\psi$ occuring in the characteristics of Eq. (182) is defined in terms of $\psi(\tilde{r}, s)$ by Eq. (179), which is determined self-consistently in terms of $F_b(X, P_X; Y, P_Y; s)$ from Poissons equation (158). Making use of Eq. (176) to express $\int d\tilde{P}_x d\tilde{P}_y \cdots = w^{-2}(s) \int dP_X dP_Y \cdots$, Eq. (158) becomes

$$\frac{1}{\tilde{r}}\frac{\partial}{\partial \tilde{r}}\tilde{r}\frac{\partial \psi}{\partial \tilde{r}} = -\frac{4\pi Z_i e^2}{\gamma_b^3 m \beta_b^2 c^2}\frac{1}{w^2(s)}\int dP_X dP_Y F_b \qquad (183)$$

for azimuthally symetric $\psi(\tilde{r}, s)$. Equations (182) and (183), together with the definition of $\delta\psi$ in Eq. (179) then provide a closed description of the nonlinear evolution of the system in the new variables $(X, P_X; Y, P_Y; s)$.

It was noted earlier, for the azimuthally aymmetric case considered here, there are often advantages to working directly in variables appropriate to cylindrical coordinates. [See the discussion leading to the cylindrical representation of the nonlinear Vlasov-Poisson equations (164) and (165) in the Larmor frame.] Therefore, to conclude Sec. V.B, we summarize briefly the appropriate transformations leading to the cylindrical analogue of Eqs. (182) and (183) in the new variables $(R, P_R; \Theta, P_\Theta; s)$. Specifically, we transform from the Larmor frame variables $(\tilde{r}, \tilde{P}_r; \tilde{\theta}, \tilde{P}_\theta, s)$ used in Eqs. (161)-(165) to the new variables $(R, P_R; \Theta, P_\Theta; s)$ by introducing the generating function F_2 defined by

$$F_2(\tilde{r}, P_r; \tilde{\theta}, P_\Theta; s) = \frac{1}{w}\tilde{r}P_R + \tilde{\theta}P_\Theta + \frac{\tilde{r}^2}{2w}\frac{dw}{ds}, \qquad (184)$$

where the envelope function $w(s+S) = w(s)$ solves Eq. (172). The generating function in Eq. (184) defines the transformation

$$R = \frac{\partial F_2}{\partial P_R} = \frac{\tilde{r}}{w}, \quad \Theta = \frac{\partial F_2}{\partial P_\Theta} = \tilde{\theta}, \qquad (185)$$

$$\tilde{P}_r = \frac{\partial F_2}{\partial \tilde{r}} = \frac{P_R}{w} + \frac{\tilde{r}}{w}\frac{dw}{ds}, \quad \tilde{P}_\theta = \frac{\partial F_2}{\partial \tilde{\theta}} = P_\Theta. \tag{186}$$

The new Hamiltonian $H_\perp(R, P_R; \Theta, P_\Theta; s)$ is given by $H_\perp = \tilde{H}_\perp + \partial F_2/\partial s$, where $\tilde{H}_\perp$ is defined in Larmor-frame variables by Eq. (161), and F_2 is defined in Eq. (184). Some straightforward algebra shows that

$$H_\perp = \frac{1}{2w^2}\left(P_R^2 + \frac{P_\Theta^2}{R^2}\right) + \psi + \frac{1}{2}w^2R^2\left[\frac{1}{w}\frac{d^2w}{ds^2} + \kappa_z(s)\right]. \tag{187}$$

Making use of Eq. (172) to eliminate $w^{-1}d^2w/ds^2 + \kappa_z$ in Eq. (187) readly gives

$$H_\perp(R, P_R; \Theta, P_\Theta; s) = \frac{1}{2w^2(s)}\left(P_R^2 + \frac{P_\Theta^2}{R^2} + R^2\right) + \delta\psi\Big(w(s)R, s\Big). \tag{188}$$

Here, the envelope function $w(s)$ solves Eq. (172), and $\delta\psi(wR, s)$ is defined in terms of $\psi(\tilde{r}, s)$ by Eq. (179). In the new variables, the equations of motion are $dR/ds = \partial H_\perp/\partial P_R$, $dP_R/ds = -\partial H_\perp/\partial R$, $d\Theta/ds = \partial H_\perp/\partial P_\Theta$, and $dP_\Theta/ds = -\partial H_\perp/\partial\Theta$. Because $\partial H_\perp/\partial\Theta = 0$, this gives

$$\frac{dR}{ds} = \frac{P_R}{w^2(s)}, \quad \frac{dP_R}{ds} = -\frac{1}{w^2(s)}\left(R - \frac{P_\Theta^2}{R^3}\right) - \frac{\partial\delta\psi}{\partial R}, \tag{189}$$

$$\frac{d\Theta}{ds} = \frac{P_\Theta}{w^2(s)R^2}, \quad \frac{dP_\Theta}{ds} = 0. \tag{190}$$

Therefore, making use of Eqs. (189) and (190), and assuming an azimuthally symmetric beam distribution with $\partial F_b/\partial\Theta = 0$, the distribution function $F_b(R, P_R; P_\Theta; s)$ evolves according to the nonlinear Vlasov equation

$$\frac{\partial F_b}{\partial s} + \frac{P_R}{w^2}\frac{\partial F_b}{\partial R} - \left[\frac{1}{w^2}\left(R - \frac{P_\Theta^2}{R^3}\right) + \frac{\partial\delta\psi}{\partial R}\right]\frac{\partial F_b}{\partial P_R} = 0. \tag{191}$$

Equation (191) should be compared with the cylindrical representation of the Vlasov equation in Eq. (164) in the Larmor-frame. As before, the particularly simple form of Eq. (191) when compared with the Cartesian representation in Eq. (182) has to do with the fact that azimuthal symmetry ($\partial/\partial\Theta = 0$) and the constancy of P_Θ are incorporated *ab initio* in Eq. (191). The effective potential $\delta\psi(wR, s)$ occurring in Eq. (191) is defined in terms of $\psi(\tilde{r}, s)$ by Eq. (179), and $w(s + S) = w(s)$ solves Eq. (172). Making use of Eq. (185) and

(186) to express $(1/\tilde{r})\int d\tilde{P}_r d\tilde{P}_\theta \cdots = (1/w^2 R)\int dP_R dP_\Theta \cdots$, the Poisson's equation (165) can be expressed as

$$\frac{1}{\tilde{r}}\frac{\partial}{\partial \tilde{r}}\tilde{r}\frac{\partial \psi}{\partial \tilde{r}} = -\frac{4\pi Z_i^2 e^2}{\gamma_b^3 m \beta_b^2 c^2}\frac{1}{w^2(s)R}\int dP_R dP_\Theta F_b. \tag{192}$$

Equation (192) relates $F_b(R, P_R; P_\Theta; s)$ in the new variables to $\psi(\tilde{r}, s)$, which in turn can be used to determine the effective potential $\delta\psi(wR, s)$ defined in Eq. (179).

To summarize, in Sec. V.A we have presented a variety of representations of the nonlinear Vlasov-Poisson equations for axisymmetric beam propagation ($\partial/\partial\tilde{\theta} = 0$) through a periodic focusing solenoidal field $B_z(s + S) = B_z(s)$. These include both cylindrical representations in Larmor-frame variables [Eq. (164)] and in tranformed variables [Eq. (191)], and Cartesian representations in Larmor-frame variables [Eq. (166)] and in transformed variables [Eq. (182)]. These equations have a wide range of applicability to beam distributions with radially nonuniform density profile $n_b(r, s)$. Which representation is most appropriate to use depends on the particular numerical or analytical technique that is best suited to the specific application under consideration.

C. Periodically Focused Rigid-Rotor Vlasov Equilibria

We now make use of the theoretical formalism developed in Sec. V.B to consider a specific example of azimuthally symmetric, periodically focused beam distributions F_b.

As an example, we consider the case where the density profile is radially uniform over the beam cross section with

$$n_b(\tilde{r}, s) = \begin{cases} N_b/\pi r_b^2(s), & 0 \le \tilde{r} < r_b(s), \\ 0, & \tilde{r} > r_b(s). \end{cases} \tag{193}$$

Here, $r_b(s + S) = r_b(s)$ is the outer radial envelope of the beam, and $N_b = 2\pi\int_o^\infty d\tilde{r}\,\tilde{r} n_b =$ const. is the number of particles per unit axial length. In this case, it follows from Poisson's equation for $\psi(\tilde{r}, s)$ [see, for example, Eq. (158)] that

$$\psi(\tilde{r}, s) = -\frac{K}{2r_b^2(s)}\tilde{r}^2 \tag{194}$$

in the beam interior, $0 \leq \tilde{r} < r_b(s)$. In Eq. (194), $K = 2N_b Z_i^2 e^2/\gamma_b^3 m\beta_b^2 c^2$ is the self-field perveance. Substituting Eq. (194) into Eqs. (171) and (179) readily gives $\kappa_s(s) = -K/r_b^2(s)$, and

$$\delta\psi(wR, s) = 0. \tag{195}$$

Equation (172) for the envelope function $w(s+S) = w(s)$ then becomes

$$\frac{d^2}{ds^2}w(s) + \left[\kappa_z(s) - \frac{K}{r_b^2(s)}\right] w(s) = \frac{1}{w^3(s)} \tag{196}$$

for the choice of step-function density profile in Eq. (193).

We choose to consider this example within the context of the nonlinear Vlasov-Poisson equations (191) and (192) expressed in the transformed cylindrical variables $(R, P_R; \Theta, P_\Theta; s)$. The question posed is what choice of azimuthally symmetric distribution function $F_b(R, P_R; P_\Theta; s)$ generates self-consistently the density profile in Eq. (193). Here, from Eq. (192), the density profile can be expressed in terms of $F_b(R, P_R; P_\Theta; s)$ by

$$n_b(\tilde{r}, s) = \frac{1}{w^2(s)R}\int dP_R dP_\Theta F_b. \tag{197}$$

For $\delta\psi(wR, s) = 0$, the Hamiltonian in Eq. (188) becomes $H_\perp = (1/2)(P_R^2 + P_\Theta^2/R^2 + R^2)/w^2(s)$, and the orbit equations in Eq. (189) and the characteristics of the nonlinear Vlasov equation (191) undergo corresponding simplification. Particularly important, while the perpendicular Hamiltonian is *not* a conserved quantity ($dH_\perp/ds \neq 0$, in general), the scaled energy variable $\mathcal{H}_\perp \equiv w^2(s)H_\perp$ *is* conserved, where

$$\mathcal{H}_\perp = \frac{1}{2}\left(P_R^2 + \frac{P_\Theta^2}{R^2}\right) + \frac{1}{2}R^2. \tag{198}$$

This follows trivially from the orbit equations for $P_R(s)$ and $R(s)$ in Eq. (189), which give

$$\frac{d}{ds}\mathcal{H}_\perp = P_R\frac{dP_R}{ds} + \frac{dR}{ds}\left(R - \frac{P_\Theta^2}{R^3}\right) = 0. \tag{199}$$

Here, use has been made of $\delta\psi = 0$ and $dP_\Theta/ds = 0$. Therefore, any distribution $F_b(R, P_R; P_\Theta; s) = F_b^0(\mathcal{H}_\perp, P_\Theta)$ that depends on R, P_R and P_Θ exclusively through $\mathcal{H}_\perp$ and P_Θ, necessarily satisfies the nonlinear Vlasov equation (191) ($dF_b/ds = 0$), and is also an

equilibrium solution to Eq. (191) with $\partial F_b/\partial s = 0$. This is true provided $F_b^0(\mathcal{H}_\perp, P_\Theta)$ *also* generates self-consistently the step-function density profile $n_b(\tilde{r}, s)$ assumed in Eq. (193).

The only known distribution function F_b^0 that self-consistently generate the density profile in Eq. (193) is

$$F_b^0(\mathcal{H}_\perp, P_\Theta) = \frac{N_b}{2\pi^2\epsilon_T}\delta\left[\mathcal{H}_\perp + \omega_b P_\Theta - \frac{1}{2}(1-\omega_b^2)\epsilon_T\right]. \tag{200}$$

Here, $|\omega_b| < 1$ is a constant parameter that measures the mean rotation of the beam in the Larmor frame, and ϵ_T =const. is the effective unnormalized transverse emittance, which includes both the directed transverse motion of the beam particles, as well as the random (or 'thermal') motion relative to the mean. Equation (200), recently considered by Chen, Pakter and Davidson [23], is an important generalization of the rigid-rotor Vlasov equilibrium in Eq. (108) (where $\partial/\partial s = 0$) to the case of a periodic focusing solenoidal field $B_z(s+S) = B_z(s)$, as well as an important generalization of the Kapchinskij-Vladimirskij distribution [24] to allow for an average beam rotation in the Larmor frame ($\omega_b \neq 0$). Making use of the definition of $\mathcal{H}_\perp$ in Eq. (198), the argument of the δ-function in Eq. (200) can be expressed as

$$\mathcal{H}_\perp + \omega_b P_\Theta - \frac{1}{2}(1-\omega_b^2)\epsilon_T = \frac{1}{2}\left[P_R^2 + \left(\frac{P_\Theta}{R} + \omega_b R\right)^2\right] - \frac{1}{2}(1-\omega_b^2)\epsilon_T\left(1 - \frac{R^2}{\epsilon_T}\right). \tag{201}$$

Substituting Eqs. (200) and (201) into the expression for the density profile $n_b(\tilde{r}, s)$ in Eq. (197) gives, after some strightforward algebra,

$$n_b(\tilde{r}, s) = \begin{cases} N_b/\pi w^2(s)\epsilon_T, & 0 \leq R/\epsilon_T^{1/2} < 1, \\ 0, & R/\epsilon_T^{1/2} > 1. \end{cases} \tag{202}$$

Equation (202) is identical to the assumed density profile in Eq. (193) provided $r_b(s)$ and $w(s)$ are related by

$$r_b(s) = \epsilon_T^{1/2} w(s). \tag{203}$$

Here, from Eq. (185), keep in mind that $R = \tilde{r}/w$, so that $R/\epsilon_T^{1/2} = \tilde{r}/\epsilon_T^{1/2} w = \tilde{r}/r_b(s)$. Therefore $0 \leq R/\epsilon_T^{1/2} < 1$ in Eq. (202) corresponds to $0 \leq \tilde{r} < r_b(s)$, as required by

Eq. (193). Substituting $w(s) = r_b(s)/\epsilon_T^{1/2}$ from Eq. (203) into Eq. (196), readily gives the familiar equation [25]

$$\frac{d^2}{ds^2} r_b(s) + \left[\kappa_z(s) - \frac{K}{r_b^2(s)}\right] r_b(s) = \frac{\epsilon_T^2}{r_b^3(s)} \tag{204}$$

for the beam envelope $r_b(s+S) = r_b(s)$. Equation (204) can be solved numerically for a broad range of functional forms of $\kappa_z(s+S) = \kappa_z(s)$, and choices of system parameters K and ϵ_T.

Having shown that the choice of $F_b^0(\mathcal{H}_\perp, P_\Theta)$ in Eq. (200) self-consistently generate the step-function density profile in Eq. (193), we now determine other statistical properties of the beam equilibrium distribution in Eq. (200). The *average* of the phase-function ψ *in the Larmor frame*, over the momentum space variables (P_R, P_Θ), is defined by

$$\langle \Psi \rangle_L \equiv \frac{1}{n_b(\tilde{r}, s) w^2(s) R} \int dP_R dP_\Theta \, \Psi \, F_b^0. \tag{205}$$

Making use of Eqs. (186), (200) and (201), some straightforward algebra shows that

$$\langle \tilde{P}_\theta \rangle_L = \langle P_\Theta \rangle_L = -\omega_b R^2 = -\omega_b \frac{\tilde{r}^2}{w^2(s)} = -\frac{\epsilon_T \omega_b}{r_b^2(s)} \tilde{r}^2, \tag{206}$$

$$\langle \tilde{P}_r \rangle_L = \left\langle \frac{P_R}{w} + \frac{\tilde{r}}{w}\frac{dw}{ds} \right\rangle_L = \frac{1}{w}\frac{dw}{ds}\tilde{r} = \frac{r_b'(s)}{r_b(s)}\tilde{r}, \tag{207}$$

where $r_b'(s) = dr_b(s)/ds$. Here, use has been made of $\epsilon_T^{1/2} w(s) = r_b(s)$ and $R = \tilde{r}/w = \epsilon_T^{1/2}\tilde{r}/r_b$. From Eq. (190), the average angular rotation velocity in the Larmor frame is $\langle \Theta' \rangle_L = \langle P_\Theta / w^2 R^2 \rangle = \langle P_\Theta \rangle / \tilde{r}^2 = -\epsilon_T \omega_b / r_b^2(s)$. Transforming to the *laboratory frame*, and using *dimensional units*, we scale velocity variables by $\beta_b c$, and make use of $\tilde{r} = r$ and the fact that Larmor frame rotates with angular velocity, $-\Omega_{cb}(s)/2 \equiv -Z_i e B_z(s)/2\gamma_b mc$, relative to the laboratory frame [see Eq. (148) and related discussion]. It readily follows that the average macroscopic beam velocity in the laboratory frame can be expressed as (with $r = \tilde{r}$)

$$\vec{V}_b(\vec{x}, s) = \beta_b c \frac{r_b'(s)}{r_b(s)} r\vec{e}_r - \Omega_b(s) r \vec{e}_\theta + \beta_b c \vec{e}_z, \tag{208}$$

where the angular rotation velocity $\Omega_b(s)$ is defined by

$$\Omega_b(s) = \frac{Z_i e B_z(s)}{2\gamma_b mc} + \frac{\epsilon_T \beta_b c}{r_b^2(s)}\omega_b. \tag{209}$$

From Eq. (208), the average radial velocity is $V_{rb}(r,s) = \beta_b c r r_b'(s)/r_b(s)$, which is slowly modulated as a function of s as the beam envelope $r_b(s+S) = r_b(s)$ oscillates. Also from Eq. (208), the average azimuthal velocity in the laboratory frame is $V_{\theta b}(r,s) = -\Omega_b(s) r$, corresponding to a rigid rotation at angular velocity $-\Omega_b(s)$. This is similar to the property obtained for the class of rigid-rotor Vlasov equilibria considered in Sec. IV for a uniform solenoidal field, with the essential difference that the angular rotation velocity $\Omega_b(s+S) = \Omega_b(s)$ is modulated by the periodic variation in the focusing field $B_z(s)$ and beam envelope $r_b(s)$.

A further interesting property of the beam distribution in Eq. (200) is the effective transverse temperature $T_{\perp b}(\tilde{r},s)$ associated with the average kinetic energy relative to the mean. Comparing Eqs. (161), (186), (206) and (207), it follows that the transverse kinetic energy $K_{\perp r}$ of a beam particle *relative to the mean* can be expressed (in dimensional units) in the Larmor frame as

$$\begin{aligned} K_{\perp r} &= \frac{1}{2}\gamma_b m\beta_b^2 c^2 \left[\left(\tilde{P}_r - \langle \tilde{P}_r \rangle_L\right)^2 + \frac{1}{\tilde{r}}\left(\tilde{P}_\theta - \langle \tilde{P}_\theta \rangle_L\right)^2\right] \\ &= \frac{1}{2}\gamma_b m\beta_b^2 c^2 \left[\frac{1}{w^2(s)} P_R^2 + \frac{1}{w^2(s)R^2}(P_\Theta + \omega_b R^2)^2\right]. \end{aligned} \tag{210}$$

The effective transverse temperature is then defined in terms of the beam distribution $F_b^0(\mathcal{H}_\perp, P_\Theta)$ in Eq. (200) by $T_{\perp b}(\tilde{r},s) = \langle K_{\perp r}\rangle_L$, i.e.,

$$T_{\perp b}(\tilde{r},s) = \frac{1}{n_b(\tilde{r},s)w^2(s)R}\int dP_R dP_\Theta\, K_{\perp r}\, F_b^0. \tag{211}$$

Substituting Eqs. (200), (201) and (210) into Eq. (211) readily gives

$$T_{\perp b}(\tilde{r},s) = (1-\omega_b^2)\frac{\epsilon_T \gamma_b m\beta_b^2 c^2}{2w^2(s)}\left(1 - \frac{R^2}{\epsilon_T}\right) = T_{\perp b}(\tilde{r}=0,s)\left[1 - \frac{\tilde{r}^2}{r_b^2(s)}\right] \tag{212}$$

in the beam interior, $0 \le \tilde{r} < r_b(s)$. Here, use has been made of $wR = \tilde{r}$ and $r_b(s) = \epsilon_T^{1/2} w(s)$ and the on-axis temperature is defined by

$$T_{\perp b}(\tilde{r}=0,s) \equiv (1-\omega_b^2)\frac{\gamma_b m\beta_b^2 c^2 \epsilon_T^2}{2r_b^2(s)}. \tag{213}$$

The parabolic transverse temperature profile in Eq. (212) is identical in form to that obtained in Sec. IV.B for a monoenergetic transverse distribution of beam particles in a uniform focusing field. The important difference, however, is that the on-axis beam temperature $T_{\perp b}(\tilde{r}=0,s)$ is modulated by the periodic oscilation of the beam envelope $r_b(s+S)=r_b(s)$. Note from Eq. (213) that $T_{\perp b}(\tilde{r}=0,s)r_b^2(s)=$ const. (independent of s).

We have implied that the constant ϵ_T occuring in the definition of $F_b^0(\mathcal{H}_\perp, P_\Theta)$ in Eq. (200) can be identified with the unnormalized transverse emittance in the Larmor frame. In this regard, the statistical average of an azimuthally symmetric phase function ψ (with $\partial\psi/\partial\Theta=0$) over the *four-dimensional phase space* $(R,P_R;\Theta,P_\Theta)$ is defined by

$$\langle\psi\rangle_\Gamma=\frac{\int dRRdP_RdP_\Theta\psi F_b^0}{\int dRRdP_RdP_\Theta F_b^0}. \tag{214}$$

The unnormalized transverse emittance ϵ in the Larmor frame is defined by

$$\epsilon\equiv 2\left[\left\langle\tilde{P}_r^2+\frac{\tilde{P}_\theta^2}{\tilde{r}^2}\right\rangle_\Gamma\left\langle\tilde{r}^2\right\rangle_\Gamma-\left\langle\tilde{r}\tilde{P}_r\right\rangle_\Gamma^2\right]^{1/2}, \tag{215}$$

where $\tilde{P}_r=w^{-1}(P_R+\tilde{r}\,dw/ds)$ and $\tilde{P}_\theta=P_\Theta$ follow from Eq. (186). Some straightforward algebra that makes use of Eq. (186), $\langle P_R\rangle_\Gamma=0$ and $\langle P_\Theta+\omega_bR^2\rangle_\Gamma=0$, shows that Eq. (215) can be expressed as

$$\begin{aligned}\epsilon &= 2\left[\left\langle P_R^2+\frac{1}{R^2}(P_\Theta+\omega_bR^2)^2+\omega_b^2R^2\right\rangle_\Gamma\left\langle R^2\right\rangle_\Gamma\right]^{1/2}\\ &= 2\left[\left\langle(1-\omega_b^2)\epsilon_T\left(1-\frac{R^2}{\epsilon_T}\right)+\omega_b^2R^2\right\rangle_\Gamma\left\langle R^2\right\rangle_\Gamma\right]^{1/2},\end{aligned} \tag{216}$$

where use has been made of Eqs. (200) and (201). As $\tilde{r}$ ranges from $\tilde{r}=0$ to $\tilde{r}=r_b(s)$, the intergration variable R covers the interval $0\le R<\sqrt{\epsilon_T}$ [compare Eqs. (193) and (202)]. Therefore, $\langle R^2\rangle_\Gamma=(\int_0^{\sqrt{\epsilon_T}}dRRR^2)/(\int_0^{\sqrt{\epsilon_T}}dRR)=\epsilon_T/2$ follows from Eq. (214), and Eq. (216) reduces to

$$\epsilon=\epsilon_T, \tag{217}$$

which is the expected result. Note that $d\epsilon/ds=d\epsilon_T/ds=0$, and the transverse emittance is a conserved quantity.

It is also convenient to introduce an unnormalized transverse *thermal emittance* ϵ_{th} in the Larmor frame, which is proportional to the transverse phase space area, subtracting out the average azimuthal and radial motions. The thermal emittance can be expressed as

$$\begin{aligned}\epsilon_{th} &= 2\left[\left\langle\frac{2K_{\perp r}}{\gamma_b m\beta_b^2c^2}\right\rangle_\Gamma\left\langle\tilde{r}^2\right\rangle_\Gamma\right]^{1/2} \\ &= 2\left[\left\langle\left(\tilde{P}_r-\langle\tilde{P}_r\rangle_L\right)^2+\frac{1}{\tilde{r}^2}\left(\tilde{P}_\theta-\langle\tilde{P}_\theta\rangle_L\right)^2\right\rangle_\Gamma\left\langle\tilde{r}^2\right\rangle_\Gamma\right]^{1/2} \\ &= 2\left[\left\langle P_R^2+\frac{1}{R^2}\left(P_\Theta+\omega_bR^2\right)^2\right\rangle_\Gamma\left\langle R^2\right\rangle_\Gamma\right]^{1/2},\end{aligned} \tag{218}$$

where use has been made of Eqs. (186), (206), (207) and (210). Comparing Eq. (218) with Eq. (216), and making use of $\langle R^2\rangle_\Gamma = \epsilon_T/2$, Eq. (218) readily gives

$$\epsilon_{th} = 2\left[\left\langle(1-\omega_b^2)\epsilon_T\left(1-\frac{R^2}{\epsilon_T}\right)\right\rangle_\Gamma\left\langle R^2\right\rangle_\Gamma\right]^{1/2} = (1-\omega_b^2)^{1/2}\epsilon_T, \tag{219}$$

where averages $\langle\cdots\rangle_\Gamma$ are defined in Eq. (214) and are over the distribution F_b^0 in Eq. (200). Because $\epsilon_{th}^2 = (1-\omega_b^2)\epsilon_T^2$, it is clear that the thermal emittance ϵ_{th} is similar to ϵ_T, subtracting out the directed azimuthal motion in the Larmor frame (proportional to ω_b^2).

The envelope equation (204) can be expressed in an alternate form by making use of $\epsilon_T^2 = \epsilon_{th}^2 + \omega_b^2\epsilon_T^2$ and Eq. (209) to express

$$\epsilon_T^2 = \epsilon_{th}^2 + \frac{r_b^4(s)}{\beta_b^2c^2}\left[\Omega_b(s)-\frac{\Omega_{cb}(s)}{2}\right]^2, \tag{220}$$

where $\Omega_{cb}(s) = Z_ieB_z(s)/\gamma_bmc$, and $\Omega_b(s)$ is the angular rotation velocity in the laboratory frame. Substituting Eq. (220) into Eq. (204) and making use of $\kappa_z(s) = (\Omega_{cb}/2\beta_bc)^2$ the envelope equation for $r_b(s)$ can also be expressed as

$$\frac{d^2}{ds^2}r_b(s)+\left\{\frac{1}{\beta_b^2c^2}\left[\left(\frac{\Omega_{cb}}{2}\right)^2-\left(\Omega_b(s)-\frac{\Omega_{cb}(s)}{2}\right)^2\right]-\frac{K}{r_b^2(s)}\right\}r_b(s) = \frac{\epsilon_{th}^2}{r_b^3(s)}. \tag{221}$$

Equation (221) is identical in content to Eq. (204), but connects more directly to the results and notation in Sec. IV. For the special case of a uniform solenoidal field with $\Omega_{cb}(s)$ and $\Omega_b(s)$ constant (independent of s) and $d^2r_b/ds^2 = 0$, the envelope equation (221) resuces exactly to the radial force balance equation (113) obtained in Sec. IV.B for the choice of equilibrium

distribution function in Eq (108). Here, we make the identification $2\hat{T}_{\perp b}/\gamma_b m\beta_b^2 c^2 = \epsilon_{th}^2/r_b^2$ in Eq. (113), which also follows from Eq. (213) and $\epsilon_{th}^2 = (1-\omega_b^2)\epsilon_T^2$.

The example of the periodically focused, rotating beam equilibrium $F_b^0(\mathcal{H}_\perp, P_\Theta)$ considered in Eq. (200) has the important feature that the corresponding self-consistent density profile $n_b(\tilde{r}, s)$ is the step-function profile in Eq. (193), with uniform density $N_b/\pi r_b^2(s)$ in the beam interior, $0 \leq \tilde{r} < r_b(s)$, and outer radial envelope $r_b(s+S) = r_b(s)$ described by Eq. (204). Consequently, the effective potentioal $\delta\psi$ defined in Eq. (179) is $\delta\psi = 0$, which leads to corresponding simplifications in the analysis of the nonlinear Vlasov equation (191). While other specific examples of periodically focused equilibrium solutions to Eqs. (191) and (192) have not yet been determined when $\delta\psi \neq 0$ and the radial density profile is nonuniform, it should be emphasized that the cylindrical representation in the transformed variables $(R, P_R; \Theta, P_\Theta; s)$ in Eqs. (191) and (192), together with the orbit equations in Eqs. (189) and (190), are particularly well-suited to analytical and numerical investigations of self-consistent distributions F_b which depart from the ideal beam equilibrium F_b^0 in Eq. (200).

D. The Method of Characteristics

The *method of characteristics* [26] is a well-estabilished technique used in plasma physics to integrate the nonlinear Vlasov equation and express the solution in terms of "*initial*" conditions. This technique can be applied directly to the form of the Vlasov equation in Eq. (159) which allows F_b and ψ to depend both on $\tilde{r}$ and $\tilde{\theta}$, or to the various forms of the Vlasov equation developed in Sec. V.B for the case of azimuthally symmetric beam propagation with $\partial/\partial\tilde{\theta} = 0$. For a brief summary of the method of characteristics, we now examine the cylindrical representation of the nonlinear Vlasov-Poisson equations given by Eqs. (164) and (165) in the Larmor frame. Here, $\partial/\partial\tilde{\theta} = 0$ is assumed, and the orbit equations in Eqs. (162) and (163) are the characteristics of the Vlasov equation (164).

In Eqs. (162) and (163), we denote the effective 'time' (really 'axial') variable by s', and the corresponding tranverse *orbits* by $\tilde{r}'(s')$, $\tilde{P}_r'(s')$, $\tilde{\theta}'(s')$ and $\tilde{P}_\theta'(s')$. From Eq. (162), the

radial orbits $\tilde{r}'(s')$ and $\tilde{P}_r'(s')$ are determined from

$$\frac{d^2}{ds'^2}\tilde{r}'(s') + \kappa_z(s')\tilde{r}'(s') = \frac{\tilde{P}_\theta^2}{\tilde{r}'^3(s')} - \frac{\partial}{\partial \tilde{r}'}\psi(\tilde{r}', s'),$$

$$\tilde{P}_r'(s') = \frac{d}{ds'}\tilde{r}'(s'). \tag{222}$$

Because $d\tilde{P}_\theta'(s')/ds' = 0$, it follows from Eq. (163) that

$$\tilde{P}_\theta'(s') = \tilde{P}_\theta = \text{const.}, \tag{223}$$

which is independent of s'. We now consider the solutions for the orbits $\tilde{r}'(s')$ and $\tilde{P}_r'(s')$ in Eq. (222) that pass through the *phase-space point* $(\tilde{r}, \tilde{P}_r)$ at 'time' $s' = s$. That is, Eq. (222) is solved subject to the boundary conditions

$$\tilde{r}'(s' = s) = \tilde{r}, \quad \left[\frac{d}{ds'}\tilde{r}'(s')\right]_{s=s'} = \tilde{P}_r. \tag{224}$$

We further consider the function $F_b[\tilde{r}'(s'), \tilde{P}_r'(s'); \tilde{P}_\theta'(s'); s']$ that satisfies

$$\frac{d}{ds'}F_b[\tilde{r}'(s'), \tilde{P}_r'(s'); \tilde{P}_\theta'(s'); s'] = 0. \tag{225}$$

Making use of Eq. (222), and the chain rule to evaluate $(d/ds)F_b(\tilde{r}', \tilde{P}_r'; \tilde{P}_\theta'; s')$, it readily follows that Eq. (225) can be expressed as

$$\left[\frac{\partial}{\partial s'} + \frac{d\tilde{r}'}{ds'}\frac{\partial}{\partial \tilde{r}'} - \left(\kappa_z\tilde{r}' - \frac{\tilde{P}_\theta^2}{\tilde{r}'^3} + \frac{\partial\psi}{\partial\tilde{r}'}\right)\frac{\partial}{\partial \tilde{P}_r'}\right] F_b(\tilde{r}', \tilde{P}_r'; \tilde{P}_\theta'; s') = 0. \tag{226}$$

In Eq. (226), the radial orbits $\tilde{r}'(s')$ and $\tilde{P}_r'(s')$ solve Eq. (222), and $\psi(\tilde{r}', s')$ is determined self-consistently from Poisson's equation (165). Most importantly, when Eq. (226) is *evaluated at* $s = s'$ and use is made of Eq. (224), it follows that Eq. (226) corresponds *exactly* to the nonlinear Vlasov equation (164), where $\tilde{r}$ and $\tilde{P}_r$ are *phase-space variables.*

The formal solution to the Vlasov equation is obtained as follows. From Eq. (225), it follows that

$$F_b[\tilde{r}'(s'), \tilde{P}_r'(s'); \tilde{P}_\theta'(s'); s'] = \text{const. (independent of } s'), \tag{227}$$

which is simply a statement that F_b is constant following the particle motion in the total (applied plus self-consistent) field configuration. Therefore, evaluating Eq. (227) at $s' = s$,

where $(\tilde{r}', \tilde{P}_r') = (\tilde{r}, \tilde{P}_r)$ from Eq. (224), and also evaluating Eq. (227) at some *initial* $s' = s_0$, we obtain for the distribution function at arbitraby $(\tilde{r}, \tilde{P}_r; \tilde{P}_\theta; s)$,

$$F_b(\tilde{r}, \tilde{P}_r; \tilde{P}_\theta; s) = F_b[\tilde{r}'(s' = s_0), \tilde{P}_r'(s' = s_0); \tilde{P}_\theta'; s' = s_0]. \tag{228}$$

Equation (228) formally determines $F_b(\tilde{r}, \tilde{P}_r; \tilde{P}_\theta; s)$ in terms the 'initial' distribution function at $s' = s_0$. The procedure to determine (e.g., numerically) the solution to the nonlinear Vlasov equation (164) is therefore the following. First, specify the functional form of the initial distribution function at $s' = s_0$. Then, make use of the orbit equations (222) to determine the orbits $\tilde{r}'(s')$ and $\tilde{P}_r'(s')$ that pass through the phase-space point $(\tilde{r}, \tilde{P}_r)$ at $s' = s$ [see Eq. (224)]. Finally, evaluate $\tilde{r}'(s' = s_0)$ and $\tilde{P}_r'(s' = s_0)$, and make use of Eq. (228) to determine $F_b(\tilde{r}, \tilde{P}_r; \tilde{P}_\theta; s)$ in terms of the initial distribution function.

Although the method of characteristics has been illustrated for the nonlinear Vlasov-Poisson equations (164) and (165) which assume azimuthal symmetry with $\partial/\partial\tilde{\theta} = 0$, it should be emphasized that an identical formalism can be developed in a straightforward manner for the nonlinear Vlasov-Poisson equations (158) and (159) which allow for general transverse spatial variation of the distribution function $F_b(\tilde{x}, \tilde{P}_x; \tilde{y}, \tilde{P}_y; s)$ and effective potential $\psi(\tilde{x}, \tilde{y}, s)$.

A very simple application of the method of characteristiscs when $\partial/\partial\tilde{\theta} = 0$ can be illustrated for the special case of a uniform focusing field with $\kappa_z(s) = \kappa_{z0} = \text{const.}$ (independent of s). In this case, assuming that $\psi(\tilde{r}, s)$ does not depend explicity on s, it is readily shown from Eq. (222) that

$$\frac{d}{ds'}\tilde{H}_\perp(s') = \frac{d}{ds'}\left\{\frac{1}{2}\left[\tilde{P}_r'^2(s') + \frac{\tilde{P}_\theta^2}{\tilde{r}'^2(s')}\right] + \frac{1}{2}\kappa_{z0}\tilde{r}'^2(s') + \psi\left[\tilde{r}'(s')\right]\right\} = 0, \tag{229}$$

where $\tilde{H}_\perp(s')$ is the energy in the Larmor frame. It follows trivially from Eq. (229) that $\tilde{H}_\perp(s') = \tilde{H}_\perp(s' = s) = \tilde{H}_\perp(s' = s_0) = \text{const.}$ (independent of s'). Defining

$$\tilde{H}_\perp = \frac{1}{2}\left(\tilde{P}_r^2 + \frac{\tilde{P}_\theta^2}{\tilde{r}^2}\right) + \frac{1}{2}\kappa_{z0}\tilde{r}^2 + \psi(\tilde{r}), \tag{230}$$

it then follows that any distribution function initially of the form

$$F_b = F_b^0(\tilde{H}_\perp, \tilde{P}_\theta) \tag{231}$$

at $s' = s_0$, necessarily maintains the functional dependence on $(\tilde{r}, \tilde{P}_r; \tilde{P}_\theta)$ in Eq. (231) for all values of s'. Therefore, for $\kappa_z(s) = \kappa_{z0} = \text{const.}$, distribution functions of the form $F_b = F_b^0(\tilde{H}_\perp, \tilde{P}_\theta)$ are automatically *equilibrium* solutions to the nonlinear Vlasov-Poisson equations (164) and (165) with $(d/ds)F_b = (\partial/\partial s)F_b = 0$ (see also Sec. IV.B).

VI. CONCLUSIONS

In this article we have developed and applied a kinetic description of intense nonneutral beam propagation through a periodic solenoidal field $\vec{B}^{sol}(\vec{x})$ based on the nonlinear Vlasov-Maxwell equations for general distribution function $f_b(\vec{x},\vec{p},t)$. Particular emphasis was placed on using the Vlasov-Maxwell description to investigate detailed beam equilibrium properties for a variety of distribution functions, both for the case of a uniform solenoidal focusing field $B_0\vec{e}_z$, where $B_0 = \text{const.}$, and for a periodic solenoidal focusing field $\vec{B}^{sol}(\vec{x})$ described by Eq. (7), where $B_z(z+S) = B_z(z)$ and S is the axial periodicity length. Following a discussion of the theoretical model and assumptions (Sec. II), the nonlinear Vlasov-Maxwell equations and the single-particle equations of motion were simplified in the thin-beam approximation (Sec. III), and an alternative Hamiltonian formulation was developed that is particularly well-suited to describing intense beam propagation in a periodic focusing system.

For the case of a uniform focusing field $B_0\vec{e}_z$, the kinetic formalism based on the nonlinear Vlasov-Maxwell equations was used (Sec. IV) to investigate a wide variety of azimuthally symmetric ($\partial/\partial\theta = 0$) intense beam equilibria characterized by $\partial/\partial t = 0 = \partial/\partial z$, ranging from distributions that are isotropic in momentum dependence in the frame of the beam, to anisotropic distributions in which the momentum spreads are different in the axial and transverse directions. In addition, a density inversion theorem was demonstrated for the class of anisotropic beam equilibria considered in Sec. IV, and a general radial force constraint condition was derived that relates the mean-square radius $\langle r^2 \rangle$ of the beam to the strength of the focusing field, the transverse thermal emittance ϵ_{th}, and other system parameters. As a general remark, for a uniform focusing field, it was found that there is enormous lattitude in the choice of equilibrium distribution function f_b^0, the corresponding equilibrium profiles and properties of the beam, and the (likely) stability behavior.

Introducing the axial coordinate $s = z$, we then made use (Sec. V) of the kinetic formalism based on the nonlinear Vlasov-Maxwell equations to investigate intense beam propagation in a periodic solenoidal field $B_z(s+S) = B_z(s)$, in which case the properties of the beam

are modulated as a function of s by the periodic focusing field. Following a transformation of the nonlinear Vlasov equation to a frame of reference rotating at the Larmor frequency $\Omega_L(s) = -\Omega_{cb}(s)/2$, the description was further simplified by assuming azimuthal symmetry $(\partial/\partial\tilde{\theta} = 0)$, in which case the canonical angular momentum $\tilde{P}_\theta$ is an exact single-particle constant of the motion. As an application of the general formalism developed in Sec. V, we considered the specific example of a periodically focused rigid-rotor Vlasov equilibrium with step-function radial density profile and average azimuthal motion of the beam corresponding to a rigid rotation (in the Larmor frame) about the axis of symmetry. This represents an important generalization of the Kapchinskij-Vladimirskij beam distribution to allow for average beam rotation in the Larmor frame, and an important generalization of the rigid-rotor Vlasov equilibrium in Eq. (108) to include the periodic focusing effects of the solenoidal field $B_z(s+S) = B_z(s)$. Finally, the method of characteristics was discussed (Sec. V) as an approach for solving the nonlinear Vlasov equation for intense beam systems with periodic focusing.

As a general remark, based on the analysis in Secs. II-V, the Vlasov-Mawell description of intense nonneutral beam propagation through a periodic solenoidal focusing field $\vec{B}^{sol}(\vec{x})$ was found to be remarkably tractable and rich in physics content. Although much remains to be done to apply the formalism developed in Secs. III and V to other choices of peroidically focused beam distributions F_b, it is clear that the Vlasov-Mawell formalism developed here for intense beam propagation through a periodic solenoidal focusing field has a wide range of applicability, and can be extended in a straightforward manner to investigate detailed stability behavior for perturbations about specific choices of beam equilibria.

ACKNOWLEDGMENTS

This research was supported by the U. S. Department of Energy, and in part by the Office of Naval Research.

REFERENCES

1. R. C. Davidson, *Physics of Nonneutral Plasmas* (Addison-Wesley Publishing Co., Reading, MA 1990), Chapter 10, and references therein.
2. D. A. Edwards and M. J. Syphers, *An Introduction to the Physics of High-Energy Accelerators* (John Wiley & Sons, Inc., New York, 1993).
3. M. Reiser, *Theory and Design of Charged Particle Beams* (John Wiley & Sons, Inc., New York, 1994).
4. J. D. Lawson, *The Physics of Charged-Particle Beams* (Oxford Science Publications, New York, 1988), and references therein.
5. R. W. Müller, in *Nuclear Fusion by Inertial Confinement: A Comprehensive Treatise*, edited by G. Velarde, Y. Ronen, and J. M. Martinez-Val (Chemical Rubber Co., Boca Raton, FL, 1993), Chap. 17, pp. 437-453.
6. E. P. Lee and J. Hovingh, Fusion Technology **15**, 369 (1989).
7. R. A. Jameson, in *Advanced Accelerator Concepts*, edited by J. S. Wurtele, American Institute of Physics Conference Proceedings **279** (American Instutite of Physics, New York, 1993), p. 969.
8. R. Gluckstern, in *Proceedings of the 1970 Proton Linear Accelerator Conference*, Batavia, IL, edited by M. R. Tracy (National Accelerator Laboratory, Batavia, IL, 1971), p. 811.
9. See, Ref. 1, p. 699.
10. H. Uhm and R. Davidson, Part. Accel. **11**, 65 (1980).
11. I. Hofmann, L. Laslett, L. Smith, and I. Haber, Part. Accel. **13**, 145 (1983).
12. J. Struckmeier and M. Reiser, Part. Accel. **14**, 227 (1984).
13. J. Struckmeier, J. Klabunde, and M. Reiser, Part. Accel. **15**, 47 (1984).
14. M. Tiefenback and D. Keefe, IEEE Trans. Nucl. Sci. **NS-32**, 2483 (1985).
15. E. P. Lee, Nucl. Instrum. Methods Phys. Res. **A15**, 576 (1987).
16. F. Guy, P. Lapostolle, and T. Wangler, in *Proceedings of the 1987 Particle Accelerator*

Conference, edited by E. R. Lindstrom and L. S. Taylor (IEEE, New York, 1987), p. 1149.

17. J. Struckmeier and I. Hofmann, Part. Accel. **39**, 219 (1992).
18. Q. Qian, R. C. Davidson, and C. Chen, Phys. Rev. **E51**, 5216 (1995).
19. Q. Qian, R. C. Davidson, and C. Chen, Phys. Plasmas **2**, 2674 (1995).
20. Q. Qian and R. C. Davidson, Phys. Rev. **E53**, 5349 (1996).
21. C. Chen, Q. Qian, and R. C. Davidson, J. Fusion Engineering and Design **32**, 159 (1996).
22. W. W. Lee, Q. Qian, and R. C. Davidson, Phys. Plasmas **4**, 1915 (1997).
23. C. Chen, R. Pakter, and R. C. Davidson, "Rigid-Rotor Vlasov Equilibrium for an Intense Charged-Particle Beam Propagating through a Periodic Solenoidal Mangetic Field," Phys. Rev. Lett., in press (1997).
24. I. Kapchinskij and V. Vladimirskij, in *Proceedings of the International Conference on High Energy Accelerators and Instrumentation* (CERN Scientific Information Service, Geneva, 1959), p. 274.
25. See, Ref. 1, pp. 673-680.
26. See Chapters 4 and 9 of Ref. 1.
27. E. D. Courant and H. S. Snyder, Annals of Physics **3**, 1 (1958).

Appendix: Particle Orbit Equations Determined from the Approximate Hamiltonian

In this Appendix, we make use of the approximate form of H in Eq. (61) obtained in the thin-beam approximation to determine the dynamical equations of motion for an individual particle. For completeness, $\phi^s(x,y,z,t)$ is allowed to have full dependence on space and time coordinates, and the solenoidal focusing field is allowed to depend on axial coordinate z according to Eqs. (6) and (7), where $\vec{B}^{sol} = \nabla \times \vec{A}_{\perp}^{sol}$ with $A_x^{sol} = -(y/2)B_z(z)$ and $A_y^{sol} = (x/2)B_z(z)$. In terms of the canonical momentum $\vec{P} = \vec{p} + (Z_i e/c)\vec{A}$, the Hamiltonian H in Eq. (61) can be expressed as

$$H = \gamma_b mc^2 + \beta_b c\delta P_z + \frac{1}{2\gamma_b m}\left(\delta P_z - \frac{Z_i e}{c}A_z^s\right)^2$$
$$+\frac{1}{2\gamma_b m}\left[\left(P_x - \frac{Z_i e}{c}A_x^{sol}\right)^2 + \left(P_y - \frac{Z_i e}{c}A_y^{sol}\right)^2\right] + \frac{Z_i e}{\gamma_b^2}\phi^s, \qquad (A1)$$

where $\delta P_z = P_z - \gamma_b m\beta_b c$, and use has been made of $\phi^s - \beta_b A_z^s = \phi^s/\gamma_b^2$. In Eq. (A1), note that $|\delta p_z| \ll \gamma_b m\beta_b c$ implies that the quadratic term proportional to $(\delta P_z - Z_i e A_z^s/c)^2$ is typically small in magnitude in comparison with the term linearly proportional to δP_z.

We now make use of Eq. (A1) to examine Hamilton's equations of motion (16) and (17). For the transverse x-y motion, it is readily shown from Eqs. (16), (17), (18), (19) and (A1) that

$$\frac{dx}{dt} = \frac{1}{\gamma_b m}\left(P_x - \frac{Z_i e}{c}A_x^{sol}\right) = \frac{p_x}{\gamma_b m}, \qquad (A2)$$

$$\frac{dy}{dt} = \frac{1}{\gamma_b m}\left(P_y - \frac{Z_i e}{c}A_y^{sol}\right) = \frac{p_y}{\gamma_b m}, \qquad (A3)$$

and

$$\frac{dp_x}{dt} = \gamma_b m\frac{d^2x}{dt^2} = Z_i e\left[-\frac{\partial\phi^s}{\partial x} + \frac{v_z}{c}\frac{\partial A_z^s}{\partial x} + \frac{v_y}{c}B_z(z) + \frac{v_z}{2c}B_z'(z)y\right], \qquad (A4)$$

$$\frac{dp_y}{dt} = \gamma_b m\frac{d^2y}{dt^2} = Z_i e\left[-\frac{\partial\phi^s}{\partial y} + \frac{v_z}{c}\frac{\partial A_z^s}{\partial y} - \frac{v_x}{c}B_z(z) - \frac{v_z}{2c}B_z'(z)x\right], \qquad (A5)$$

where $v_z = dz/dt$, $v_x = dx/dt$ and $v_y = dy/dt$. On the other hand, for the axial motion, Eqs. (16), (17) and (A1) give

$$\frac{dz}{dt} = \beta_b c + \frac{1}{\gamma_b m}\left(\delta P_z - \frac{Z_i e}{c}A_z^s\right) = \beta_b c + \frac{\delta p_z}{\gamma_b m}, \qquad (A6)$$

and

$$\frac{d\delta p_z}{dt} = \gamma_b m \frac{d^2 z}{dt^2} = Z_i e \left[-\frac{\partial \phi^s}{\partial z} - \frac{v_x}{c}\frac{\partial A_z^s}{\partial x} - \frac{v_y}{c}\frac{\partial A_z^s}{\partial y} + \frac{1}{2c} B_z'(z)(x v_y - y v_x) \right], \qquad (A7)$$

where $\delta p_z = p_z - \gamma_b m \beta_b c$. Consistent with Eq. (25), we note that Eq. (A7) can be expressed in the equivalent form

$$\frac{d\delta P_z}{dt} = \frac{d}{dt}\left(\delta p_z + \frac{Z_i e}{c} A_z^s \right) = Z_i e \frac{\partial}{\partial z}\left[-\phi^s + \frac{v_z}{c} A_z^s + \frac{1}{2c} B_z(z)(x v_y - y v_x) \right], \qquad (A8)$$

where $\delta P_z = P_z - \gamma_b m \beta_b c$.

The role of the quadratic term proportional to $(\delta p_z)^2$ in Eq. (61) [or equivalently, in Eq. (A1)] is an interesting one. From Eq. (61), we find

$$\frac{dH}{dt} = \frac{p_z}{\gamma_b m}\frac{d\delta p_z}{dt} + \frac{1}{\gamma_b m}\left(p_x \frac{dp_x}{dt} + p_y \frac{dp_y}{dt} \right) + Z_i e \frac{d\phi^s}{dt}, \qquad (A9)$$

where $p_z = \delta p_z + \gamma_b m \beta_b c$ in Eq. (A9), and $(d/dt)\phi^s(x,y,z,t) = \partial\phi^s/\partial t + \vec{v}\cdot\nabla\phi^s$. Substituting Eqs. (A4), (A5), (A7) and $\vec{v} = \vec{p}/\gamma_b m$ into Eq. (A9) then gives the expected result

$$\frac{dH}{dt} = Z_i e \frac{\partial \phi^s}{\partial t} \qquad (A10)$$

by direct calculation. In this regard, to the level of accuracy of the orbit equations given by Eqs. (A4), (A5) and (A7), then energy conservation ($dH/dt = 0$ whenever $\partial\phi^s/\partial t = 0$) *necessarily requires* that the quadratic term proportional to $(\delta p_z)^2$ in Eq. (61), or in Eq. (A1), be retained in the definition of H.

Keeping in mind the discussion in the preceding paragraph, it is nonetheless useful to further simply the equations of motion. Consistent with Eq. (9), we make use of $|\delta p_z| \ll \gamma_b m \beta_b c$ and it follows from Eq. (A6) that $v_z = dz/dt = p_z/\gamma_b m$ can be approximated to leading order by

$$v_z = \frac{dz}{dt} = \beta_b c. \qquad (A11)$$

Substituting Eq. (A11) and $A_z^s = \beta_b \phi^s$ into the transverse dynamical equations (A4) and (A5) then gives the approximate results,

$$\frac{dp_x}{dt} = \gamma_b m \frac{d^2 x}{dt^2} = Z_i e \left[-\frac{1}{\gamma_b^2}\frac{\partial \phi^s}{\partial x} + \frac{1}{c}\frac{dy}{dt} B_z(z) + \frac{\beta_b}{2} y B_z'(z) \right], \qquad (A12)$$

$$\frac{dp_y}{dt} = \gamma_b m \frac{d^2 y}{dt^2} = Z_i e \left[-\frac{1}{\gamma_b^2} \frac{\partial \phi^s}{\partial y} - \frac{1}{c} \frac{dx}{dt} B_z(z) - \frac{\beta_b}{2} x B_z'(z) \right], \qquad (A13)$$

where $\gamma_b^{-2} = 1 - \beta_b^2$. If we make the identification $z = s = \beta_b ct$, then Eqs. (A12) and (A13) are identical to the transverse dynamical equations (45) and (46) obtained in Sec. III.B.

While $dp_z/dt = \gamma_b m dv_z/dt \cong 0$ to the level of accuracy of Eq. (A11), we can make use of Eqs. (A7) or (A8) to calculate leading-order corrections to $dp_z/dt = 0$. We readily obtain

$$\frac{d\delta P_z}{dt} = \frac{d}{dt}\left(\delta p_z + \frac{Z_i e}{c} A_z^s\right) = Z_i e \frac{\partial}{\partial z}\left[-\frac{\phi^s}{\gamma_b^2} + \frac{1}{2c} B_z(z)(x v_y - y v_x)\right], \qquad (A14)$$

or equivalently,

$$\frac{d\delta p_z}{dt} = \gamma_b m \frac{d^2 z}{dt^2} = Z_i e \left[-\frac{\partial \phi^s}{\partial z} - \frac{\beta_b}{c}\left(v_x \frac{\partial}{\partial x} + v_y \frac{\partial}{\partial y}\right)\phi^s + \frac{1}{2c} B_z'(z)(x v_y - y v_x)\right]. \qquad (A15)$$

Note that Eq. (A14) plays an important role in assuring energy conservation, when combined with Eqs. (A12) and (A13). To the same level of accuracy as Eqs. (A12), (A13) and (A14), and consistent with $|\delta p_z| \ll \gamma_b m \beta_b c$, we approximate Eq. (61) by

$$H = \gamma_b m c^2 + \beta_b c \delta p_z + \frac{1}{2\gamma_b m}(p_x^2 + p_y^2) + Z_i e \phi^s, \qquad (A16)$$

or equivalently, Eq. (A1) by

$$H = \gamma_b m c^2 + \beta_b c \delta P_z + \frac{1}{2\gamma_b m}\left[\left(P_x - \frac{Z_i e}{c} A_x^{sol}\right)^2 + \left(P_y - \frac{Z_i e}{c} A_y^{sol}\right)^2\right] + \frac{Z_i e}{\gamma_b^2}\phi^s. \qquad (A17)$$

Making use of Eqs. (A12), (A13) and (A15), and $d\phi^s/dt = \partial\phi^s/\partial t + \vec{v}\cdot\nabla\phi^s$, to calculate dH/dt from Eq. (A16), we obtain the expected result that $dH/dt = Z_i e \partial\phi^s/\partial t$, implying that energy is conserved ($dH/dt = 0$) whenever $\partial\phi^s/\partial t = 0$.

FIGURE CAPTIONS

Fig. 1 Plot of normalized density $n_b^0(r)/\hat{n}_b$ versus r/λ_D calculated numerically from Eqs. (64) and (72) for the choice of thermal equilibrium distribution in Eq. (71). Here, $\lambda_D = (\gamma_b^2 k_B T/4\pi\hat{n}_b Z_i^2 e^2)^{1/2}$ is the effective Debye length, and ϵ is the dimensionless parameter defined by $\epsilon \equiv (\Omega_b\Omega_{cb} - \Omega_b^2)/(\hat{\omega}_{pb}^2/2\gamma_b^2) - 1$.

Fig. 2 Plots of (a) normalized density $n_b^0(r)/\hat{n}_b$ and (b) temperature $T_b(r)/\hat{T}_b$ versus r/r_b calculated numerically from Eqs. (85)-(87) for $\epsilon = 0.001$, 0.01 and 0.1 with corresponding values of $\lambda_D/r_b = 0.088$, 0.127 and 0.222. Here, the dimensionless parameter ϵ is defined in Eq. (88), $\lambda_D = (3\gamma_b^2\hat{T}_b/8\pi\hat{n}_b Z_i^2 e^2)^{1/2}$ is the effective Debye length, and the equilibrium distribution is defined in Eq. (82).

Fig. 3 Plots of normalized density $n_b^0(r)/\hat{n}_b$ and transverse temperature $T_{\perp b}(r)/\hat{T}_{\perp b}$ versus r/r_b obtained from Eqs. (110) and (115) for the choice of equilibrium distribution in Eq. (108). Here, the beam radius is determined self-consistently in terms of other system parameters from Eq. (113).

Fig. 4 Plot of the normalized density $n_b^0(r)/\hat{n}_b$ versus r/r_b obtained from Eq. (122) for the choice of equilibrium distribution in Eq. (116). Here, the two cases correspond to the choices $r_b/\lambda_D = 5$ and $r_b/\lambda_D = 10$ [see Eq. (121)].

Fig. 5 Plot of the normalized density $n_b^0(r)/\hat{n}_b$ versus r/r_b obtained from Eq. (125). The density inversion theorem shows that the corresponding equilibrium distribution that generates this density profile self-consistently is given by Eq. (128).

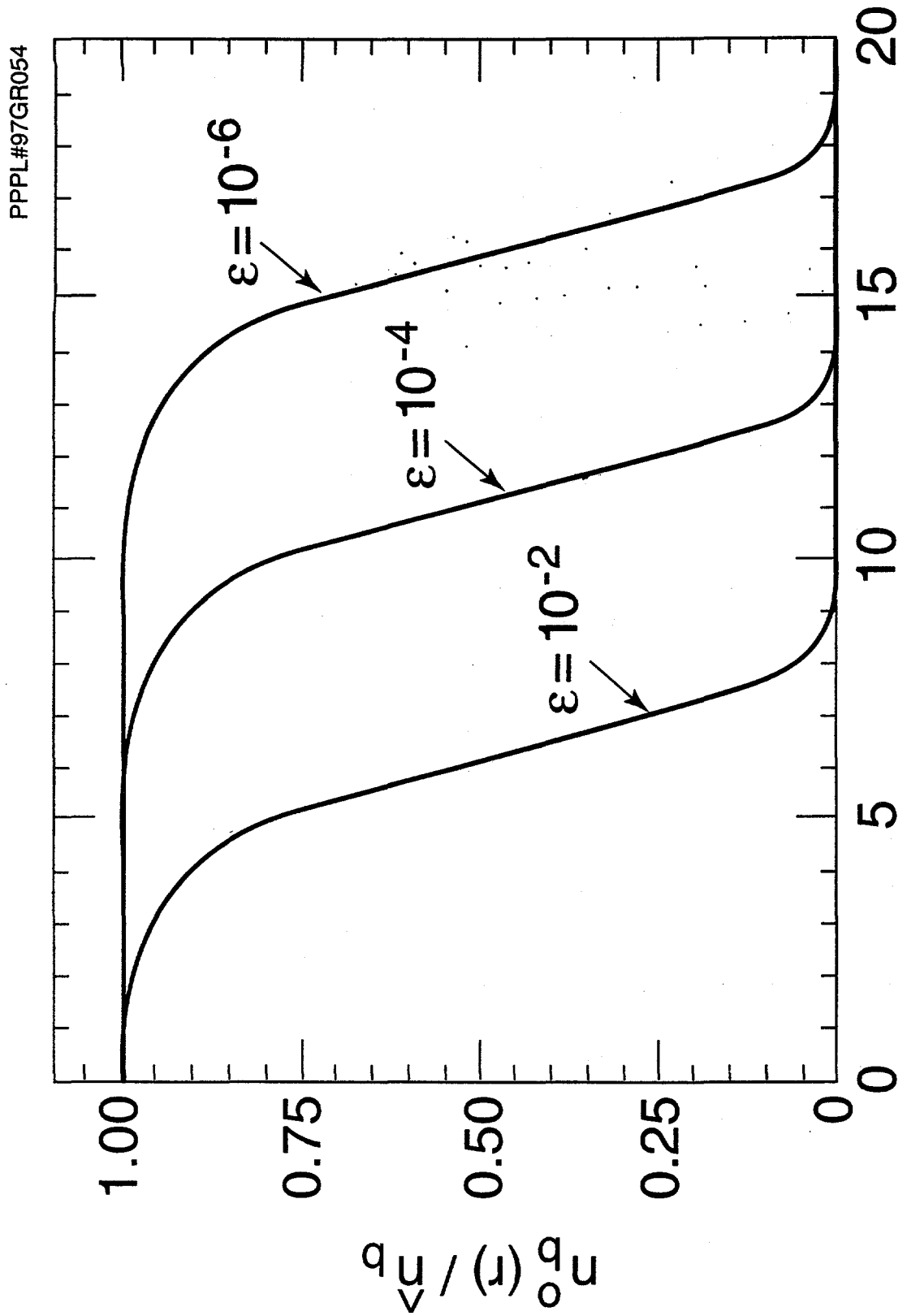
PPPL#97GR054
$n_b^o(r) / \hat{n}_b$
1.00
0.75
0.50
0.25
0
0
5
10
15
20
r/λ_D
$\varepsilon = 10^{-6}$
$\varepsilon = 10^{-4}$
$\varepsilon = 10^{-2}$

Fig. 1

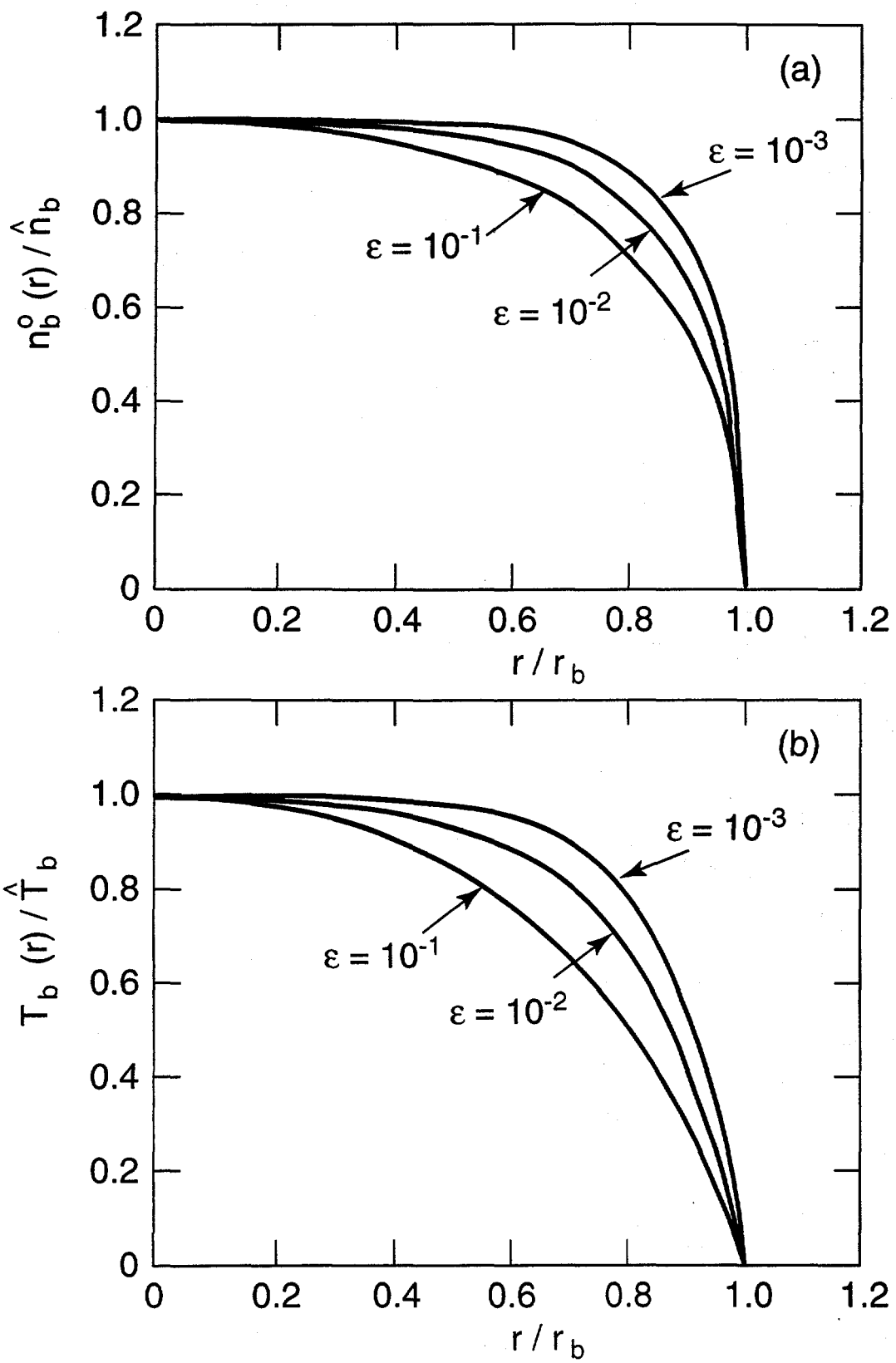
(a)
$\varepsilon = 10^{-3}$
$\varepsilon = 10^{-1}$
$\varepsilon = 10^{-2}$
$n_b^o(r) / \hat{n}_b$
r / r_b
(b)
$\varepsilon = 10^{-3}$
$\varepsilon = 10^{-1}$
$\varepsilon = 10^{-2}$
$T_b(r) / \hat{T}_b$
r / r_b

Fig. 2

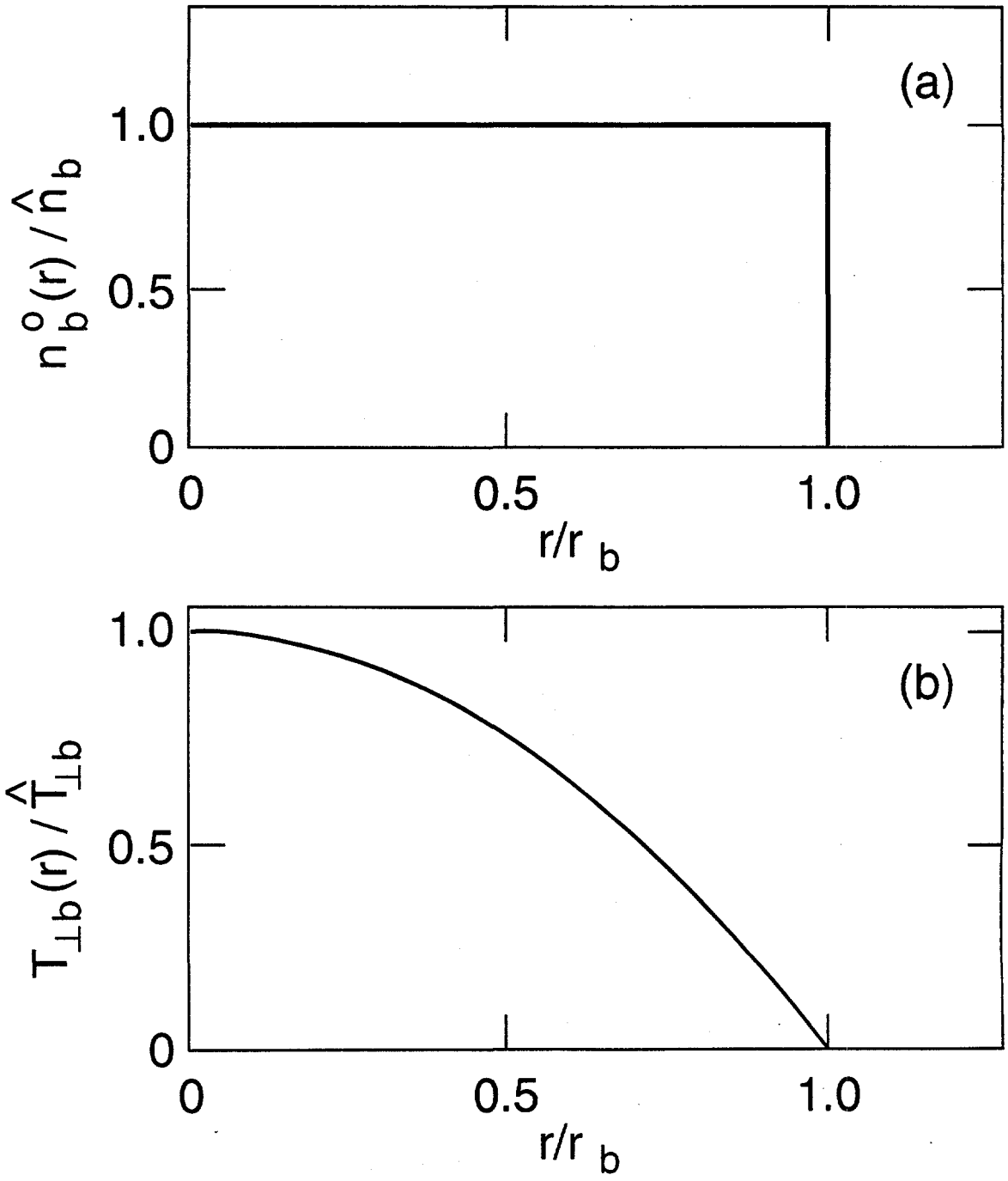
(a)
1.0
0.5
0
$n_b^o(r) / \hat{n}_b$
0
0.5
1.0
r/r_b
(b)
1.0
0.5
0
$T_{\perp b}(r) / \hat{T}_{\perp b}$
0
0.5
1.0
r/r_b

Fig. 3

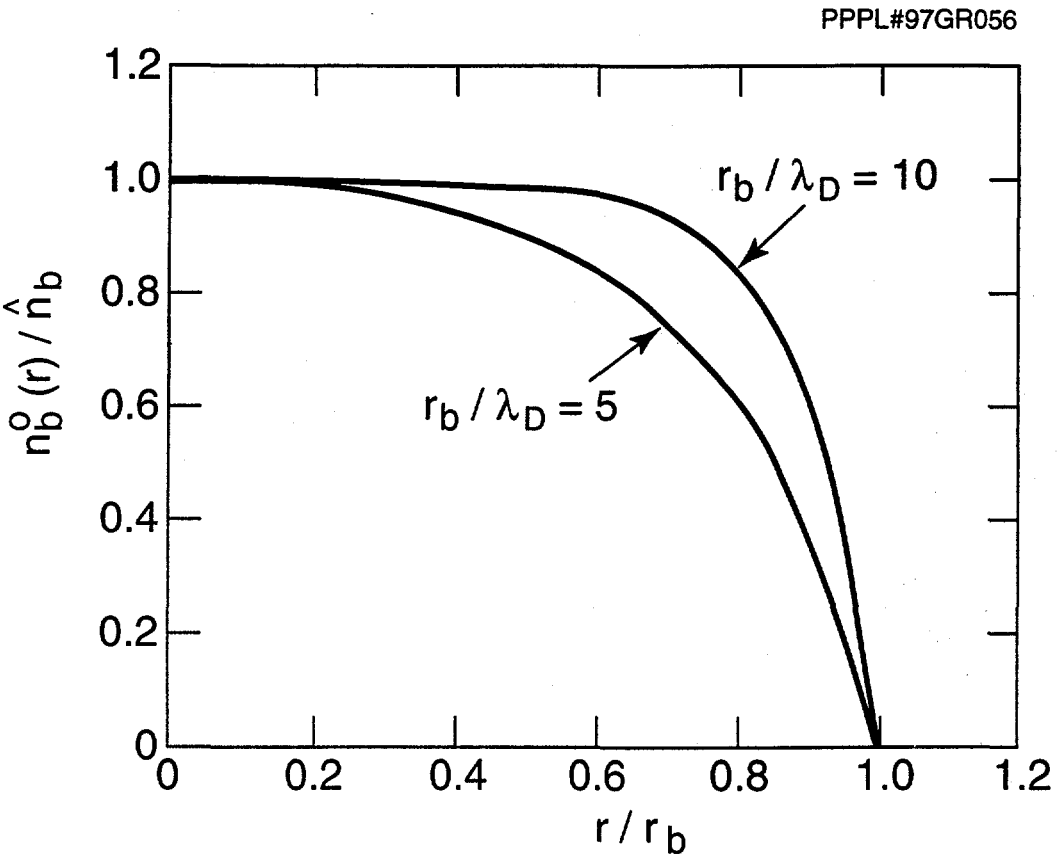
PPPL#97GR056
1.2
1.0
0.8
0.6
0.4
0.2
0
0
0.2
0.4
0.6
0.8
1.0
1.2
$n_b^o(r) / \hat{n}_b$
r / r_b
$r_b / \lambda_D = 10$
$r_b / \lambda_D = 5$

Fig. 4

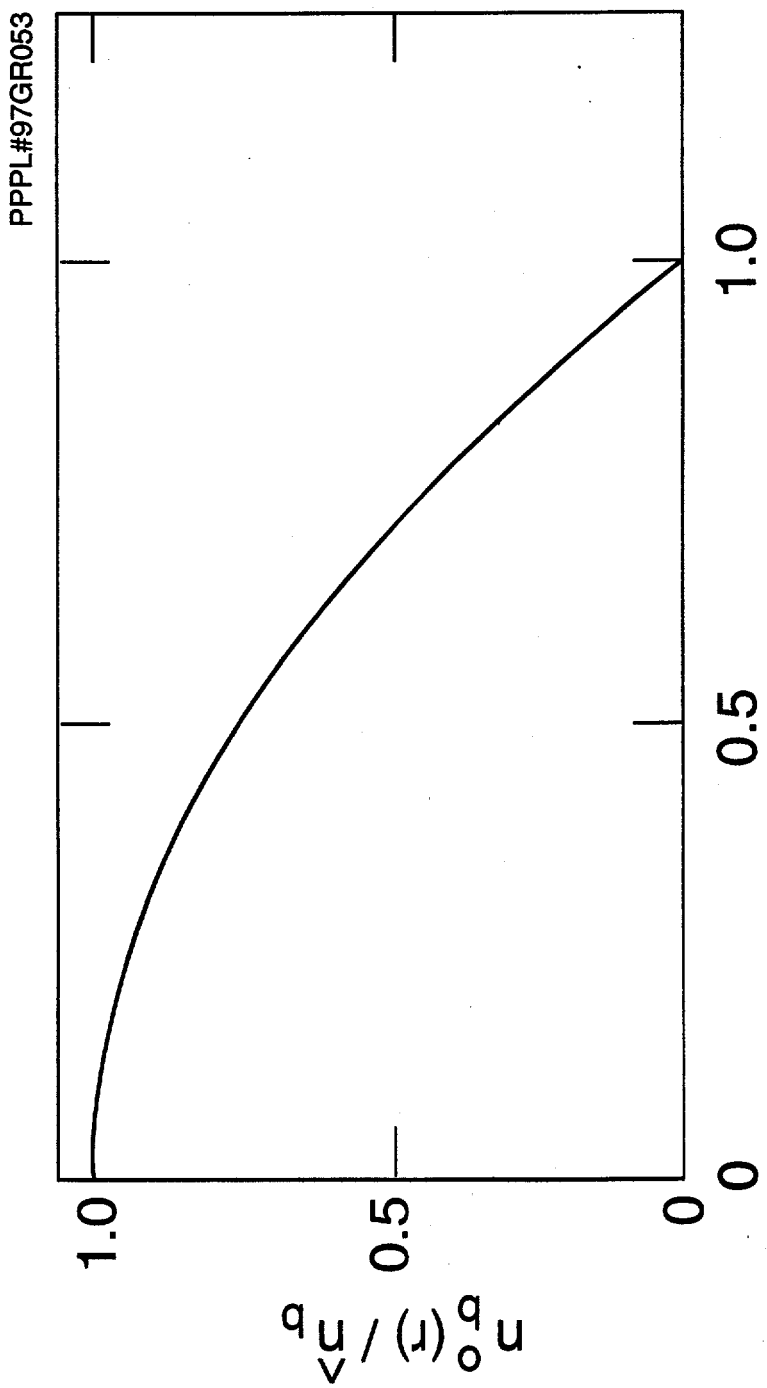

Fig. 5

External Distribution in Addition to UC-420

Professor Joao Canalle, Instituto de Fisica DEQ/IF - UERJ, Brazil
Mr. Gerson O. Ludwig, Instituto Nacional de Pesquisas, Brazil
Dr. P.H. Sakanaka, Instituto Fisica, Brazil
Library, R61, Rutherford Appleton Laboratory, England
The Librarian, Culham Laboratory, England
Professor M.N. Bussac, Ecole Polytechnique, France
Dr. F. Moser, Bibliothek, Institute für Plasmaforschung der Universitüt Stuttgart, Germany
Jolan Moldvai, Reports Library, MTA KFKI-ATKI, Hungary
Ms. Clelia de Palo, Associazione EURATOM-ENEA, Italy
Dr. G. Grosso, Instituto di Fisica del Plasma, Italy
Librarian, Naka Fusion Research Establishment, JAERI, Japan
Library, Plasma Physics Laboratory, Kyoto University, Japan
Dr. O. Mitarai, Kyushu Tokai University, Japan
Library, Academia Sinica, Insitute of Plasma Physics, People's Republic of China
Shih-Tung Tsai, Insitute of Physics, Chinese Academy of Sciences, People's Republic of China
Dr. S. Mirnov, Triniti, Troitsk, Russian Federation, Russia
Dr. V.S. Strelkov, Kurchatov Institute, Russian Federation, Russia
Mr. Dennis Bruggink, Fusion Library, University of Wisconsin, USA
Alkesh Punjabi, Center for Fusion Research and Training, Hampton University, USA
Dr. W.M. Stacey, Fusion Research Center, Georgia Institute of Technology, USA
Mr. Paul H. Wright, Indianapolis, Indiana, USA